IL
NUOVO CIMENTO
ORGANO DELLA SOCIETÀ ITALIANA DI FISICA
SOTTO GLI AUSPICI DEL CONSIGLIO NAZIONALE DELLE RICERCHE

VOL. VII, N. 2 *Serie decima* 16 Gennaio 1958

Study on α Radioactivity in Low Concentration.

R. DUGNANI LONATI, U. FACCHINI and I. IORI
Laboratori CISE - Milano

F. G. HOUTERMANS
Physikalisches Institut der Universität - Bern

E. TONGIORGI
Istituto di Paletnologia dell'Università - Pisa

(ricevuto il 12 Settembre 1957)

Summary. — With an ionization chamber filled with A (98%) and N_2 (2%) and with an emitting surface of 1 100 cm^2 it is possible to analyse by means of their α spectrum, samples of radioactive material containing up to concentrations of about 10^{-5} units. This investigations are interesting for instance, in the study of the age of a mineral deposit or a fossil; in the study of ocean sediments and of the radioactivity of lava.

1. – Introduction.

A previous work that in this paper will be referred to as (I) described a method of analysis of radioactive minerals based on the study of the α-particle spectrum (1).

The measurement of this spectrum is obtained easily by means of a grid ionization chamber filled with a mixture of argon (98%) and nitrogen (2%). About 10 g of sample is finely ground and mixed with water and sodium silicate. A known volume of the mixture is spread over a clean metal disc which is successively introduced into the chamber. The results obtained with concentrations of uranium up to about 10^{-3} were described in (I).

(1) U. FACCHINI, M. FORTE, A. MALVICINI and T. ROSSINI: *Nucleonics*, **14**, 126 (1956).

The aim of this work is to describe the extension of this method to lower concentrations.

As is well known, uranium and thorium, along with their decay products, are widely diffused in low concentrations. The study of their concentrations, the degree of their radioactive equilibrium, the concentrations of various decay products such as radium and ionium, radioactive emanations, etc., can in many cases furnish interesting information on a number of geophysical processes undergone by the radioactive families.

For the sake of illustration it is recalled how it is possible to determine the age of a mineral deposit up to about 10^5 years through the study of uranium, ionium and radium equilibrium. The study and age estimate of the ocean sediments can be made through ionium concentrations. In fact the surface sediments contain a notable concentration of ionium produced from the decay of the uranium dissolved in all the waters on the earth and subsequently precipited.

Another interesting study is that of the radioactivity of lava from various eruptions. Many researches were carried out along these lines but no complete radioactive analysis has so far been possible in view of the low radioactivity involved.

Generally speaking, while the study of high concentrations is predominantly of mining interest, that of low concentrations is mostly of geophysical interest.

2. – Experimental method.

The limitations of the method described in (I) are of two kinds, background and counting time.

A preliminary study has been conducted on the chamber described in (I), whose constructional design is being reproduced in Fig. 1 for convenience.

This chamber permits the use of samples spread over a surface of 110 cm^2, and in order to obtain the α spectrum with reasonable accuracy the thickness of the sample should be less than ~ 0.3 mg/cm^2. On the emitting electrode a total quantity of about 30 mg of the sample is deposited, about 10 mg of which being sodium silicate.

Taking into consideration the well known emission data for uranium and thorium, we obtain the following figures for a 20 mg sample:

$7 \cdot 10^{-3}$ pulses per minute per part per million of U and for α line;
$2.3 \cdot 10^{-3}$ pulses per minute per part per million of Th and for α line.

These figures correspond to every α emitter of the respective families of uranium and thorium in supposed radioactive equilibrium.

The sensitivity of the method is limited by the chamber background, i.e. by the number of pulses per minute, corresponding to α particle pulses of ener-

gies exceeding 3÷4 MeV, occurring when no radioactive sample is introduced in the chamber.

The background pulses are of two types; those due to electromagnetic disturbance induced in the chamber, which generally are difficult to screen completely, and those due to radioactive contaminations.

The electromagnetic disturbances were practically eliminated by means of a suitable circuit consisting of an antenna placed near the chamber to collect

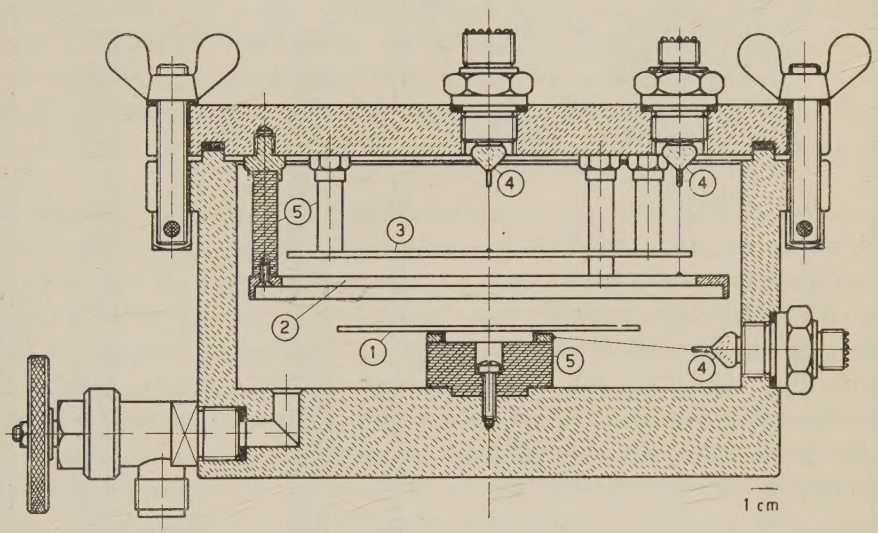

Fig. 1. – Ionization chamber of type I: 1) emitting electrode; 2) grid; 3) collector; 4) kovar-glass seals; 5) lucite.

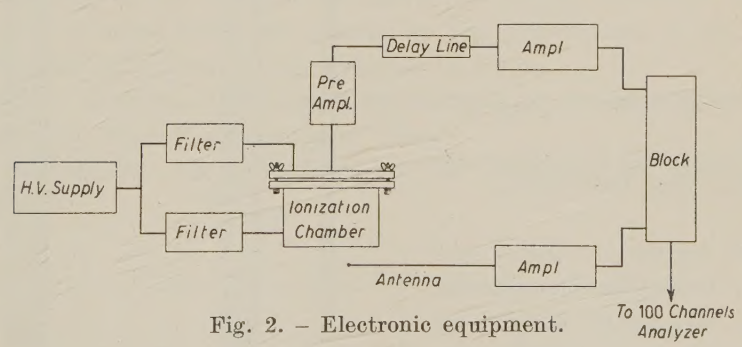

Fig. 2. – Electronic equipment.

those electromagnetic disturbances which can be induced on the chamber. The signal of the antenna is suitably amplified and relayed to drive a block circuit. The pulses originating in the chamber are passed across the same circuit which, normally open, is closed when an electromagnetic disturbance takes place. Fig. 2 illustrates the electronic equipment.

The radioactive contaminations were noted to be caused by two effects:

1) Contaminations due to the α radioactivity included in the materials constituting the chamber electrodes, and cosmic ray background.
2) Contaminations due to active deposit of emanation coming from the laboratory air.

A study has been conducted of the materials constituting the discs on which the radioactive sample is spread and of those constituting the grid and the collecting electrodes.

The best results were obtained using chromated brass or stainless

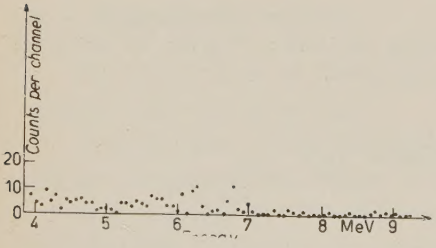

Fig. 3. – Spectrum of the background. Counting time 1360 minutes.

steel both for the electrodes and the discs. Under these conditions, the total background is equal to 0.2 pulses/min for α particle energies above 3 MeV.

The contamination due to the room air is easily detected by simply exposing the metallic disc to the air and introducing it after a while in the chamber.

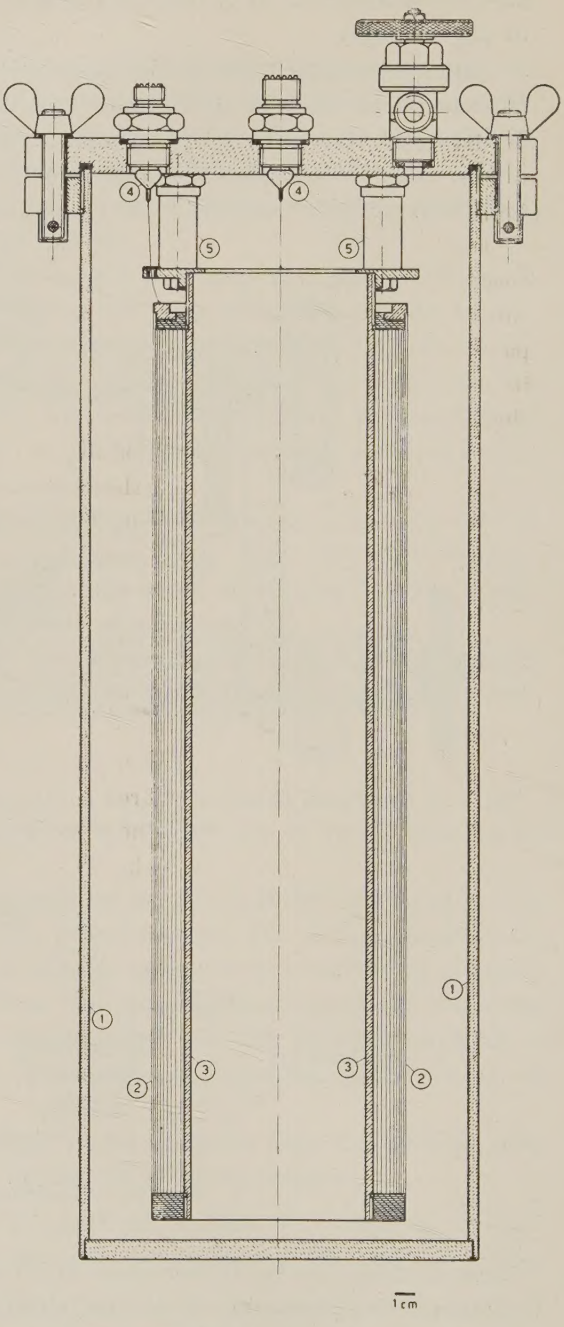

Fig. 4.
Ionization chamber of type II: 1) emitting electrode; 2) grid; 3) collector; 4) kovar-glass seals; 5) lucite.

This contamination is due to the active deposit contained in the atmosphere dust and increases the background up to 1-3 pulses/min.

After a few score hours when the active deposits of Rn and Tn have decayed, the background is reduced to the lowest value. If, under these conditions, the background is analyzed with a hundred channel pulse analyzer, the curve in Fig. 3 is obtained. Throughout the hundred channels the background varies from $\sim 7 \cdot 10^{-3}$ to $\sim 7 \cdot 10^{-4}$ pulses per minute per channel.

Observing that an α line corresponds to about 10 channels and taking into account the data discussed above, it is concluded that in the region of 4 MeV the background is equivalent to ~ 10 parts per million of uranium or ~ 30 parts per million of thorium, while in the more favourable region of 8 MeV it is equal to ~ 1 part per million of uranium or ~ 3 parts per million of thorium.

In principle, therefore, it is possible to reveal against the background samples of U and Th concentrations in the order of a few parts per million.

With so low an intensity, long time is rather needed to reveal a spectrum of sufficient statistics: about a hundred hours. With the chamber of (I) it is reasonably possible to measure the spectrum of a sample containing around 40 parts per million in about 24 hours.

For the purpose of reducing the measurement time, a new chamber has been constructed having a surface 25 times that of the chamber in Fig. 1, and in order to reduce the electrostatic capacity of the collecting electrode and simplify the construction, the chamber was built in the shape of a cylinder (Fig. 4). The sample is prepared on a suitable metal sheet with the same technique described above. The sheet is then rolled and placed inside the external cylinder of the chamber to serve as emitting electrode. The grid consists of steel wires stretched parallel to the generatrices of the cylinder with a diameter of 0.3 mm and a distance of 3 mm.

Finally the collecting electrode is represented by an internal cylinder of chromated brass having a diameter of 10 cm.

Table I illustrates the advantages of this chamber with respect to the previous one.

TABLE I.

	I	II
Surface of sample (cm^2)	110	2800
Weight of sample (mg)	20	500
Sensitivity in pulses per minute per part per million	$7 \cdot 10^{-3}$	$175 \cdot 10^{-3}$
Integral background above 4 MeV (pulses per minute)	0.2	7
Background in ppm of U at 8 MeV	1	1.5
Measuring time in hours needed for sample of 20 ppm of U	50	2

As will be noted, the longer time required in preparing the sample is compensated by the shorter time needed for measurement.

In order to show the resolution obtained with this chamber, Fig. 5 illustrates a spectrum of a Th salt.

3. – Measurement.

To give an example of the kind of results which can be obtained with such a method we will discuss two cases examined with the chamber of Fig. 1.

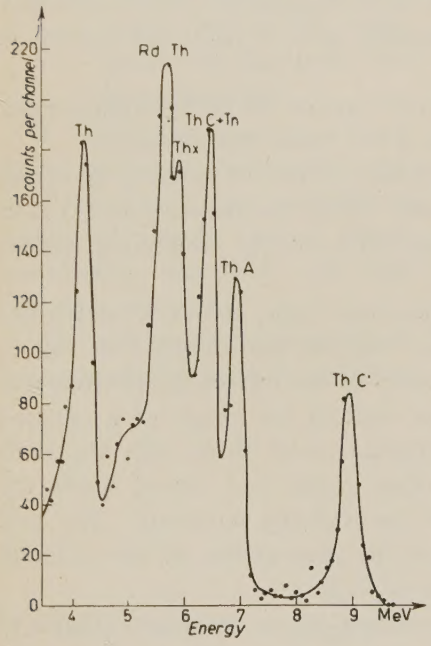

Fig. 5. – α spectrum of a Th salt mixed with non-active sand.

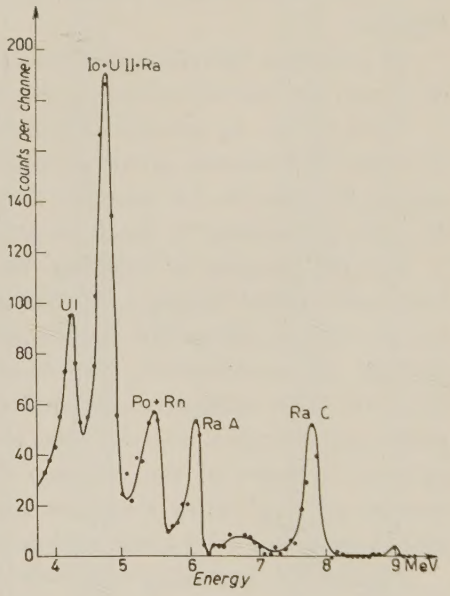

Fig. 6. - α spectrum of a fossil hippopotamus bone from Viterbo.

1) The spectrum of Fig. 6 is obtained from a bone of fossil hippopotamus coming from Viterbo.

The figures are as follows:

weight of sample	4.1 mg
measurement time	270 minutes
$\frac{\text{intensity of } U^{238} \text{ line}}{\text{intensity of } U^{234} + \text{Io} + \text{Ra lines}}$	0.3
equilibrium degree between Ra and U:	> 0.9

uranium concentration deduced from ^{238}U, ^{234}U, Io and Ra lines: $6.26.2 \cdot 10^{-4} \pm 10\,\%$
uranium concentration deduced from the whole spectrum including the Rn decay products: $5.3 \cdot 10^{-4} \pm 10\,\%$
(the last value may be reduced by a possible radon escape)
thorium content from ThC″ lines $< 6 \cdot 10^{-5}$.

The upper limit of torium content was only estimated, no line was measured. The hippopotamus was situated below a layer of sand, and above that a layer of tuff.

To clear the situation better, we have studied the activity of the tuff and sand, the latter studied in two positions, the first (I) just above the hippopotamus bone and the second (II) at the top of the layer below the tuff.

The α activities of the various samples are listed in Table II.

TABLE II.

Pulses/min/mg		U content	Th content
Hippopotamus bone	1.6	$6.2 \cdot 10^{-4}$	$< 6 \cdot 10^{-5}$
Tuff	0.093	$1.5 \cdot 10^{-5}$	$7 \cdot 10^{-5}$
Sand . . . I	0.0405	not analysed	
II	0.024	» »	

In the case of tuff the α analysis was done by obtaining the spectrum of Fig. 7; it is possible to deduce the indicated figures for U and Th contents.

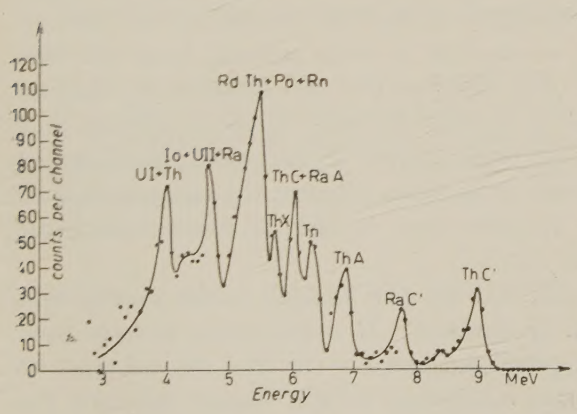

Fig. 7. – α spectrum of tuff layer.

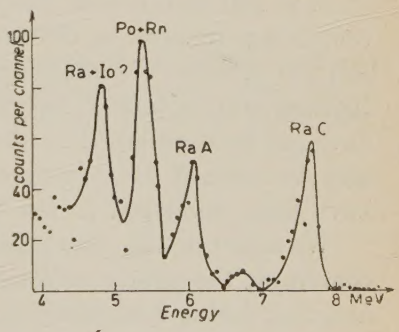

Fig. 8. – α spectrum of a volcanic glass sample from Mt. Vesuvius.

2) The spectrum of Fig. 8 corresponds to a vulcanic glass (from Mt. Vesuvius (1906)); the background as in Fig. 3 has been substracted.

weight of sample: 15 mg
measurement time: 1360 min

From the measurement of the various lines a concentration of radium of the order of $2.5 \cdot 10^{-11}$ is deduced.

The corresponding concentration of uranium would be $7 \cdot 10^{-5}$, though it is interesting to note that such a quantity of uranium was not present in the sample; the line of ^{238}U at 4.2 MeV is practically absent.

It is noteworthy that the total α activity found in the sample agrees with the results given by M. FERRETTI SFORZINI, C. FESTA, F. IPPOLITO ([2]) and obtained with the method of nuclear emulsions.

4. – Conclusions.

All the conclusions drawn from the spectra given above must be considered as quite tentative. Yet Fig. 6, 7, 8 clearly show that by using the ionization chambers I and II the α-spectrometer described in (I) is suitable for age determination in cases of radioactive non-equilibrium and therefore may be developed into a very valuable research tool for suitable cases in pleistocene palaeontology and in the study of prehistoric volcanism as well as in oceanography for studies of ocean sediments.

1) The hippopotamus bone from Viterbo shows an almost radioactive equilibrium between ^{238}U and its descendant elements, especially ionium, and an almost complete absence of the thoirum series. From this the following facts may be concluded: the high activity found in the bone material seems to exclude that it has been incorporated during the lifetime of the animal.

It is well known that uranium is absorbed by bone material from solutions containing uranium in the form of uranyl-ions ([3]). The absence of thorium and the presence of ionium almost in equilibrium leads to the conclusion that thorium and its isotope ionium were either absent in the passing solutions or have not been absorbed by the bone. A decision between the two possibilities may be reached by experiment. In both cases Io and its descendants must have been developed in the bone itself.

We might in this case distinguish between two limiting model assumptions concerning the uptake of uranium by the bone. It might either *a*) have been absorbed during a relatively short period compared to the time elapsed since its uptake or *b*) the absorption has been continuous since it began. Between the

([2]) M. FERRETTI SFORZINI, C. FESTA and F. IPPOLITO: *Atti del I Convegno di Geologia Nucleare*, p. 57 (1955).

([3]) Prof. LEHMANN, private communication.

two limiting cases an experimental decision may seem possible from a measurement of the uptake of uranium by bones to be put in the same conditions, within a relatively short time. From the fact that Io and its descendants are at present in a state of near equilibrium, above 4/5, with respect to ^{238}U, a maximum age of at least 3 half lives of Io, 250 000 years, may be calculated since the date of the uptake of uranium. It will not be too difficult to measure the Io content more accurately by chemical separation of U, Th and Ra from the bone material in order to determine more accurately the Io/^{238}U ratio, thus narrowing the limits of error in deducing the maximum age ([4]). Let us note also that if case *b*) (continuous uptake of U) is closer to reality the value for maximum age since the beginning of U-absorption should be even further lowered.

Fig. 8 reveals the very surprising fact that in the volcanic glass from Mt. Vesuvius (1906) uranium and thorium have been found to be absent within the limits of error, in spite of the fairly high radium content corresponding to a U concentration of 70 ppm. This proves that the application of the photographic method to volcanic materials and the attempts of determining a U/Th ratio on the basis of assumed equilibrium ([2-5]) does not seem sufficient in similar cases.

However it seems premature to draw any generalized conclusion from the α-analysis of this single sample. It will be necessary to make a systematic study of the equilibrium state and absolute Ra content of lava's volcanic tuffs and glasses of known historic date in order to obtain the original Ra-content for an eventual application in dating prehistoric volcanic materials.

* * *

Thanks to Prof. G. Occhialini for interesting discussions.

([4]) N. Isaac and E. Picciotto: *Nature*, **171**, 742 (1953).

([5]) S. Milone Tamburino and A. Stella: *Nuovo Cimento*, **9**, 253 (1952); L. Barbera, M. Curatolo, M. Indovina, D. Palumbo and M. Santangelo: *Ann. Geof.*, **6**, 161 (1953); G. Imbò and L. Casertano: *Ann. Geof.*, **6**, 315 (1953); G. Imbò: *Atti I Congresso Geologia Nucleare*, 1955, pag. 47.

RIASSUNTO

Con una camera di ionizzazione riempita con A (98%) e N_2 (2%) e con superficie emittente di 1100 cm^2 si possono esaminare, attraverso lo spettro α, campioni di materiale radioattivo con concentrazioni fino a 10^{-5} unità. L'esame di questi spettri è di interesse, per esempio, nello studio dell'età di minerali o di fossili; nello studio di sedimenti oceanici e nello studio della radioattività delle lave.

Cross Sections for K^--p Interactions.

R. G. Glasser and N. Seeman

U. S. Naval Research Laboratory - Washington, D.C.

G. A. Snow

U. S. Naval Research Laboratory - Washington, D.C.
and Brookhaven National Laboratory - Upton, N.Y.

(ricevuto il 12 Settembre 1957)

Summary. — Nine K^-+p elastic scattering events and eight $K^-+p \to \Sigma^\pm+\pi^\mp$ avents have been observed in nuclear emulsion. These events yield $\sigma_{(K^-+p\to K^-+p)} = 33^{+13}_{-9}$ mb and $\sigma_{(K^-+p\to\Sigma^\pm+\pi^\mp)} = 29^{+12}_{-9}$ mb averaged over the energy region $0 \div 82$ MeV. The data indicate that $\sigma_{(K^-+p\to\Sigma^\pm+\pi^\mp)}$ rises as the K^- energy decreases.

A search for K^--meson collisions on free hydrogen in nuclear emulsion has been carried out in the energy region $0 \div 82$ MeV. Similar emulsion experiments have been summarized by Ceccarelli [1]. K^--p interactions near zero energy observed in a liquid hydrogen bubble chamber have been reported by Rosenfeld [2].

A stack of 128 Ilford G.5 nuclear emulsions, 600 μm × 4 in. × 6 in., was exposed to the separated K^--meson beam at the bevatron [3]. The mean energy of the incident K^- mesons as determined from the mean range of those that come to rest is 81.6 MeV. (The range-energy relation of Barkas [4] was used, correcting for the difference (0.1%) between the measured density of our emulsion and the « standard » density of 3.815 g/cm³). This energy corresponds to a grain density in our stack of 53 grains/100 μm. The method of scanning was to select, at a fiducial line approximately 2 mm in from the leading edge, all tracks within 10° of the beam direction in projected angle

(1) M. Ceccarelli: *Report on Rochester Conference* (1957).

(2) A. H. Rosenfeld: *Report on Rochester Conference* (1957).

(3) W. H. Barkas, W. F. Dudziak, P. C. Giles, H. H. Heckman, F. W. Inman C. J. Mason, N. A. Nickels and F. M. Smith: *Phys. Rev.*, **105**, 1417 (1957).

(4) W. H. Barkas: *UCRL*-3769 (1957), unpublished.

and 6° in dip angle. These tracks were grain counted, and if the count was between 45 and 62 grains per hundred microns, the track was followed until it decayed, interacted in flight, came to rest, or was shown not to be a K-meson. (87% of the tracks which satisfied these criteria were K^--mesons.)

2600 K^--mesons were followed; of these, 480 interacted or decayed in flight. All interactions in flight with two outgoing prongs were checked for consistency with their being K^- interactions on free hydrogen nuclei ([5]). The principal interactions which can occur are:

(1) $K^- + p \to K^- + p$ (elastic scattering)

(2) $K^- + p \to K^0 + n$ (charge exchange scattering)

(3) $K^- + p \to \Sigma^+ + \pi^-$

(4) $K^- + p \to \Sigma^- + \pi^+$

(5) $K^- + p \to \Sigma^0 + \pi^0$ } (absorption)

(6) $K^- + p \to \Lambda^0 + \pi^0$

Of these, (2), (5) and (6) are seen in emulsion only as abrupt endings (0 prongs stars) which are indistinguishable from the larger number of such stars due to collisions on heavier emulsion nuclei and are therefore not identifiable. For reactions (1), (3) and (4), conservation of energy and momentum yield stringent kinematic tests which were applied to each two-prong event. Each event was required to be coplanar within the measurement error ($(1 \div 4)°$) depending on the orientation and scattering of the tracks.) For all K^--p elastic scattering events the range and angle with respect to the incident K^--meson of each outgoing track were required to fit the kinematic relations. In the reactions (3) and (4) the only range to which the stringent kinematic tests can be applied is that of the hyperon since the pion in general has a range too long to end in our stack. If the hyperon decays in flight into a pion which leaves the stack, then the only kinematic tests which are available are much less sensitive since they depend on measurements of ionization for determination of the hyperon and K^--meson energies. Even if the hyperon is not identifiable by its characteristic decay or visible interaction, the event might still be a K^--p interaction, e.g., the hyperon could be a Σ^- ending in a 0-prong star. The kinematic tests will identify these events also.

Applying the above tests to the two-prong stars produced by K^--mesons in flight, we have found nine K^--p elastic scatters and eight absorption events of types (3) and (4). Table I contains the essential characteristics of each of

([5]) The NRL group has tabulated the kinematics of reactions (1), (3) and (4) for K^--meson energies from $0 \div 200$ MeV.

the elastic scattering events. Table II describes the eight absorption events. The total K^--meson path length followed is 85.4 meters.

The average cross-section in the region (0 ÷ 82) MeV for elastic scattering is:

(7) $$\sigma_{(K^- + p \to K^- + p)} = 33^{+13}_{-9} \text{ mb}$$

TABLE I. – *Characteristics of* K -p *elastic scatters.*

Event	K star (a)	Path length (b) (mm)	T_{K^-} (c) (MeV)	$\chi^{CM}_{KK'}$ (d)
82–37	(0, 0, 4, 2)	32.4	22.7	135°
96–25	(0, 0, 0, 1)	29.8	36.3	76°
81–22	(1, 0, 1, 1)	15.8	39.9	60°
94–36	(0, 0, 5, 0)	24.7	40.9	102°
88–9	(0, 1, 2, 1)	15.9	53.9	100°
81–26	(0, 1, 3, 0)	13.4	62.1	74°
76–36	(0, 0, 0, 1)	11.6	68.2	123°
76–67	(0, 0, 4, 0)	9.9	73,1	96°
36–34	(0, 0, 2, 1)	6.2	81.2	132°

(*a*) Description of star made by outgoing K^-. The four numbers in parentheses denote the number of light, gray, black, and recoil or electron tracks respectively.
(*b*) The path length denotes the length of K^- track followed to the point of scatter.
(*c*) T_{K^-} is the energy of the K^- meson at the point of scatter as determined from the kinematics of the event.
(*d*) $\chi^{CM}_{KK'}$ is the angle through which the K^- scatters in the (K^-, p) center of mass system.

TABLE II. – *Characteristics of* $K^- + p \to \Sigma^\pm + \pi^\mp$ *events.*

Event	Hyperon (a)	Path length (b) (mm)	T_{K^-} (c) (MeV)	$\chi^{CM}_{K^-\pi}$ (d)
85–35 (e)	$\Sigma^\pm \to \pi^\pm + n$ (f)	34.8	14	84°
33–35	Σ^- star (0, 0, 0, 1)	37.2	14	149°
48–20	$\Sigma^+ \to \pi^+ + n$ (r)	31.5	15.0	134°
76–60	Σ^- star (0, 0, 2, 1)	33.9	15.7	87°
40–33	$\Sigma^+ \to p + \pi^0$ (r)	32.5	25	27°
82–35 (e)	$\Sigma^\pm \to \pi^\pm + n$ (f)	22.7	47.3	172°
32–1	$\Sigma^+ \to \pi^+ + n$ (r)	9.7	57	94°
35–56	$\Sigma^+ \to \pi^+ + n$ (r)	7.1	75	53°

(*a*) The four numbers in parentheses after Σ^- stars are the number of light, gray, black, and recoil or electron tracks respectively. (f) or (r) after a decay mode indicates decay in flight or at rest.
(*b*) The path length denotes the length of K^- track followed to the point of scatter.
(*c*) T_{K^-} is the energy of the K^-meson at the point of scatter as determined from the kinematics of the event.
(*d*) $\chi^{CM}_{K^-\pi}$ is the angle between the K meson and the π-meson directions in the (K^-, p) center of mass system.
(*e*) These two events fit the kinematics better with the assumption that the hyperon is a Σ^-, but the possibility of its being a Σ^+ cannot be ruled out.

at a mean energy ($\bar{T}_{K^-}$) of 52.2 MeV. (We have used the value of .0536 g/cm^3 of H_2 in our emulsion.) From our limited data there is no indication of any variation of cross-section with energy (see Table I). This result can be compared with the result reported by CECCARELLI [1] of about 46 mb at a similar average energy, and with the result reported by ROSENFELD [2] of 40 mb at an average energy of about 15 MeV.

For the absorption cross-sections of reactions (3) and (4) the result is

$$\sigma_{(K^-+p\to\Sigma^\pm+\pi^\mp)} = 29^{+12}_{-9}\ \text{mb} \qquad (\bar{T}_{K^-} = 52.5\ \text{MeV}) \tag{8}$$

over the same energy interval as before. In this case there is a definite indication of a variation of cross-section with energy. If we consider just the energy interval below 30 MeV, corresponding to a K^--meson path length of 13.54 m, there are five events. This yields a cross-section of

$$\sigma_{(K^-+p\to\Sigma^\pm+\pi^\mp)} = 115^{+65}_{-41}\ \text{mb} \qquad (\bar{T}_{K^-} = 20.8\ \text{MeV})\,, \tag{9}$$

while for the energy interval 30÷82 MeV the result is

$$\sigma_{(K^-+p\to\Sigma^\pm+\pi^\mp)} = 13^{+10}_{-6}\ \text{mb} \qquad (T_{K^-} = 62.1\ \text{MeV})\,. \tag{10}$$

Although the number of events is small, the difference between (9) and (10) is suggestive of a real effect in view of the difference between the ~ 100 mb cross-section reported by ROSENFELD at an average energy of 17 MeV and the ~ 11 mb cross-section reported by CECCARELLI at an average energy of ~ 50 MeV.

The rapid rise of the absorption cross-section as T_{K^-} approaches zero suggests that the K^-+p absorption process takes place predominantly in the $l=0$ state at energies $T_K \lesssim 30$ MeV. Since, ignoring the variation of absorption matrix element with energy, it follows that the absorption cross-section varies as k^{-1} for S waves and as k for P waves as T_K approaches zero [6]. (k is the wave number of the K^--meson in the center of mass system, $k=(1/\hbar)\sqrt{2M_{K^-}\bar{T}_{K^-}}$). Another possible explanation of the rapid variation of the absorption cross-

[6] E. P. WIGNER: *Phys. Rev.*, **73**, 1002 (1948). Strictly speaking, since there is an attractive Coulomb potential in the K^-+p system, the absorption cross-section varies as $1/k^2$ for all l states when T_{K^-} is very near zero ($T_{K^-} \ll 1$ MeV). However at the energies of observation considered here the Coulomb potential acts as a very small perturbation to the total absorption cross-section and the energy dependences quoted above, which are correct for neutral particles, are more appropriate. A necessary condition for the validity of these results however is that $ka \ll 1$, where a is the radius of the region of interaction. This condition is not well satisfied even in the energy region $T_{K^-} < 30$ MeV. If $a=\hbar/m_{K^-}c$ then ka varies from 0.14 to 0.35 as T_{K^-} goes from 5 to 30 MeV. Certainly, for $ka > 0.35$ the simple energy dependences for different l values quoted above cannot be relied upon. On the other hand if $a=\hbar/m_\pi c$ then already $T_{K^-}=5$ MeV, $ka=0.33$, and the simple argument given above in favor of S state K^-+p capture would be unreliable.

section with energy could arise from the concept of « global symmetry » [7] of the baryon interactions with π-mesons. If the $\Sigma\pi$ system has a strong resonance similar to the $n\pi$ system but shifted to lower energy, so that it occurs in the $\Sigma\pi$ system at an energy corresponding to $K^- + p$ capture near zero energy, then the $\Sigma\pi$ final state interaction could give rise to a rapid variation of the K^- absorption cross-section with energy.

* * *

We wish to thank Dr. MAURICE M. SHAPIRO for helpful discussions, Dr. E. LOFGREN and Dr. W. BARKAS and his group for their aid in exposing the plates. We would like also to acknowledge the many hours spent by the scanning staff, Mrs. LEEK, Mrs. RONES, Miss TRYON, Mrs. GRADY, Miss DEANGELIS, and Mr. BAILEY. We are indebted to Messrs. F. O'DELL and B. STILLER for their advice and aid in the processing of the emulsions.

[7] M. GELL-MANN: *Phys. Rev.*, **106**, 1296 (1957); and J. SCHWINGER: *Proc. of Rochester Conference* (1957).

RIASSUNTO (*)

In emulsione nucleare si sono osservati 9 scattering elastici $K^- + p$ e 8 $K^- + p \to \Sigma^\pm + \pi^\mp$. Questi eventi danno, mediando sull'intervallo energetico $0 \div 82$ MeV, $\sigma_{(K^- + p \to K^- + p)} = 33^{+13}_{-9}$ mb e $\sigma_{(K^- + p \to \Sigma^\pm + \pi^\mp)} = 29^{+12}_{-9}$ mb. I risultati indicano che $\sigma_{(K^- + p \to \Sigma^\pm + \pi^\mp)}$ cresce mentre l'energia del K^- decresce.

(*) *Traduzione a cura della Redazione*

IL NUOVO CIMENTO Vol. VII, N 2. 16 Gennaio 1958

Fluctuations of Track Parameters in Nuclear Emulsions.

B. J. O'Brien

The F.B.S. Falkiner Nuclear Research and Adolph Basser Computing Laboratories, School of Physics (*), *The University of Sydney - Sydney, N. S. W., Australia*

(ricevuto il 16 Settembre 1957)

Summary. — The fluctuations in nuclear-emulsion track parameters have been studied in a G5 emulsion of low minimum grain density by measurements of the blob density and integral gap length of long tracks of relativistic heavy nuclei. The intrinsic variations arising from the statistical nature of the process of track formation were found to be in good agreement with those predicted by the Blatt fluctuation theory. Subjective, emulsion and other variations were found in some cases to be comparable to the intrinsic variations. A method of estimating these fluctuation effects in any general experimental measurement is given.

1. – Introduction.

In experimental investigations of particles traversing nuclear emulsions, information about the particles is obtained by measurements of various characteristics of the tracks left by the particles. The characteristics usually measured may be classified in three groups, involving

a) along-the-track characteristics such as grain or blob density, gap-length distribution, and so on,

b) off-the-track characteristics, such as δ-ray density, and

c) the Coulomb scattering of the particle.

In the following we shall be concerned only with characteristics of group *a*).

(*) Also supported by the Nuclear Research Foundation within the University of Sydney.

Several theories of track formation have been proposed ([1-4]), by means of which all characteristics of group *a*) may be expressed for a given portion of a track in terms of a single parameter called the probability of development (p) pertaining to that portion of the track, and other parameters characteristic of the developed emulsion in the immediate vicinity of the track. Some experimental checks have been made of these theories ([3-8]).

However, besides a model which permits prediction of the mean value of a particular parameter given certain emulsion characteristics and the value of p, the experimentalist is interested also in the distribution of values of this parameter about the mean and in the accuracy of his measurements.

Methods of estimating these distributions have been derived by BLATT ([6,9]) who presented explicit expressions for the spread of the distribution assuming various models of track formation. The present paper covers an experimental investigation of the Blatt predictions and an analysis of other fluctuations present in experimental measurements.

In Sect. 2 are outlined the types of fluctuations which may occur in measurements of track parameters. The following section is devoted to a brief survey of the various models of track formation, leading in Sect. 4 to the Blatt fluctuation theory. The experimental details are given in Sect. 5, and the analysis of these in Sect. 6, and the resultant experimental implications in Sect. 7. Finally in Sect. 8 are given the conclusions and recommendations from the work.

2. – Types of fluctuations of track parameters.

Suppose a beam of particles having the same charge and velocity has traversed a nuclear-emulsion sheet. Suppose also that in the emulsion region under consideration, their rate of energy loss remained constant. For example, one might have a monoenergetic beam of relativistic protons entering the emulsion. Then if a series of measurements of any parameter Y is made on various tracks, or along any one track, Y will be found to have a mean value $\overline{Y}$ say, and the measured values of Y_i $(i = 1, 2, ..., k)$ will be distributed about

(1) C. O'CEALLAIGH: *Rep. Cosmic Ray Congress* (Bagnères-de-Bigorre, 1953), p. 73.
(2) W. W. HAPP, T. E. HULL and A. H. MORRISH: *Can. Journ. Phys.*, **30**, 699 (1952).
(3) M. DELLA CORTE, M. RAMAT and L. RONCHI: *Nuovo Cimento*, **10**, 509 (1953).
(4) A. J. HERZ and G. DAVIS: *Aust. Journ. Phys.*, **8**, 129 (1955).
(5) P. H. FOWLER and D. H. PERKINS: *Suppl. Nuovo Cimento*, **4**, 238 (1956).
(6) J. M. BLATT: *Aust. Journ. Phys.*, **8**, 248 (1955).
(7) C. CASTAGNOLI, G. CORTINI and A. MANFREDINI: *Nuovo Cimento*, **2**, 301 (1955).
(8) P. H. FOWLER and D. H. PERKINS: *Phil. Mag.*, **46**, 587 (1955).
(9) J. M. BLATT: (*Corrigendum.*) *Aust. Journ. Phys.*, **8**, 573 (1955).

$\overline{Y}$ with a standard deviation of σ, where

$$\sigma^2 = \frac{1}{K_i} \sum_{i=1}^{K} (Y_i - \overline{Y})^2 . \tag{1}$$

The standard deviation and hence the spread in the values of Y_i will arise from four sources

1) from variations in measurement techniques and judgments from observer to observer,

2) from variation of the decision and measurement efficiencies of one particular observer with time. In this we include setting or instrument errors,

3) from variations in the emulsion, e.g. perhaps arising from development or fixing gradients and

4) from the statistical nature of the process of track formation.

In the following all measurements were made by one observer, so that factor 1) will not enter into our considerations.

In making rough estimates of the accuracy of blob or grain counts it is sometimes assumed that there are no subjective or emulsion variations and that the distribution of the blobs along the track is random, resulting in a Poissonian distribution of the counts. The standard deviation of each measurement is thus taken to be the square root of the number counted.

This rough method usually gives results which are of the correct order of magnitude, but it has been known for some time that the spread in blob counts is often less than the Poissonian spread ([9,10]) and that the error is in general best obtained from the spread in measurements on calibration tracks. This may be attributed to the influence of saturation on various along-the-track characteristics and to the finite size of the grains.

In this experiment, measurements were made on the tracks of relativistic heavy nuclei where the rate of energy loss is essentially constant. The energy loss in each crystal determines the probability (p) of that crystal giving a grain when developed. Then for consideration of along-the-track parameters the effective energy loss in the crystals follows a Landau distribution, with a high-energy-loss cut-off due to the escape of δ rays from the crystals.

It is seen, therefore, that there will be a fluctuation in the energy loss in addition to the four fluctuation factors given above. By choosing a suitably long interval in which many energy-loss events take place, we may reasonably expect this effect to be small.

([10]) P. E. Hodgson: *Brit. Journ. Appl. Phys.*, **3**, 11 (1952).

3. – Models of track formation.

Several theories explaining the variation of along-the-track characteristics with the rate of energy loss have been proposed. These theories are basically of two types. The first, called the continuum model, has been developed by O'CEALLAIGH (1) and others (2). The second—the discrete model—is that proposed by HERZ and DAVIS (4) and by DELLA CORTE *et al.* (3).

The continuum model assumes a random distribution of AgBr crystals in the nuclear emulsion, so that there is a constant probability per unit path length for activating the next crystal.

The Herz model assumes an ordered array of crystals arranged in a lattice of regular spacing along the path of the particle.

These models give similar characteristics for a light track where the spacing between grains is generally many grain diameters. However, in the limit of a very clogged track were the probability of activating each crystal traversed approaches unity, there is no longer any agreement.

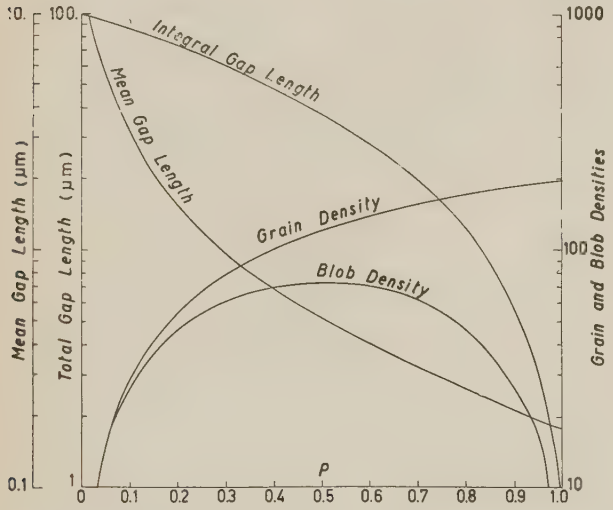

Fig. 1. – Variation of track characteristics with the probability of development p, for an original crystal diameter of 0.34 μm, a growth factor of 1.5, and a cell length of 100 μm.

The continuum model predicts that, in this limit, the average gap size reduces to zero. The Herz model, on the other hand, predicts that all the gaps should become zero-order gaps, i.e. gaps of a definite length dictated by the original lattice spacing and the growth of the crystals during development.

In order to account for the observed distribution of finite gaps at very high rates of energy loss, FOWLER and PERKINS (8) modified the O'Ceallaigh model by taking such gaps to be due to the presence of gelatin between the AgBr crystals.

A detailed comparison of the O'Ceallaigh and the Herz-Davis models was made by CASTAGNOLI *et al.* (7). They found that the Herz-Davis model was satisfactory for both thin and clogged tracks, whereas the O'Ceallaigh model was unsatisfactory for clogged tracks. A survey of the various theories of

track formation has also been given by BLATT ([6]) and by FOWLER and PERKINS ([8]) and no detailed comparison of the models will be made here.

Although the Herz-Davis model is an oversimplification which appears to break down for very heavy tracks, the results of CASTAGNOLI *et al.* ([7]) and our own measurements have shown that the Herz-Davis model is satisfactory for thin and medium tracks, and we shall adopt this model throughout the following. In Fig. 1 is shown the predicted effect of variation of the probability of development (p) on some along-the-track parameters

$$N_g = \text{grain density per 100 } \mu\text{m of track},$$

$$N_b = \text{blob density per 100 } \mu\text{m of track},$$

$$L_g = \text{total gap length per 100 } \mu\text{m of track},$$

$$\overline{w} = \text{mean gap width } (\mu\text{m}),$$

for a mean grain diameter (2γ) of 0.51 μm and an undeveloped crystal diameter (β) of 0.34 μm (see Sect. 5·3). For methods of calculation of various parameters given the two above values the reader is referred to HERZ and DAVIS ([4]).

The fit of the Herz model is indicated by comparison of predicted and experimental values for various tracks as shown in Table I. It is seen that the fit is reasonably good for light and medium tracks. The violent disagreement for the very heavy track is probably due both to the essential artificiality

TABLE I. – *Comparison of Herz' predictions with experiment*

$\beta = 0.34$ μm $\quad (2\gamma = 0.51) \quad t = 100$ μm

Charge	Track	Observed			Calculated		
		$\overline{w}$	N_b	$\overline{L}_g$	p	N_b	$\overline{L}_g$
2	α	2.5	31.3	78.2	0.13	32.5	81.0
5	B	0.46	71.0	32.7	0.54	72.5	33.6
5	B	0.44	65.7	28.8	0.57	72.0	31.5
5	B	0.38	68.0	25.6	0.63	68.0	25.5
~ 26	~ Fe	0.30	16.9	5.03	0.74 (*)	55	17
~ 26	~ Fe	0.27	18.6	5.03	0.78 (*)	49	13.5

(*) These values of p were calculated from the mean gap length $\overline{w}$. The value of p obtained from the gap length L_g is 0.92, and it is this value which will be used in subsequent calculations.

of the model in this region and also to experimental difficulties in observing and measuring the very small gaps. For high rates of energy loss, p is only

slowly dependent on L_g but varies rapidly with $\overline{w}$. Since any gaps missed by the observer will be small, they will consequently have less effect on a value of p determined from L_g than on p estimated from $\overline{w}$. Accordingly for the iron-nucleus track we estimate p from the measured value of L_g.

4. – Blatt fluctuation theory.

Following BLATT (6), we define $n_r(t)$ as the number of countable gaps, each one of length equal to or greater than r, in a cell length t, and $x_r(t)$ is the total length of these n_r gaps, counting for each gap only the excess of its length over r.

Clearly then, for $r = 0$, $n_r(t)$ and $x_r(t)$ for $t = 100$ μm, equal the blob density N_b and integral gap length L_g defined in Sect. 3.

Also, in order to check the Blatt model experimentally, we follow the Blatt definition of a countable gap, where

i) the initial point $t = 0$ of each cell length must be inside a blob, and

ii) the grain terminating each countable gap must have its centre within the cell length t.

We introduce, following BLATT, fluctuation parameters μ_n and μ_x which are defined as the ratios of the standard deviations to the square root of the mean values of n_r and x_r, viz. $\overline{n}_r$ and $\overline{x}_r$. Thus

$$(\mu_n)^2 = (\overline{n_r^2} - \overline{n}_r^2)/\overline{n}_r \tag{2}$$

and

$$(\mu_x)^2 = (\overline{x_r^2} - \overline{x}_r^2)/\overline{x}_r \,. \tag{3}$$

Explicit expressions for $(\mu_n)^2$ and $(\mu_x)^2$ may be derived by applying the Blatt theory to particular models of track formation. We consider only the Herz model, and here, using the notation of BLATT (6),

$$(\mu_n)^2 = 1 - (2R+1)p(1-p)^R + \text{order}\left(\frac{2\gamma + r}{t}\right), \tag{4}$$

$$(\mu_x)^2 = \overline{w} + q\,\frac{\beta^2}{p^2\overline{w}} + 2q^R\left\{\overline{w}\left(1 - \frac{p}{2}\right) - (R+1)pw_0 - (R\beta + w_0)q - \frac{2q}{p}\,\beta\right\}, \tag{5}$$

where $R =$ integral part of $(2\gamma + r)/\beta$

$$q = 1 - p \,, \tag{6}$$

$$w_0 = \lim_{p \to 1} \overline{w} = \beta(R+1) - (2\gamma + r) \,. \tag{7}$$

In Fig. 2 we show the variation of these two fluctuation parameters with the probability of development, using the Herz model and the measured characteristics of our emulsion,

with $r = 0$ (i.e. all gaps counted),
$R = 1$ (i.e. growth factor having a value between 1 and 2)
$w_0 = 0.17$ μm (the zero-order gap length)
$\beta = 0.34$ μm (the original crystal diameter)
$2\gamma = 0.51$ μm (the developed grain diameter).

Some intuitive picture of the significance of the Blatt fluctuation parameters may be gained by considering the variation of $(\mu_n)^2$ with the value of p

For $p \to 0$, i.e. for a very light track, all blobs will be single grains, and their distribution along the track will be Poissonian. Thus the variance will equal the mean blob density, and hence $(\mu_n)^2 \to 1$.

As p increases, the individual grains occur closer together, and two or more will occasionally merge to form a blob. Thus the finite size of the grains will result in a cut-off to the lower end of the distribution of blobs along the length of the track, and this distribution will have a spread which is less than Poissonian. Thus $(\mu_n)^2$ will be less than one.

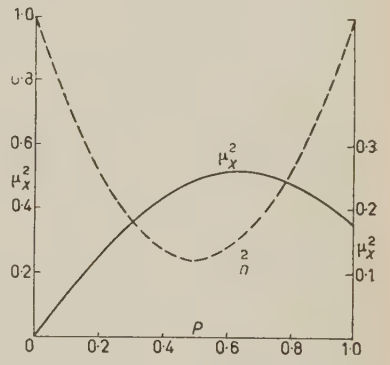

Fig. 2. – Variation of the fluctuation parameters with p.

Further increase in p results in greater saturation or clogging, and there will be a progressive decrease in $(\mu_n)^2$. Finally as $p \to 1$ we will have the situation of zero-order gaps distributed along the track in a Poissonian form and again $(\mu_n)^2 \to 1$. In the case $p \to 1$ the zero-order gaps are distributed along the track in much the same way that single grains were for $p \to 0$.

5. – Experimental details.

5·1. *Emulsion stack.* – Measurements were carried out using a sheet of G5 emulsion which was one of the outside sheets of a stack flown at 110 000 feet over Texas in February 1956 [12].

[11] R. R. Daniel and D. H. Perkins: *Proc. Roy. Soc.*, A **221**, 351 (1954).
[12] J. H. Noon, A. J. Herz and B. J. O'Brien: *Nuovo Cimento*, **5**, 854 (1957).

The plateau grain density for a singly-charged particle in this emulsion was about 8 grains per 100 μm. Thus the fluctuation studies were carried out in G5 emulsion of low minimum grain density, since normal G5 has a plateau grain density of about 25 grains per 100 μm. If the only effect of a higher minimum grain density of a G5 emulsion is to increase the value of p for any particular rate of energy loss, we may reasonably expect the fluctuations to be essentially similar regardless of the minimum grain density. It is not possible at this stage to state with certainty whether this expectation is justified, especially as we have not been able as yet to investigate the effects of physical development.

The variation of the track characteristics with p are shown in Fig. 1, where p is experimentally determined from the mean gap width w. A fast α particle has a value of p around 0.12, boron around 0.56 and iron around 0.92. Fig. 1 is derived from the mean measured grain diameter of 0.51 μm assuming an original crystal diameter of 0.34 μm.

A good fit for the tracks of light and medium nuclei can also be obtained if we assume an original crystal diameter of 0.20 μm, but the shape of the curves in Fig. 1 will be altered if we do this. For example, N_b will then have a maximum at $p = 0.33$. Since no measurement of the crystal diameters in this emulsion is available, it is not possible to choose between the two values.

However, we are concerned here only with fluctuation estimates from the Blatt model, and it can be shown that these estimates will be the same regardless of which choice we make for all tracks where p is not very close to unity. This is reasonable since one expects the fluctuation estimates to be dependent only upon the physical characteristics of the track. Accordingly, throughout this paper we will adopt the first model, i.e. with original crystal diameter of 0.34 μm and a growth factor of 1.5.

The background grain density was less than 0.2 grains per 100 μm, and thus was negligible in all the following measurements.

5·2. *The gap counter.* – In the measurements use was made of a gap counter developed in this laboratory by Dr. A. J. Herz along the lines of those in use elsewhere ([13,14]). The track is aligned parallel to the x direction of a Koristka microscope, and the stage is moved at the rate of 20 μm per minute by means of a suitably geared motor. One dekatron scaling unit records continuously while the track moves, and another only when a microswitch is depressed whilst a gap is crossing a hair line as seen by the observer. The ratio of the registers of the two dekatron scaling units gives a direct measure of the value of L_g. The gap (or blob) density is found by measurement of

([13]) G. Baroni and C. Castagnoli: *Suppl. Nuovo Cimento*, **12**, 364 (1954).
([14]) H. M. Mayer: C.E.R.N. Document BS20 (10-V-1955).

the number of times the microswitch is depressed for the track length which is read from the barrel of the microscope. In this experiment the click-stop device of the Koristka was used so that each measurement was over a 100 μm interval.

5·3. *Grain-size distribution.* – In order to make use of the Herz-Davis model of track formation, the mean diameter of single developed grains in the emulsion must be found. This value was determined by using the gap counter on a light track where most of the grains are single. About 250 blobs were measured along an α-particle track, and the mode of the resultant distribution found. This value is taken to be the mean grain diameter ($\alpha\gamma$ in Herz formulae, and 2γ in Blatt's notation). It was found to be 0.51 μm. In the use of the Herz-Davis model, it is assumed that all developed grains have this diameter.

5·4. *Experimental method.* – Several tracks with lengths of more than 15 mm in the 9 in. × 10 in. plate studied were selected from different charge groups. These tracks are shown in Fig. 3. All these tracks could be followed through the stack for more than 30 g cm^{-2}. Measurements were made on the tracks in the central 400 μm of the emulsion.

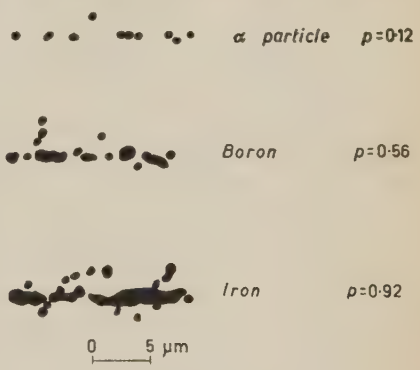

Fig. 3. – Typical sections of the three tracks measured.

Measurements of the blob number and integral gap length were made using the gap counter. A measurement was made for each 100 μm cell, and 100 successive cells were measured on each track. For purposes of analysis and discussion, we shall say that 10 successive cells constitute a group. Thus 10 successive groups, each of 10 cells, were measured for each track.

One group in each track was selected at random, and measured in the same way five times. Since this was done with the object of estimating subjective errors, these five repeat determinations were made over a similar time interval to the overall track measurements. In this way allowance could be made for any long-term subjective fluctuations as well as for subjective fluctuations such as setting and decision errors.

6. – Analysis of results.

6·1. *Nomenclature.* – As pointed out in Sect. 2, the errors which may influence measurements of blob densities and integral gap lengths fall into three categories:

subjective (S), emulsion (E), and track (T) effects.

We shall denote for any one track the overall standard deviations of the blob density and integral-gap-length measurements as S_n and S_x respectively.

Let $(S_n)_S$, $(S_n)_E$, and $(S_n)_T$ be the standard deviations introduced into the blob-density measurements by the three types of fluctuations mentioned earlier.

An analogous notation will hold for the integral-gap-length measurements.

Then

$$(S_n)^2 = (S_n)_S^2 + (S_n)_E^2 + (S_n)_T^2 , \tag{8}$$

provided we make the reasonable assumption that these three sources of variance are independent.

6·2. *Fluctuations of the fluctuation parameter.* – The fluctuation parameter for each of the ten groups can be calculated by considering the ten readings for each group as being distributed about the appropriate mean value for that group. The resultant estimates are set out in Table II.

TABLE II. – *Values of the fluctuation parameters for each group of ten cells.*

Type of track	Thin		Medium		Clogged	
Charge	2		5		~ 26	
p	0.12		0.58		0.92	
	μ_n^2	μ_X^2	μ_n^2	μ_X^2	μ_n^2	μ_X^2
	0.7	0.09	0.19	0.06	0.5	0.13
	1.7	0.22	0.20	0.78	1.2	0.34
	0.7	0.10	0.20	0.30	1.0	0.48
	0.7	0.13	0.24	0.11	0.7	0.31
	0.6	0.09	0.38	0.09	1.2	0.27
	2.6	0.07	0.65	0.18	0.6	0.14
	0.6	0.10	0.77	0.65	0.9	0.27
	1.6	0.23	0.46	0.25	0.6	0.11
	0.8	0.14	0.81	0.26	0.5	0.49
	0.9	0.09	0.78	0.18	0.4	0.34

It is seen that the fluctuation parameters themselves show considerable fluctuations, as may be expected with the small samples involved.

6·3. *Subjective variations.* – Within the category of subjective variations we include, for the purposes of analysis, such factors as

i) judgment errors, e.g. arising from decisions as to what constitutes a gap, or what is the minimum observable gap length,

ii) setting errors, arising from the pressing of the microswitch,

iii) instrument errors.

Accordingly we require some method of numerically estimating the spread in the blob and gap-length measurements which is introduced by the subjective fluctuations alone. Thus estimates of $(S_n)_s$ and $(S_x)_s$ are required for the measurements on each track.

Such estimates were made by selecting one group in each track at random, and making five sets of measurements on each of the ten cells within this group. These repeat measurements were carried out over the same time interval as the overall measurements, so as to make allowance for any possible long-term subjective variation.

Since the mean values of each of the ten cells will vary and since it is desirable to avoid any corresponding weighting of the standard-deviation estimates, the subjective fluctuation parameters are calculated for each of the ten cells to give $(\mu)_i^2$ $(i = 1, 2, ..., 10)$ for both gap numbers and gap lengths for each track. These values are set out in Table III.

TABLE III. – *Estimates of subjective fluctuations.*

Type of track	Thin		Medium		Clogged	
p	0.12		0.58		0.92	
Charge	2		5		~ 26	
	μ_n^2	μ_X^2	μ_n^2	μ_X^2	μ_n^2	μ_X^2
	.012	.045	.049	0.05	0.35	0.12
	.033	.022	.10	0.02	0.42	0.03
	.037	.020	.11	0.02	0.67	0.15
	.008	.036	.01	0.08	0.06	0.02
	.008	.008	.07	0.07	0.06	0.08
	.015	.027	.09	0.1	0.10	0.04
	.007	.017	.13	0.11	0.13	0.05
	.007	.016	.03	0.21	0.03	0.03
	.023	.003	.00	0.10	0.36	0.10
	.006	.012	.07	0.01	0.02	0.01

Then if

$$(S_n)_s^2 = N_b(\mu_n)_s^2, \tag{9}$$

following the usual statistical methods

$$(\mu_n)_s^2 = \sum_{i=1}^{10} (\mu_n)_i^2/9 \tag{10}$$

and similarly for the gap-length measurements. The values of $(S_n)_s$ and $(S_x)_s$ which are derived from equations (9) and (10) are included in the summary Table IV.

TABLE IV. – *Summary of standard deviation estimates.*

TABLE IV (*a*). – Blob density.

Cause of fluctuation	Track p	0.12	0.58	0.92
	Charge	2	5	~ 26
Large scale emulsion effects $(S_n)_E$		1.4	2.7	1.0
Subjective effects $(S_n)_S$		0.7	2.5	2.1
Track effects $(S_n)_T$		4.6	4.5	3.2
Blatt prediction		4.6	4.3	3.7
Poissonian prediction		5.5	8.3	4.2
Overall effects S_n		4.9	6.2	3.9

TABLE IV (*b*). – Integral gap length.

Cause of fluctuation	Track p	0.12	0.58	0.92
	Charge	2	5	~ 26
Large scale emulsion effects $(S_X)_E$		1.6	3.0	0.4
Subjective effects $(S_X)_S$		1.3	1.6	0.6
Track effects $(S_X)_T$		3.1	2.6	1.1
Blatt prediction		2.3	2.7	1.0
Poissonian prediction		9.0	5.4	2.2
Overall effects S_X		3.7	4.2	1.3

These values will be slight onverestimates of the subjective fluctuations, since there was a setting error of the order of 1 μm in the repeat measurements. However, only for the α-particle blob counts will this setting error be important in the subjective error, and in no case will it be comparable with the overall error.

As would be expected from the physical nature of the tracks, the proportionate importance of the subjective variations increases with the density of the track.

6·4. *Analysis of variance.* – By using the standard analysis-of-variance techniques ([15]) on the measurements for each of the 100 cells of any track, one can obtain three values of variance:

i) the variance between groups (σ_B^2),

ii) the variance within groups (σ_W^2),

iii) the overall variance $(S)^2$.

([15]) C. G. PARADINE and B. H. P. RIVETT: *Statistics for Technologists* (London, 1953), p. 232.

If there is no significant difference in the track parameters from group to group, one would expect all three variances to be approximately equal.

If, on the other hand, there is a significant variation in the measurements from group to group, σ_B^2 will be significantly greater than σ_W^2. The test of significance is made using the Fisher F-test.

In every case in this experiment, σ_B^2 and σ_W^2 were significantly different at a 90% confidence level and indeed in every case except the blob measurements along the iron track, they were significantly different at a 95% confidence level.

This difference could be due either to a long-term subjective variation, or to a definite variation in the emulsion from one 1 mm section to another, or to a combination of these factors. Estimates of the subjective errors were carried out as described in the preceding section and since these repeat measurements were made over the same time interval as the overall measurements, it was possible to eliminate the effects of subjective variations.

Thus it can be concluded that there existed significant variations in the emulsion from one 1 mm section to another. It should be emphasized that the measurements were made in the central 400 μm of the 600 μm sheet, and that the three tracks were located at different positions in the 9 in. ×10 in. sheet. Further, when the grain densities of relativistic α-particles were measured in various portions of this sheet, they were consistent statistically with a constant minimum grain density over the sheet. Some evidence for similar emulsion variations has been given recently ([16]).

Again using standard statistical methods

$$\sigma_B^2 = \sigma_W^2 + 10(S_E^2)\,, \tag{11}$$

where $(S)_E$ is the standard deviation introduced into the measurements because of the variations in the emulsion over 1 mm intervals. The values of the « emulsion » standard deviations are listed in the summary Table IV.

6·5. *Comparison with Blatt estimates.* – In the preceding sections are given the methods of estimating the subjective and large-scale emulsion variations. We have seen also that we may estimate the variance σ_W^2 for measurements within the groups, and that this value of σ_W^2 will be independent of large-scale (> 1 mm) emulsion variations.

Then, assuming that the small-scale (100 μm) emulsion variations are

([16]) G. Alexander and R. H. W. Johnston: *Nuovo Cimento*, **5**, 363 (1957).

negligible,

$$\sigma_W^2 = (S)_S^2 + (S)_T^2 , \tag{12}$$

for both blob densities and integral gap lengths. Since we have obtained prior estimates of $(S)_S^2$, we now have values of $(S_n)_T^2$ and $(S_x)_T^2$ with which to compare those values which can be predicted using the Blatt theory.

It is seen in Table IV that final agreement with the Blatt estimates is good. We may reasonably conclude, therefore, that our assumption regarding small-scale (100 μm) emulsion effects was justified, i.e. emulsion variations over 100 μm were found to be small compared to the intrinsic track fluctuations.

7. – Experimental implications.

The measurements in this G5 emulsion of low minimum grain density have shown that for measurements of along-the-track parameters the Blatt fluctuation theory allowed reliable estimates of those errors which arose from the intrinsic fluctuations in the track itself.

However, as is apparent from comparison of the overall and track standard deviations listed in Table IV, one has considerable additional errors in most experimental work. These errors may arise from subjective, instrument, emulsion or person-to-person fluctuations. The magnitude of these errors will vary with the circumstances. The measurements outlined in this paper were carried out with near-ideal conditions viz. *a*) with very long, flat tracks, *b*) with very good illumination and ×1600 magnification, *c*) on a Koristka microscope, *d*) with a measured normal distribution in the setting errors, *e*) reasonably uniform emulsion (as shown by α-particle grain-density measurements) and *f*) by only one observer.

Accordingly it is probable that the measured values of the subjective variances and, to a lesser extent, the emulsion variances, which were given above, will be less than those in any comparable experiment. Indeed, they may prove to be considerably less.

For any portion of a track in a G5 emulsion where the crystals grow during development by a factor less than two the appropriate value of p, the probability of development, may be found to a rough approximation by use of Fig. 1, and by measurement of the mean gap width. One can then find from Fig. 2 the corresponding values of μ_x^2 and μ_n for this track, and these values will place a limit upon the accuracy of any measurement on this track.

Thus, if one measures n blobs and L μm of gap along this track, the errors in these measurements are *at least* $\mu_n\sqrt{n}$ and $\mu_x\sqrt{L}$ respectively, where μ_n and μ_x can be obtained from Fig. 2. If the growth factor is greater than two, corresponding curves may be drawn as mentioned in Sect. 5 above.

Errors arising from other causes—subjective and emulsion—should be estimated in each experiment. The subjective error and person-to-person errors may be readily obtained by repeat measurements on a suitable track over a suitable time interval. The emulsion errors are more difficult to obtain, but some estimate should be made. In the experiment outlined in this paper, emulsion variations over 1 mm intervals within a length of 1 cm in one plate were found to be comparable with the intrinsic variations in each track.

In general experiments, the region of fluctuation study should be extended to cover all sections of emulsion in which measurements are made.

For steeply-dipping tracks, where the smallest gaps will be obscured by the track itself, it is probable that the fluctuation theory will be useless unless the value of r (the minimum gap size) is increased until obscuration is negligible.

Finally, as regards the very clogged tracks such as that of the iron nucleus in this experiment, the great density of δ rays curling around and along the track will add further difficulties and fluctuations to any set of measurements. The fluctuations may be estimated by direct measurements in the manner outlined previously, and the integral gap length should be used in the application of the Herz-Davis model, since obscuration of zero-order gaps will make the mean gap width an unreliable parameter.

8. – Conclusions and recommendations.

The work reported in this paper has shown that the Blatt fluctuation theory may be used to estimate the intrinsic fluctuations of along-the-track parameters. This investigation has shown also that other sources of fluctuation may prove comparable with the Blatt fluctuations.

The methods of general experimental application of the Blatt theory and of the track-analysis techniques which were given are such that in any experiment an estimate may be made of the accuracy of a measurement of an along-the-track parameter.

If the exact value of the error of any measurement is a matter of importance it will not be sufficient to assume that this error is equal to or less than the Poissonian error. The error itself should be measured in the manner described using the Blatt theory and the Herz-Davis model for the particular emulsion. Alternatively, of course, the errors may be estimated empirically from the spread in measurements of calibration tracks.

If only a rough estimate is required, the Poissonian errors may be adequate.

* * *

The author wishes to acknowledge with thanks the interest and helpful discussions of Drs. B. A. Chartres, A. J. Herz and J. H. Noon, and Mr. C. S.

WALLACE, who have done much to relieve the tedium of the measurements.

Thanks are also due to Professor H. MESSEL and the Nuclear Research Foundation for providing the excellent research facilities, and to the Research Committee within the University of Sydney and the Atomic Energy Commission for providing a Research Studentship.

RIASSUNTO (*)

In una emulsione G5 di bassa densità minima di granuli si sono studiate le fluttuazioni dei parametri di traccia per mezzo di misure di densità dei blob e della intera lunghezza di gap di lunghe tracce di nuclei pesanti relativistici. Le variazioni intrinseche derivanti dalla natura statistica del processo di formazione della traccia furono trovate in buon accordo con quelle predette dalla teoria delle fluttuazioni di Blatt. Variazioni soggettive inerenti all'emulsione ed altre variazioni furono in alcuni casi trovate confrontabili alle variazioni intrinseche. Si dà un metodo per la valutazione di questi effetti di fluttuazione in qualsiasi serie di misure sperimentali.

(*) *Traduzione a cura della Redazione.*

IL NUOVO CIMENTO Vol. VII, N. 2 16 Gennaio 1958

Interactions and Decays of K^--Mesons.

E. Lohrmann (*), M. Nikolić (+), M. Schneeberger,
P. Waloschek (×) and H. Winzeler
Physikalisches Institut der Universität - Bern

(ricevuto il 18 Settembre 1957)

Summary. — Results on interactions in flight, elastic scatterings and decays of K^- mesons in nuclear emulsion in the energy interval between 5 and 130 MeV are given. A total K^--path of 112 m was followed. 11 K^--proton elastic scatterings and 5 K^--(free) proton absorptions were found. The differential cross-section for elastic scatterings by complex nuclei for the two average energies of 45 and 100 MeV are listed. The mean free path for star production in the energy interval from 20 to 130 MeV is (27.7 ± 1.4) cm. The secondary tracks of the stars were, as far as possible, identified. 3 K^- reemissions were observed. Finally the K^--lifetime and some identified decays are discussed. From one of the two τ^--mesons observed we got a mass value of $(966.0 \pm 1.8)\, m_e$. One possible example of the $K_{\pi 2}$-decay mode was found.

1. – Experimental procedure.

A stack of 150 stripped emulsions, Ilford G-5, 6 in. × 7 in. × 600 μm, was exposed to the not enriched Berkeley K^--beam of approximately 435 MeV/c momentum. During the exposure the paper layers between the emulsions had been removed; the original thickness of all emulsions had been measured at this time (†).

(*) Also from the Istitut für Kernphysik, Frankfurt - Main.

(+) On leave of absence from Istitute for Nuclear Sciences, Boris Kidrich, Belgrade.

(×) On leave of absence from the Argentine Comision Nacional de la Energía Atómica, now at the Istituto di Fisica dell'Università di Bologna, Italy.

(†) The whole exposure and also the thickness measurements were done for us in Berkeley by Drs. L. Jauneau and M. Teucher.

The « scanning along the track » method was used. The mean kinetic energy of the K^--mesons at the pickup was 130 MeV. Their tracks were selected by the usual angular and grain-density criteria. A total track length of 112 m was followed. This corresponds to about 1600 K^--mesons.

The events found were at first roughly classified in the following way:

1) K^--capture stars at rest, 978 events.

2) Tracks leading to class 1) making single deflections $> 5°$, 244 events.

3) Interactions in flight, including K^--proton collisions and « stops », which are suddenly disappearing tracks with no visible secondaries, 404 events (*).

4) « Decays », comprising real decays and stars in flight having only one thin prong, 49 events.

5) Tracks produced by particles coming to rest without leading to any visible interaction.

The number of real K^--interactions given in class 3) was determined by tracing back each primary of this class from the pickup to the point of entering of the beam into the stack. By this manner the proton contamination from nuclear collisions inside the stack was eliminated. Further on, by following back a sample of sure proton tracks, we could estimate the small ratio of entering protons to protons from inside the stack. With this ratio the number of entering protons which cause interactions of the class 3) became 43. It is already subtracted in class 3).

With respect to class 5) we did not apply the same « cleaning »-procedure, since the fraction of $K^- - \varrho$'s is already well known and is according to reference (1) and reference (2) about 15% of class 1). This information enabled us to evaluate the total K^--track-length scanned.

2. – K^--proton-interactions in flight.

In Fig. 1 the K^--path scanned is shown as a function of the kinetic energy. The energy interval considered ranged essentially from 5 to 130 MeV. On this track length we have found 11 K^--proton scatterings and 5 K^--proton absorptions in flight giving rise to charged hyperons and π-mesons. The cor-

(*) The present paper contains a first analysis of the experimental data. More detailed work is in progress.

(1) W. ALLES, N. N. BISWAS, M. CECCARELLI and J. CRUSSARD: Preprint, 1957.

(2) W. H. BARKAS, W. F. DUDZIAK, P. C. GILES, H. H. HECKMANN, F. W. INMAN, C. J. MASON, N. A. NICKOLS and F. M. SMITH: *Phys. Rev.*, **105**, 1417 (1957).

responding kinetic energy for these events is also marked in Fig. 1. The details of the events are given in Tables I and II.

TABLE I. – K *-proton collisions*; χ *is the scattering angle of the* K *in the center of mass system.*

T (MeV)	41	114	23	58	95	135	81	122	26	122	64
χ^0	100	28	38	123	123	74	95	126	106	41	82

TABLE II. – K^-*-proton absorptions.* χ *is the angle between the* K^-*- and the* π*-direction of flight in the center of mass system.*

T (MeV)	20	30	110	55	101
χ^0	60	66	47	112	106
Products	$\Sigma^+ \to \pi^+$	$\Sigma^- \to \rho^{\prime\prime}$	$\Sigma^+ \to p$	$\Sigma^- \to$ blob	$\Sigma^\pm \to \pi^\pm$

Adding our data to those collected at the Rochester Conference 1957 (about 60 scatterings and 11 absorptions) we got the angular distribution shown in Fig. 2). It remains fairly isotropic. The cross-section for K^--proton scattering seems to decrease slightly with increasing energy. The cross-section in the energy interval from 5 to 130 MeV is (46 ± 6) mb; it is (60^{+11}_{-9}) mb in the interval from 5 to 60 MeV and (34^{+8}_{-6}) mb in the interval from 60 to 110 MeV.

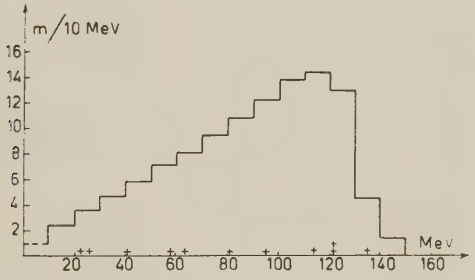

Fig. 1. – K^--path scanned. The crosses indicate the K^--collisions.

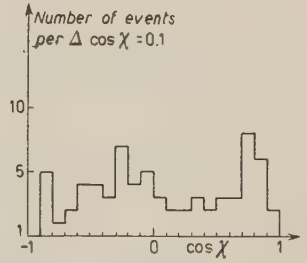

Fig. 2. – K^--proton scattering angular distribution in CMS.

3. – Elastic scatterings by complex nuclei.

While all deflections having a projected angle $\geqslant 5°$ were noted, only those with a projected angle $\geqslant 7°$ were used for the final analysis. Furthermore, to be sure of the identity and energy of the particles only those tracks, which

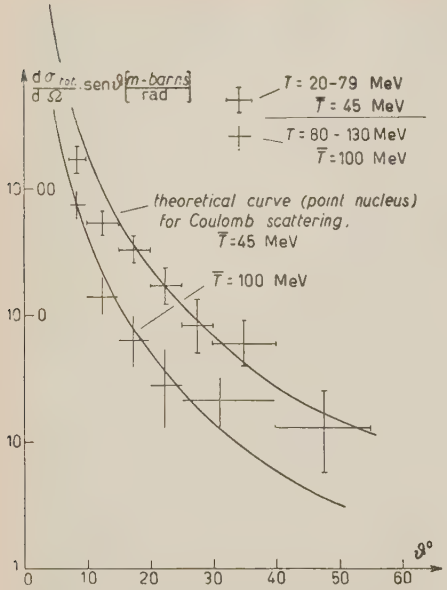

Fig. 3. – Elastic scattering.

led to capture stars at rest were considered. The corresponding total observed path was 79 m.

The range distribution of the scattered K-mesons agreed with the distribution of those which had not sufferend a deflection $\geqslant 5°$. Especially there was no asymmetry in the range distribution of the scattered mesons, i.e. no low energy «tail», within the limits of the statistical accuracy, neither for low- nor for high-energy scatterings. We may thus conclude that the scatterings considered are essentially elastic.

Fig. 3 shows the angular distribution of the scatterings for two energy intervals, having the mean energies of 45 and 100 MeV. For comparison we have also drawn in the theoretical curves for pure Coulomb scattering according to the Rutherford formula. No deflections $> 55°$ were observed in the energy interval from (20 to 130) MeV.

4·1. – Interactions in flight.

These events comprise absorptions, charge exchanges and inelastic scatterings of K-mesons with complex nuclei. 34 stops and 9 stars with one thin prong only, are included in these statistics. (This point is discussed in the section on the decays.) The mean free path for star production so defined, as a function of energy, is shown in Fig. 4. Its average value is (27.7 ± 1.4) cm.

We were able to investigate 95% of the prongs of these stars. Table III gives the number of identified K^--mesons, hyperons, π-mesons and hyperfragments emerging from them.

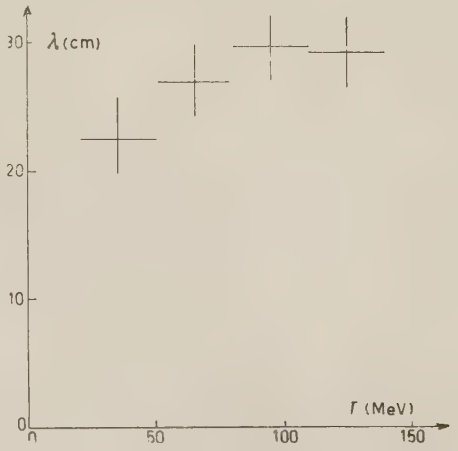

Fig. 4. – Mean free path for star production.

TABLE III. – *Particles emerging from 395 stars in flight.*

	Number	% per star
$\pi^{\pm}$ mesons	81	20
$\Sigma^{+} \rightarrow$ p at rest	3	0.9
$\Sigma^{+} \rightarrow \pi$ at rest	2	0.6
$\Sigma^{+} \rightarrow$ p in flight	2	0.6
Σ^{-} at rest, star	10	2.9
Σ^{-} at rest, blob	6	1.7
$\Sigma^{\pm} \rightarrow \pi^{+}$ in flight	15	4.2
Secondary tracks which are « stops »	10	2.9
K^{-}-reemissions	3	0.9
Hyperfragments	2	0.6
Not identified (short π's, K's hyperfragments, hyperons)	25	

4·2. – Inelastic scatterings of K^{-}-mesons.

In 3 cases of these 395 stars in flight the K^{-}-meson was found to be reemitted. The details are shown in Table IV. Each primary energy was determined by mean gap-length measurements.

The last two events probably happened on light elements. One has to

TABLE IV. – K^{-}-*reemissions.*

Primary energy T_1 (MeV)	Secondary energy T_2 (MeV)	$\Delta T/T_1$	« Scattering » angle	Number of prongs besides the reemitted K^{-}
45	29	0.40	149°	0
73	46	0.37	13°	3
87	48	0.45	25°	3

keep in mind that here possibly inelastic scatterings with small reemission energies are lost, in which the K^--absorption at rest could not be identified with certainty. On the other hand there may be a bias with respect to the cases of small energy loss which neither led to a visibile star nor were recognized by a change in grain density so that they have been classified amongst the 244 single deflections. Nevertheless the reemission probability of K^--mesons is low. This was already discussed in reference [1]. According to our data the probability of reemission is of the order of 1%. In the energy interval (90÷150) MeV (53% of the total track length) no inelastic scattering events were found.

5. – Decays in flight.

5·1. *The lifetime of the* K^-. – We observed 47 events in flight where the K-track gave rise to only one thin track. These could represent decays or one prong stars. Furthermore, we had 36 stops, i.e. sudden disappearings of K-tracks, with no visible secondary track. Amongst these there might be also some few decays and one prong stars, the thin secondary tracks of which we had lost. The rest of real « zero prong events » consists of zero prong nuclear interactions, K^--proton charge exchange scatterings and K^--proton absorptions with emission of neutral hyperons and π's.

Before we go on to discuss reasonable values for the mean life-time and for the remaining fraction of nuclear interactions, we will set a lower limit for the lifetime, assuming all one-thin- and zero-prong events to belong to decays. Disregarding events lying within a distance of 20 μm from the surface or the glass, leaving off the last 300 μm of rest-range in calculating the corresponding time of flight and adding one τ^--meson (one other τ^--meson was cut-off) we got

$$\tau_{K^-} > (0.75 \pm 0.09) \cdot 10^{-8} \text{ s} .$$

This value evidently is a lower limit.

In order to get a reasonable value for the lifetime we chose the following way. First we estimated our « loss » by examining the zero prong events at least 3 times carefully by different observers, with the result that only 3 one prong events were discovered amongst stops in addition to the 44 one prong events seen at first. This indicates the « loss » to be small. On the other hand there may be a certain number of thin tracks which could not be seen by any observer at all. To get an estimate for this, we examined 64 μ-e decays. In 61 cases the electron track could be observed (*).

(*) Naturally the situation with the μ-e decays at rest is not exactly the same as with the K decays in flight because the rest-points are known within the limits of 1 μm, but the comparison should be well applicable within the large limits of the statistical, accuracy.

With the assumption that about 5% of the stops are in fact overlooked one prong events, separating 9 one prong stars which were connected with an apparent blob or an electron (*) and adding the τ^--decay, we get the following result:

42 decays
9 one-thin-prong- and
34 zero-prong stars.

Thus our estimate for the K^--lifetime is

$$\tau_{K^-} = (1.5 \pm 0.3) \cdot 10^{-8} \text{ s} .$$

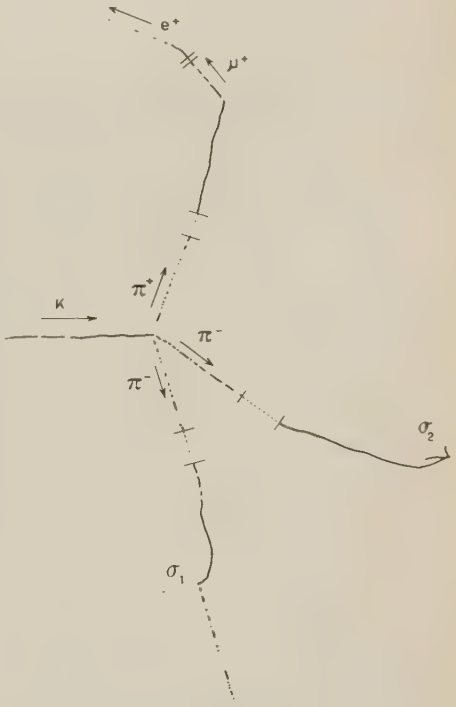

Fig. 5. – τ^--event from which a mass value of $(966.0 \pm 1.8)\, m_e$ was obtained.

5·2. *Decay modes.* – Two examples of negative τ-decays were found. In one of these cases the kinetic energy of the τ at the point of decay was only 4.6 MeV, belonging to a rest-range of 230 μm. The event is shown in Fig. 5. All the π-mesons could be followed and identified. Since in addition to the small kinetic energy of the τ, the plane of decay in the center-of-mass system was nearly perpendicular to the direction of flight, we got an accurate value of the mass of the τ^- (+). We found $Q = 75.1$ MeV; the mass is

$$m_\tau = (966.0 \pm 1.8)\, m_e .$$

From the events with one thin prong we selected 2 favorable cases with no blob, where the thin track was flat and going in the backward direction, and followed them. Both tracks belonged to π^--mesons producing σ-stars. The

(*) This seems to be justified, since among 80 single deflections we found only 4 which were connected with a blob. The 9 events would also agree reasonably with the prong distribution of the observed stars.

(+) The range energy tables of BARKAS were used. W. H. BARKAS- *UCRL*, 3769 (1957). The errors include those arising from the straggling in range and emulsion thickness and the inaccuracy connected with angular determinations. A calibration with 100 π-μ-decays was done and is also included. $m_\pi = 273.0\, m_e$.

kinematics of one of these events is well compatible with the $K_{\pi 2}$ decay mode. The kinetic energy of the charged π in the center-of-mass system would be (108 ± 3) MeV.

* * *

We are very grateful to Drs. L. JAUNEAU, E. J. LOFGREN and M. TEUCHER who arranged the exposure. Without their co-operation this work would not have been possible.

We are also indebted to Profs. F. G. HOUTERMANS, Ch. PEYROU and E. SCHOPPER for their continuous interest in this investigation, to Prof. M. C. CECCARELLI for helpful discussions, and to the scanning team of Bern for their efficient work. Mrs. B. ALBRECHT made some precise measurements for us. Our further thanks are due to the Schweizer Nationalfonds for financial help, one of us (E.L.) is indebted to the Deutsche Forschungsgemeinschaft and P. W. thanks very much Prof. F. G. HOUTERMANS for the kind hospitality in his Institute.

RIASSUNTO (*)

Si danno risultati su interazioni in volo, scattering elastici e decadimenti di mesoni K in emulsioni nucleari nell'intervallo di energia tra 5 e 130 MeV. Sono state seguite in totale tracce di K^- per 112 m. Si trovarono 11 scattering elastici K^--protone e 5 assorbimenti di K^- (liberi) in protoni. Si elencano le sezioni d'urto differenziali per gli scattering elastici su nuclei complessi alle due energie medie di 45 e 100 MeV. Il cammino libero medio per la produzione di stelle nell'intervallo di energie da 20 a 130 MeV è (27.7 ± 1.4) cm. Furono, per quanto possibile, identificate le tracce secondarie delle stelle. Si osservarono 3 riemissioni di K^-. Si discutono finalmente la vita media dei K e alcuni decadimenti identificati. Da uno dei due mesoni τ osservati abbiamo ottenuto per la massa un valore di $(966.0 \pm 1.8)\, m_e$. È stato trovato un possibile esempio del modo di decadimento $K_{\pi 2}$.

(*) *Traduzione a cura della Redazione.*

IL NUOVO CIMENTO Vol. VII, N. 2 16 Gennaio 1958

On the Pursey-Pauli Invariants in the Theory of Beta Decay (*).

G. Lüders (+)

Radiation Laboratory, University of California - Berkeley, Cal.

(ricevuto il 24 Settembre 1957)

Summary. — The assumption of a vanishing neutrino mass leads to a group of transformations on the neutrino field which transform the β-decay interaction into equivalent interactions. By physical observations one cannot distinguish between equivalent interactions. The results of observations can be expressed in terms of nuclear matrix elements and combinations of the coupling constants which are invariant under the group. These invariants have recently been put forward by Pursey and on a more general basis by Pauli. They are explored further in this paper. Their mathematics is studied and relations between them are established. The conditions for invariance with respect to reflections in space, charge conjugation, and time reversal are expressed in terms of these invariants. Interactions which conserve lepton charge and/or couple to only two components of the neutrino field are characterized by relations between the invariants. (For a reader who does not want to follow the detailed arguments the main results are summarized in the last section.) In the Appendix possible experiments on β-decay are expressed in terms of the invariants.

1. – As recently shown by Pauli [1] the assumption that the mass of the neutrino is exactly equal to zero leads to a group of linear transformations of the neutrino field operators which leave both commutation relations and free field Hamiltonian invariant. This group is generated by the following

(*) This work was performed under the auspices of the U. S. Atomic Energy Commission.

(+) Fulbright Grantee on leave of absence from Max-Planck-Institut für Physik, Göttigen, Germany.

(1) W. Pauli: *Nuovo Cimento*, **6**, 204 (1957). We shall use the symbol LC when referring to this paper.

two commuting subgroups

$$\psi' = a\psi + b\gamma_5 C^{-1}\bar{\psi}\,; \qquad \bar{\psi}' = a^*\,\bar{\psi} + b^*\psi C\gamma_5\,, \tag{1}$$

with

$$|a|^2 + |b|^2 = 1 \tag{2}$$

(transformation (I) in LC) and ([2])

$$\psi' = \exp[i\alpha\gamma_5]\psi\,; \qquad \bar{\psi}' = \bar{\psi}\exp[i\alpha\gamma_5]\,, \tag{3}$$

with α real (transformation (II) in LC) ([3]). The symbol C in Eq. (1) denotes the 4×4 charge conjugation matrix ([4]). Throughout this paper the conventional four-component theory of the neutrino shall be used; the two-component theory can be treated as a special case in which only one half of the degrees of freedom of the neutrino appears in the interaction Hamiltonian (cf. Sect.6). The existence of especially transformation (I) shows that the concept of particles versus antiparticles is note well defined for free neutrinos. For each momentum and spin parallel or antiparallel to the momentum, there are two linearly independent states of the neutrino; but it is not clear which particular linear combination of these states has to be used to define the neutrino (in the conventional sense) or the antineutrino. Therefore the concept of antineutrino shall be avoided in this paper and the word neutrino shall be used for the whole physical entity described by the four-component spinor.

Pauli's discussion of β-decay is based upon the interaction Hamiltonian

$$H_{\text{int}} = \sum_{i=1}^{5} (\bar{\psi}_N O_i \psi_P)[g_{\text{I},i}(\bar{\psi}_\nu O_i \psi_e) - f_{\text{I},i}(\bar{\psi}_\nu \gamma_5 O_i \psi_e) + \\ + g_{\text{II},i}(\psi_\nu C O_i \psi_e) + f_{\text{II},i}(\psi_\nu C\gamma_5 O_i \psi_e)] + \text{herm. conj.} \tag{4}$$

(LC, Eq. (1)) where local interaction is assumed but neither parity conservation nor conservation of lepton charge in the conventional sense. An application of the transformations of the neutrino field does not leave the inter-

([2]) Transformation (II) was often used in the literature. It forms the basis of a discussion by D. L. PURSEY: *Nuovo Cimento*, 6, 266 (1957).

([3]) In the following we shall refer to these two transformations by (I) and (II) as done in LC.

([4]) We use the definition given in LC. The present author used a slightly different definition in a recent paper (*Ann. of Phys.*, 2, 1 (1957)). The relation between these two definitions is $C_{\text{Pauli}} = -C^{-1}_{\text{Lüders}}$

action Hamiltonian invariant but rather can be expressed as a linear transformation of the four coupling constants carrying the same subscript i, i.e., referring to the same type of coupling. PAULI indicates that physical results are not affected by such a transformation (cf. also Sect. 2) and, therefore, can depend only upon invariant combinations of the coupling constants. A complete list of these invariants is given by

$$K_{ij} = K_{ji}^* = g_{\mathrm{I}i}^* g_{\mathrm{I}j} + f_{\mathrm{I}i}^* f_{\mathrm{I}j} + g_{\mathrm{II}i}^* g_{\mathrm{II}j} + f_{\mathrm{II}i}^* f_{\mathrm{II}j} , \tag{5}$$

$$L_{ij} = L_{ji}^* = g_{\mathrm{I}i}^* f_{\mathrm{I}j} + f_{\mathrm{I}i}^* g_{\mathrm{I}j} - g_{\mathrm{II}i}^* f_{\mathrm{II}j} - f_{\mathrm{II}i}^* f_{\mathrm{II}j} , \tag{6}$$

$$I_{ij} = I_{ji} = g_{\mathrm{I}i} g_{\mathrm{II}j} + g_{\mathrm{II}i} g_{\mathrm{I}j} + f_{\mathrm{I}i} f_{\mathrm{II}j} + f_{\mathrm{II}i} f_{\mathrm{I}j} , \tag{7}$$

$$J_{ij} = J_{ji} = g_{\mathrm{I}i} f_{\mathrm{II}j} - f_{\mathrm{II}i} g_{\mathrm{I}j} + f_{\mathrm{I}i} g_{\mathrm{II}j} - g_{\mathrm{II}i} f_{\mathrm{I}j} . \tag{8}$$

We mention that K_{ii} and L_{ii} are both real and that

$$K_{ii} \geqslant 0 ; \qquad -K_{ii} \leqslant L_{ii} \leqslant +K_{ii} . \tag{9}$$

The sign of equality in the first equation only holds if that particular type of interaction does not appear at all in the Hamiltonian.

The general structure of these invariants is better understood when one looks at three special transformations contained in the group:

a) Phase transformation of the neutrino field (transformation (I) with $b = 0$). This transformation amounts to multiplying coupling constants with subscript I by some phase factor and multiplying those with subscript II by the complex conjugate phase factor. Consequently there appear in the invariants either products of coupling constants and complex conjugate coupling constants carrying the same Roman subscript (K_{ij} and L_{ij}) or products of two coupling constants carrying different Roman indices (I_{ij} and J_{ij}).

b) Charge conjugation of the neutrino field (apply first (I) with $a = 0$, $b = -i$ and subsequently (II) with $\alpha = \pi/2$). This transformation essentially (i.e., apart from signs) leads to an exchange of coupling constants with subscripts I and II. So these couplings have to appear in an essentially symmetrical manner.

c) Multiplication of ψ_ν by γ_5. This case has been discussed already in LC. As a consequence the constants f and g enter in an essentially symmetrical way (5).

(5) These considerations could in fact be used for a systematic construction of the invariants starting from any product of coupling constants. C. P. ENZ: *Nuovo Cimento*.

The invariants K_{ij} and L_{ij} on the one hand and I_{ij} and J_{ij} on the other hand are not quite on the same footing since the neutron, proton, and electron fields can be multiplied by an arbitrary phase factor without changing any physical results. If this transformation again is expressed as a transformation of the coupling constants, K_{ij} and L_{ij} still stay invariant whereas I_{ij} and J_{ij} take up the same phase factor. So physical results must be expressable in terms of K_{ij}, L_{ij} and the combinations $I_{ji}I^*_{lm}$, $I_{ij}J^*_{lm}$, $J_{ij}J^*_{lm}$.

In LC also relative invariants are given, i.e., expressions whic hremain invariant under (I) but take up a phase factor under (II). If one, however, forms strictly invariant combinations, e.g., $N_{\mathrm{I},ij}N_{\mathrm{II},lm}$ ([6]), one sees that they can be expressed in terms of bilinear combinations of the original invariants. This is a consequence of the completeness of the bilinear invariants (cf. Sect. **3**).

The whole physics of β-decay including all double processes can be expressed in terms of the invariants (5) through (8). Particularly, ordinary β-decay depends only on the invariants K_{ij} and L_{ij} (and, of course, the nuclear matrix elements). Double β-decay can be expressed in terms of I_{ij} and J_{ji} (or rather their fully invariant combinations). The chain β-decay-inverse β-decay depends either on I_{ij} and J_{ij} or on K_{ij} and L_{ij} depending on whether the charge of the electron emitted in the two processes is the same or opposite. These statements are true in the lowest non-vanishing order. Practically uninteresting higher order terms might depend on all four types of invariants. *We believe that these invariants are not only of theoretical interest but that they also might represent an effective tool for the analysis of experimental data* ([7]). Therefore we explored these invariants beyond the analysis given by PURSEY and PAULI in their papers.

2. – It has already been shown by PAULI that states which contain neutrons, protons, and electrons but no neutrinos are not affected by the group of transformations. But the same holds with slight modifications for final states which do contain neutrinos. If the neutrinos are not absorbed, e.g., in some subsequent inverse β-decay, they escape essentially unobserved. The most one can hope to measure is their linear momentum (in the case of only one neutrino

---

6, 250 (1957), treated the case of double processes with non-vanishing neutrino mass. The bilinear combinations of coupling constants which in the results appear multiplied by m_ν can be constructed in a similar manner if one observes that a neutrino with non-vanishing rest mass still admits the group generated by phase transformations, charge conjugation, and γ_5 multiplication combined with the substitution $m_\nu \to -m_\nu$. The latter transformation was used in a different context by D. C. PEASLEE: *Phys. Rev.*, **91**, 1447 (1953).

([6]) For the notation see LC, Eqs. (18*a*) and (18*b*).

([7]) Cf. the Appendix to this paper.

from momentum conservation) and perhaps the component of the spin parallel to the momentum. Therefore in all statements of physical significance one has to sum over internal degrees of freedom of the neutrino. Such a situation can be expressed by formulating the final situation in terms, not of a state vector, but of a projection operator (density matrix).

For this purpose the neutrino operator shall be decomposed in the usual way in terms of plane waves

$$\psi_\sigma(\boldsymbol{r}) = \frac{1}{\sqrt{V}} \sum_{\boldsymbol{p},\lambda} (a_{\boldsymbol{p}\lambda} u_{\boldsymbol{p}\sigma}{}^{\lambda} e^{i\boldsymbol{p}\cdot\boldsymbol{r}} + b^*_{\boldsymbol{p}\lambda} v_{-\boldsymbol{p}\sigma}{}^{\lambda} e^{-i\boldsymbol{p}\cdot\boldsymbol{r}}) \,. \tag{10}$$

$u_{\boldsymbol{p}\sigma}{}^{\lambda}$ ($\lambda = 1, 2$) are, for fixed $\boldsymbol{p}$, a pair or orthonormal four-spinors ([8,9]) obeying

$$(\boldsymbol{\gamma}\cdot\boldsymbol{e} + i\gamma_4)_{\varrho\sigma} u_{\boldsymbol{p}\sigma}{}^{\lambda} = 0 \,, \tag{11}$$

where $\boldsymbol{e}$ is the three dimensional unit vector in the direction of motion. In the same way one has ([10])

$$(\boldsymbol{\gamma}\cdot\boldsymbol{e} + i\gamma_4)_{\varrho\sigma} v_{-\boldsymbol{p}\sigma}{}^{\lambda} = 0 \,. \tag{12}$$

On the one hand $a_{\boldsymbol{p}\lambda}$, $b_{\boldsymbol{p}\lambda}$ and $a^*_{\boldsymbol{p}\lambda}$, $b^*_{\boldsymbol{p}\lambda}$ on the other hand are the well known annihilation and creation operators for neutrinos of momentum $\boldsymbol{p}$. For the present discussion it is advisable to relate the spinors $u_{\boldsymbol{p}}{}^{\lambda}$ and $v_{-\boldsymbol{p}}{}^{\lambda}$ in the following manner,

$$v_{-\boldsymbol{p}}{}^{\lambda} = \gamma_5\gamma_4 C^{-1}(u_{\boldsymbol{p}}{}^{\lambda})^* \,. \tag{13}$$

This correspondence is compatible with the Dirac equations (11) and (12) and conserves orthonormality. If the spinors are eigenstates of the spin component in the direction of motion, Eq. (12) relates spinors of equal eigenvalue ([11]). Once this correspondence has been established the creation operators transform under (I) in the following way

$$a'^*_{\boldsymbol{p}\lambda} = a^* a^*_{\boldsymbol{p}\lambda} + b^* b^*_{\boldsymbol{p}\lambda} \,; \qquad b'^*_{\boldsymbol{p}\lambda} = -\, b a^*_{\boldsymbol{p}\lambda} + a b^*_{\boldsymbol{p}\lambda} \,. \tag{14}$$

([8]) The normalization is $a^*_{\boldsymbol{p}\lambda} a_{\boldsymbol{p}\mu} = \delta_{\lambda\mu}$ etc. A covariant normalization (using $\bar{a}_{\boldsymbol{p}\lambda} a_{\boldsymbol{p}\mu}$) is not possible for mass zero.

([9]) The spinors $u_{\boldsymbol{p}}{}^{\lambda}$ and $v_{-\boldsymbol{p}}{}^{\lambda}$ actually do not depend upon the magnitude of the momentum vector $\boldsymbol{p}$ but only on its direction, the unit vector $\boldsymbol{e}$.

([10]) Notice that because of the absence of a mass term there is no real difference between spinors of positive and negative energy.

([11]) This follows without calculation from the observation that relation (13) does not depend upon any space direction apart from $\boldsymbol{e}$.

Transformation (II) on the other hand leads to a multiplication of each creation operator separately by a phase factor if the spinors have been chosen as eigenstates of the spin component in the direction of motion.

Now we can take up the discussion of projection operators. For the sake of simplicity this discussion shall be limited to final states containing only one neutrino. Let $|\rangle$ be a state of the system which is different from this final state only by the absence of the neutrino and $a^*_{p\lambda}|\rangle$ as well as $b^*_{p\lambda}|\rangle$ be the neutrino containing states which actually appear as final states. Let

$$P = |\rangle\langle| \tag{15}$$

be the projection operator corresponding to $|\rangle$. The projection operator for the states with neutrino, summed over the internal degrees of freedom of the neutrino, is then given by

$$P_{p\lambda} = a^*_{p\lambda} P a_{p\lambda} + b^*_{p\lambda} P b_{p\lambda} . \tag{16}$$

Here we assume that the neutrino states correspond to a particular spin component in the direction of the momentum. In most cases one will have to sum over $\lambda\,(=1, 2)$. Now it is easily seen that this projection operator is indeed invariant under the transformation (14) (which corresponds to transformation (I)) and of course also under a multiplication of the creation operators by phase factors (corresponding to transformation (II)) [12] .

Neutrinos in initial states cannot be treated in an analogous way. One rather has to include their production mechanism in the physical process.

These considerations show that interaction Hamiltonians which can be transformed into each other by a combination of the transformations (I) *and* (II) *lead to the same physical conclusions.* Within the framework of β-decay there is no possibility of distinguishing between them. Such Hamiltonians shall be called equivalent. The invariants (5) through (8) are the same for equivalent Hamiltonians. In the following section we shall show that if two interaction Hamiltonians lead to the same values for the invariants then there is one and generally only one transformation of the group which transforms these Hamiltonians into each other. So equality of the invariants is a necessary and sufficient condition for the equivalence of interaction Hamiltonians. We shall also show that these invariants form a complete set but are not entirely independent.

---

[12] In the second case a simpler proof can be given in terms of the Casimir projection operator in spinor space. One only has to check that

$$\exp\,[i\alpha\gamma_5](\boldsymbol{\gamma}\cdot\boldsymbol{e} + i\gamma_4)\,\exp\,[i\alpha\gamma_5] = (\boldsymbol{\gamma}\cdot\boldsymbol{e} + i\gamma_4) .$$

3. – For discussions of a more mathematical character [13] the coupling constants g_{I}, g_{II}, f_{I}, f_{II} are less practical than the following linear combinations [14]

$$(17)\quad F_1 = g_{\mathrm{I}} - f_{\mathrm{I}}\,, \qquad G_1 = g_{\mathrm{I}} + f_{\mathrm{I}}\,, \qquad F_2 = g_{\mathrm{II}} + f_{\mathrm{II}}\,, \qquad G_2 = -\,g_{\mathrm{II}} + f_{\mathrm{II}}\,;$$

here the subscript i referring to the type of coupling has been omitted. If one further introduces

$$(18)\qquad H_1 = G_2^*\,, \qquad H_2 = -\,G_1^*\,,$$

the transformation of the coupling constants is simply given by [15]

$$(19)\qquad (F_1', F_2') = (F_1, F_2)T\,, \qquad (H_1', H_2') = (H_1, H_2)T\,,$$

with

$$(20)\qquad T = \exp\,[-\,i\alpha]\begin{pmatrix} a & -\,b^* \\ b & a^* \end{pmatrix}.$$

So the pairs F_1, F_2 and H_1, H_2 transform under the same irreducible representation of the group. If one regards $\boldsymbol{F} = (F_1, F_2)$ and $\boldsymbol{H} = (H_1, H_2)$ as vectors in a two-dimensional complex vector space [16] one recognizes that the group generated by transformations (I) and (II) induces a unitary transformation in this space [17].

The invariants under this group of unitary transformations are given by the scalar products

$$(21)\qquad \boldsymbol{A}\cdot\boldsymbol{B} = A_1^* B_1 + A_2^* B_2$$

of pairs of vectors or, more explicitly, by

$$(22)\qquad \boldsymbol{F}_i\cdot\boldsymbol{F}_j\,, \qquad \boldsymbol{H}_i\cdot\boldsymbol{H}_j\,, \qquad \boldsymbol{H}_i\cdot\boldsymbol{F}_j\,,$$

---

[13] The reader not interested in mathematical rigor might very well skip this section. He should however take notice of the inequalities (25), (26) and (27) between the invariants and of the existence of rather complicated identities between them.

[14] LC Eq. (5).

[15] LC Eq. (10).

[16] To avoid misunderstanding we should like to mention that the ordinary complex plane in the sense of this terminology is not a two-dimensional but a one-dimensional complex space.

[17] This incidentally shows that the group of transformations of the neutrino field is isomorphic with the unitary group in two dimensions.

where now the subscripts referring to types of coupling have been written down explicitly. The relation between these invariants and the invariants (5) through (8) is given by

$$(23)\qquad \begin{cases} \boldsymbol{F}_i\cdot\boldsymbol{F}_j = K_{ij} - L_{ij}\,, \qquad \boldsymbol{H}_i\cdot\boldsymbol{H}_j = K_{ij} + L_{ij}\,, \\ \boldsymbol{H}_i\cdot\boldsymbol{F}_j = -I_{ij} - J_{ij} = -I_{ji} + J_{ji}\,. \end{cases}$$

The invariants (22), i.e. (5) through (8), are obviously characteristic for the unitary group in two dimensions and consequently for the group of transformations of the neutrino field ([18]). From the theory of invariants of the unitary group it also follows that all invariant combinations of the coupling constants can be expressed in terms of the basic invariants (22) ([19]); these invariants form a complete set.

At present we are interested in a different question. Provided there are two sets of vectors $\boldsymbol{F}_i$, $\boldsymbol{H}_i$ and $\boldsymbol{F}'_i$, $\boldsymbol{H}'_i$ which lead to the same invariants (22) (or (5) through (8)), does there always exist a transformation of the group which transforms one set into the other? In other words, is equality of all invariants not only a necessary but also a sufficient condition for the equivalence of the two interactions in the sense explained in Sect. 2 (identical values for all physically meaningful quantities)? From simple geometrical considerations, or from the theory of the unitary group, if follows that the answer is indeed in the affirmative. From the equality of the scalar products between corresponding dashed and undashed vectors one concludes that lengths and relative orientations of the two sets of vectors are the same; therefore they can be transformed into each other by a unitary transformation. If there are at least two linearly independent vectors the transformation is determined uniquely.

The scalar products (or invariants) are not all independent. First there are inequalities between them which are a consequence of the Cauchy Schwarz inequality

$$(24)\qquad (\boldsymbol{A}\cdot\boldsymbol{A})(\boldsymbol{B}\cdot\boldsymbol{B}) \geqslant |\boldsymbol{A}\cdot\boldsymbol{B}|^2\,.$$

In terms of the invariants (5) through (8) one finds

$$(25)\qquad (K_{ii} \pm L_{ii})(K_{jj} \pm L_{jj}) \geqslant |K_{ij} \pm L_{ij}|^2\,,$$

$$(26)\qquad (K_{ii} + L_{ii})(K_{jj} - L_{jj}) \geqslant |I_{ij} + J_{ji}|^2\,.$$

([18]) This has already been shown in LC. The author realizes that it is more difficult to establish a mathematical fact than to simplify a proof already given.

([19]) This is especially true for invariant products of the relative invariants (LC, Eq. (18)-(18*b*)).

Inequality (25) is valid both for upper and lower sign. Putting $i = j$ in the second inequality one obtains

$$(K_{ii})^2 \geqslant (L_{ii})^2 + |I_{ii}|^2 , \tag{27}$$

which is a stronger relation than Eq. (9) ([20]).

There are also identities between the invariants which are obtained in the following way. Since the number of dimensions of the complex vector space is equal to two, any three vectors $\boldsymbol{A}$, $\boldsymbol{B}$, $\boldsymbol{C}$ are linearly dependent, i.e. there are numbers λ, μ, ν not all equal to zero so that

$$\lambda \boldsymbol{A} + \mu \boldsymbol{B} + \nu \boldsymbol{C} = 0 . \tag{28}$$

Forming scalar products of this relation with three vectors $\boldsymbol{D}$, $\boldsymbol{E}$, $\boldsymbol{G}$ one obtains three equations which can be regarded as linear equations for λ, μ, ν. The condition for a non-trivial solution is

$$\begin{vmatrix} \boldsymbol{D}\cdot\boldsymbol{A} & \boldsymbol{D}\cdot\boldsymbol{B} & \boldsymbol{D}\cdot\boldsymbol{C} \\ \boldsymbol{E}\cdot\boldsymbol{A} & \boldsymbol{E}\cdot\boldsymbol{B} & \boldsymbol{E}\cdot\boldsymbol{C} \\ \boldsymbol{G}\cdot\boldsymbol{A} & \boldsymbol{G}\cdot\boldsymbol{B} & \boldsymbol{G}\cdot\boldsymbol{C} \end{vmatrix} = 0 . \tag{29}$$

From this general expression one can derive relations between the invariants (5) through (8) but at present it seems not worthwhile to do so. An experimental test of such relations might eventually mean a test of the general ansatz (4) for the interaction.

4. – Since there is no physical distinction between equivalent Hamiltonians the concept of invariance with respect to symmetry operations (especially reflections in space, charge conjugation, and time reversal) is to be modified. One might very well use the usual definitions of these operations ([21]) but it would be unphysical to require that the interaction Hamiltonian is unchanged by such a transformation. One rather has to postulate that the transformed Hamiltonian is equivalent to the original one in the sense of this paper. This means that one only has to study the action of a symmetry operation on the invariants (5) through (8). The conditions that a particular theory is

([20]) It should be noticed that Eq. (9) is *not* a consequence of Eq. (24) but rather follows immediately from Eq. (23) since a scalar product of a vector with itself is a real non-negative quantity.

([21]) Cf. e.g., G. LÜDERS: *Ann. of Phys.*, **2**, 1 (1947). Before application of charge conjugation notice, however, footnote ([3]) of the present paper.

invariant with respect to a symmetry operation have to be expressed entirely in terms of these invariants.

As an example we treat reflections in space in some detail. If one applies the customary parity operation one obtains the following transformation of the coupling constants

$$(30)\qquad \begin{cases} g'_{\mathrm{I}i} = g_{\mathrm{I}i} \exp[i\eta], & g'_{\mathrm{II}i} = -g_{\mathrm{II}i} \exp[i\zeta], \\ f'_{\mathrm{I}i} = -f_{\mathrm{I}i} \exp[i\eta], & f'_{\mathrm{II}i} = f_{\mathrm{II}i} \exp[i\zeta], \end{cases}$$

where $\exp[i\eta]$ and $\exp[i\zeta]$ are arbitrary phase factors. This leads to the following transformation of the invariants

$$(31)\qquad \begin{cases} K'_{ij} = K_{ij}, & L'_{ij} = -L_{ij}, \\ I'_{ij} = -I_{ij} \exp[i(\eta+\zeta)], & J'_{ij} = J_{ij} \exp[i(\eta+\zeta)]. \end{cases}$$

The conditions for invariance with respect to reflections in space (or conservation of parity) are therefore given by ([22])

$$(32)\qquad L_{ij} = 0, \qquad I_{ij} J^*_{kl} = 0.$$

The last condition of course means that either all I_{ij} or all J_{ij} have to vanish. In ordinary β-decay all effects from which a non-conservation of parity can be recognized depend upon the invariants L_{ij}; parity violating effects in double β-decay can be expressed in terms of $I_{ij} J^*_{kl}$.

If one treats the operations of charge conjugation and time reversal in a similar manner one obtains the following conditions ([23]): invariance with respect to charge conjugation:

$$(33)\qquad \mathrm{Im}\, K_{ij} = \mathrm{Re}\, L_{ij} = \mathrm{Re}\, I_{ij} I^*_{kl} = \mathrm{Re}\, I_{ij} J^*_{kl} = \mathrm{Re}\, J_{ij} J^*_{kl} = 0$$

invariance with respect to time reversal:

$$(34)\qquad \mathrm{Im}\, K_{ij} = \mathrm{Im}\, L_{ij} = \mathrm{Re}\, I_{ij} I^*_{kl} = \mathrm{Im}\, I_{ij} J^*_{kl} = \mathrm{Re}\, J_{ij} J^*_{kl} = 0.$$

Incidentally, since the quantities L_{ii} are real, one sees that invariance with respect to charge conjugation requires the vanishing of all L_{ii}. One result of the TCP theorem is immediately recognized from the conditions (32) through (34): from the invariance with respect to any two of these symmetry operations, invariance with respect to all three can be inferred. The condition for inva-

([22]) For the more special case $I_{ij}=J_{ij}=0$ these conditions and the others presented in this section were already given by Pursey, l.c.

([23]) Re = real part, Im = imaginary part.

riance under all three operations is indeed given by

$$\text{Im } K_{ij} = L_{ij} = \text{Re } I_{ij} I^*_{ke} = I_{ij} J^*_{ki} \text{ Re } J_{ij} j^*_{ke} = 0 . \tag{35}$$

5. – The question whether a particular interaction Hamiltonian conserves lepton charge is to be handled in a similar way. One has to analyse whether there is an equivalent Hamiltonian in which all coupling constants with subscript II vanish. One condition on the invariants is easily recognized

$$I_{ij} = J_{ij} = 0 . \tag{36}$$

Since double β-decay depends only on I_{ij} and J_{ij} this condition physically means that there is no double β-decay (and no effect in the chain β-decay–inverse β-decay with the emission of equally charged electrons in both processes).

The other conditions are obtained if one puts all $f_{\text{II},i}$ and $g_{\text{II},i}$ equal to zero in the invariants K_{ij} and L_{ij} ([24]). One gets

$$(K_{ij} \pm L_{ij})(K_{kl} \pm L_{kl}) = (K_{il} \pm L_{il})(K_{kj} \pm L_{kj}) ; \tag{37}$$

the equations are to be postulated both with plus signs and with minus signs. We shall show presently that Eqs. (36) and (37) are not only necessary but also sufficient conditions for the conservation of lepton charge. It is remarkable that Eq. (36) alone constitutes almost a sufficient condition ([25]). If

$$K_{ij} \pm L_{ij} = 0 \tag{38}$$

(with upper and lower sign) does not hold for all combinations of indices then Eq. (37) can be inferred from (36) through the identities (29). If, however, (38) holds, one of the conditions (37) is evidently satisfied but the other has to be postulated ([26]). It should also be mentioned that once the conditions for the conservation of lepton charge are satisfied, all inequalities (24) and identities (29) between the invariants are automatically fulfilled; so no further information can be obtained from them ([27]).

([24]) The derivation of these equations is more easy if one works with the first two invariants (22) putting $F_{2i}=G_{2i}=0$; cf. also Eq. (39). The equations are equivalent to the conditions $N_{\text{I},ij}=N_{\text{II},ij}=0$ in LC.

([25]) The reverse, however, is not true; Eq. (36) cannot be concluded from Eq. (37). Equation (37) also holds if there is no conservation of lepton charge but only two components of the neutrino field are coupled to the other fields (cf. Sect. **6**).

([26]) ENZ, l. c., got hold of such an exceptional case with $K_{SS}+L_{SS}=K_{ST}+L_{ST}=$ $=K_{TT}+L_{TT}=0$.

([27]) Inequality (25) is obviously satisfied with the sign of equality; inequality (26) is fulfilled with vanishing right hand side since both terms on the left hand side are positive (Eq. (9)). In the identity (29) all possible choices of the vectors have to be discussed separately.

We now want to show that conditions (36) and (37) together are sufficient for conservation of lepton charge in the sense that there exists an equivalent interaction Hamiltonian with $f_{\mathrm{II},i} = g_{\mathrm{II},i} = 0$. For this purpose we assume that there is a set of coupling constants $g'_{\mathrm{I},i}$, $g'_{\mathrm{II},i}$ $f'_{\mathrm{I},i}$, $f'_{\mathrm{II},i}$ which leads to invariants fulfilling these relations. Then we ask whether it is possible to choose another set of coupling constants $g_{\mathrm{I},i}$, $f_{\mathrm{I},i}$, to put $g_{\mathrm{II},i} = f_{\mathrm{II},i} = 0$, and still to obtain the same invariants. If Eq. (37) is expressed in terms of the invariants (22) one has

$$(39) \qquad (\boldsymbol{F}_i \cdot \boldsymbol{F}_j)(\boldsymbol{F}_k \cdot \boldsymbol{F}_l) = (\boldsymbol{F}_i \cdot \boldsymbol{F}_l)(\boldsymbol{F}_k \cdot \boldsymbol{F}_j)\,; \qquad (\boldsymbol{H}_j \cdot \boldsymbol{H}_i)(\boldsymbol{H}_l \cdot \boldsymbol{H}_k) = (\boldsymbol{H}_l \cdot \boldsymbol{H}_i)(\boldsymbol{H}_j \cdot \boldsymbol{H}_k)$$

and the question is whether it is possible to choose constants $F_{1,i}$ and $H_{2,i}$ so that

$$(40) \qquad \boldsymbol{F}_i \cdot \boldsymbol{F}_j = F^*_{1i} F_{1j}\,, \qquad \boldsymbol{H}_i \cdot \boldsymbol{H}_j = H^*_{2i} H_{2j}\,.$$

For the general argument it is only necessary to analyse in more detail the invariants $\boldsymbol{F}_i \cdot \boldsymbol{F}_j$. First we put

$$(41) \qquad F_{1j} = \exp[i\alpha_j] \sqrt{\boldsymbol{F}_j \cdot \overline{\boldsymbol{F}_j}}\,,$$

for all j where the phase factors $\exp[i\alpha_j]$ remain to be determined. We can fix one of these phase factors, e.g., $\exp[i\alpha_1]$, ambiguously ([28]) and determine the others from putting

$$(42) \qquad F^*_{11} F_{1j} = \exp[i(\alpha_j - \alpha_1]) \sqrt{(\boldsymbol{F}_1 \cdot \boldsymbol{F}_1)(\boldsymbol{F}_j \cdot \boldsymbol{F}_j)} = \boldsymbol{F}_1 \cdot \boldsymbol{F}_j\,.$$

for all $j \neq 1$. That this is indeed possible follows from (39) with a special choice of indices

$$(43) \qquad |\boldsymbol{F}_1 \cdot \boldsymbol{F}_j|^2 = (\boldsymbol{F}_1 \cdot \boldsymbol{F}_1)(\boldsymbol{F}_j \cdot \boldsymbol{F}_j)\,.$$

The F_{1j} determined in this way also give the correct value for $\boldsymbol{F}_i \cdot \boldsymbol{F}_j$ $(i \neq 1)$ ([29]) since

$$(44) \qquad = \boldsymbol{F}_i \cdot \boldsymbol{F}_j \frac{(\boldsymbol{F}_i \cdot \boldsymbol{F}_1)(\boldsymbol{F}_1 \cdot \boldsymbol{F}_j}{\boldsymbol{F}_1 \cdot \boldsymbol{F}_1}\,.$$

6. – In contrast to PAULI in LC we do not want to treat the two-component theory of the neutrino as a different case for which new invariants have to be formulated. We rather want to work with the full four-component form-

([28]) It is assumed that $\boldsymbol{F}_1 \cdot \boldsymbol{F}_1 \neq 0$.

([29]) This argument shows that not all conditions (37), (39), respectively, are independent.

ulation throughout and to treat the two-component theory as a specialization. This means that we always work with the same invariants (5) through (8) and express experimental information in terms of these invariants only. If one has a two-component neutrino there are identities between the various four-component invariants which one has to test on the experimental data.

The ordinary two-component theory of the neutrino can be written either in the Weyl formulation or in the Majorana formulation. If one works with the Weyl formulation and translates it into the four-component theory it means that one has the following conditions on the coupling constants

$$g_{\mathrm{I}i} = \pm f_{\mathrm{I}i}\,; \qquad g_{\mathrm{II}i} = \pm f_{\mathrm{II}i}\,, \tag{45}$$

with either the upper or the lower signs throughout. The Majorana formulation is in four-component language given by

$$g_{\mathrm{I}i} = \mp g_{\mathrm{II}i}\,; \qquad f_{\mathrm{I}i} = \pm f_{\mathrm{II}i}\,. \tag{46}$$

The equivalence between the two formulations ([30]) can be expressed as equivalence in the sense of this paper by recognizing that Eq. (45) is transformed into (46) under transformation (I) ([31]) with $a = -b = \sqrt{\frac{1}{2}}$.

The statement that we have a two-component theory does not mean that the interaction Hamiltonian really has to fulfill the conditions (45), (46), respectively. It rather means that the particular interaction Hamiltonian is equivalent to a two-component theory fulfilling either of these conditions. Therefore the two-component character can be expressed in terms of identities between the invariants (5) through (8). Inserting either (45) or (46) into these invariants one sees that the following relation is a necessary condition for a two-component theory in the above sense ([32])

$$(K_{ij} + L_{ij})(K_{kl} - L_{kl}) = (I^*_{ik} + J^*_{jk})(I_{il} + J_{il})\,. \tag{47}$$

([30]) J. SERPE: *Physica*, **18**, 295 (1952) and more recent papers by other authors.

([31]) This follows most easily from LC, Eq. (6) if it is noticed that Eq. (45) (for upper sign) is equivalent to $F_{1i} = G_{2i} = 0$ and Eq. (46) equivalent to $F_{1i} + F_{2i} = G_{1i} - G_{2i} = 0$. A slightly more general condition on a and b is $a + b^* = 0$. Both the Weyl and Majorana formulation still admit transformation (II) (cf., LC, Eq. (7)) and charge conjugation; the latter operation changes upper into lower signs in the conditions (45), and (46).

([32]) This equation is equivalent to $(\boldsymbol{H}_j \cdot \boldsymbol{H}_i)(\boldsymbol{F}_k \cdot \boldsymbol{F}_l) - (\boldsymbol{H}_i \cdot \boldsymbol{F}_k)^*(\boldsymbol{H}_j \cdot \boldsymbol{F}_l)$. The necessity of this condition and of Eq. (37) in the form of Eq. (39) is most conveniently derived in the Weyl formulation with $F_{1i} = G_{2i} = 0$, cf. footnote ([31]). This representation is also suitable for proving the sufficiency of the conditions.

Further Eq. (37) has to be satisfied [33] so that from ordinary β-decay alone (i.e., K_{ij} and L_{ij}) one cannot decide between a four-component interaction which conserves lepton charge and a two-component interaction for which conservation of lepton charge has not been postulated. All inequalities (25) and (26) and identities (29) are again satisfied; in fact all two-rowed subdeterminants of (29) vanish. That the conditions (37) and (47) are also sufficient is shown in a similar manner as in Sect. 5 for the conservation of lepton charge.

Now the particular case of a two-component theory which conserves lepton charge [34] shall be treated. It follows from Eqs. (36) and (47) that

$$(K_{ij} + L_{ij})(K_{kl} - L_{kl}) = 0\,, \tag{48}$$

or [35]

$$K_{ij} \pm L_{ij} = 0\,, \tag{49}$$

with the same sign for all indices. Consequently Eq. (37) reduces to

$$K_{ij}K_{kl} = K_{il}K_{kj}\,. \tag{50}$$

Eqs. (49) and (50) together form necessary and sufficient conditions for a two-component interaction with conservation of lepton charge [36]. For all i with $K_{ii} \neq 0$ [37] one finds L_{ii} $(= \pm K_{ii}) \neq 0$. Consequently one necessarily has violation of both parity and charge conjugation (cf. Eqs. (32) and (33)) in a two-component theory which conserves lepton charge [38]. Since the second inequality (9) imposes a limitation on the possible values of L_{ii} one so gets maximum violation of parity and charge conjugation.

Both the Weyl equation and the Majorana equation lead to a neutrino the physical state of which is entirely specified by momentum and component of the spin in the direction of the momentum. In the four-component theory these quantum numbers do not specify the state of a neutrino completely; one rather has an additional two-fold degeneracy. The fact that the group

---

[33] One also derives $(I_{ij}+J_{ij})(I_{kl}+J_{kl})=(I_{il}+J_{il})(I_{kj}+J_{kj})$ or $(\boldsymbol{H}_i\cdot\boldsymbol{F}_j)(\boldsymbol{H}_k\cdot\boldsymbol{F}_l)=(\boldsymbol{H}_i\cdot\boldsymbol{F}_l)(\boldsymbol{H}_k\cdot\boldsymbol{F}_j)$ which, however, is not independent of Eqs. (37) and (47).

[34] In most of the current literature such a theory is simply called a two-component theory.

[35] The relations for $i \neq j$ can be inferred from those for $i=j$ by means of inequality (25).

[36] Notice that inequality (26) leads to Eq. (36) as a consequence of Eq. (49).

[37] Cf. our remarks in connection with Eq. (9).

[38] This has been recognized recently by several physicists on the basis of less general formulations of β-decay theory.

generated by transformations (I) and (II) acts on this additional degree of freedom but does not change physical results means that this degree of freedom is physically redundant. This could be regarded as an argument in favor of the realization of the two-component neutrino in nature. We think, however, that one should be most reluctant with arguments of this kind.

7. – All experimental information in the field of β-decay can, under the assumption of vanishing neutrino rest mass and local interactions (Eq. (4)), be expressed in terms of the bilinear combinations (invariants) (5) through (8) of the coupling constants and of nuclear matrix elements. Especially ordinary β-decay depends only on the quantities K_{ij} and L_{ij}; without additional assumptions or conventions more detailed information about the coupling constants themselves cannot be obtained from experiments. Invariance with respect to reflections in space (i.e. conservation of parity), charge conjugation, and time reversal are expressed by the conditions (32), (33), (34), respectively. Conservation of lepton charge is fulfilled if the conditions (36) and (37) are satisfied; these conditions do not only forbid double β-decay but they also put limitations on the quantities entering into ordinary β-decay. If β-decay is adequately described by a two-component neutrino, Eqs. (37) and (47) have to be fulfilled. A two-component theory which conserves lepton charge is characterized by Eqs. (49) and (50). Unfortunately Eq. (37) connecting quantities which can be derived from ordinary β-decay alone is a necessary condition for both conservation of lepton charge and two-component interaction (with no requirements as to conservation of lepton charge). So from single β-decay data one cannot decide between the two cases. The stronger requirement of a two component neutrino interaction which simultaneously conserves lepton charge can, however, be tested on information from β-decay alone.

* * *

The author is indebted to Professor W. Pauli and Drs. C. Enz and D. L. Pursey for having sent him preprints of their papers. He also wishes gratefully to acknowledge a stimulating correspondence with Professor Pauli and Dr. Enz as well as discussions with Dr. S. A. Bludman.

Note added in proof.

S. Kahana and D. L. Pursey in a recent paper (*Nuovo Cimento*, to be published) reach similar conclusions. We took over from them two additional terms in Eqs. (33) through (35) which were erroneously omitted in our original manuscript. The present author agrees with Kahana and Pursey that phase transformations of the nucleon and electron fields should be incorporated in the concept of equivalence. The definitions of conservation of lepton charge differ in the two papers.

Appendix

Allowed transitions.

For more detailed formulae one has to specify the Dirac matrices O_i in Eq. (4). This can for instance be done by postulating that the square of each of them is equal to unity which leads to the following list [39]

$$1\,, \quad \gamma_\mu\,, \quad i\gamma_{\mu\nu}\,, \quad i\gamma_\mu\gamma_5\,, \quad \gamma_5\,.$$

Pauli's notation for the coupling constants is not identical with the one used in current β-decay theory. The relation between Pauli's coupling constants $g_{\mathrm{I}i}$, $f_{\mathrm{I}i}$ and C_i, C_i' [40] is given by

$$g_{\mathrm{I}i} = C_i^*\,, \qquad f_{\mathrm{I}i} = C_i'^*\,.$$

Here, it is understood that in the term for tensor interaction it is to be summed only once over each pair of tensor indices (or that a factor of $\frac{1}{2}$ is to be added if free summation is permitted).

In the following table [41,42]) many observable quantities in allowed β-decay are expressed in terms of the invariants K_{ij} and L_{ij}. To obtain such expressions one only has to make use of calculational results for an interaction containing both $g_{\mathrm{I}i}$ and $f_{\mathrm{I}i}$ (or C_i and C_i'); from the general arguments given in LC and in this paper it then follows that the coupling constants $g_{\mathrm{II}i}$ and $f_{\mathrm{II}i}$ can only occur in such a way as to complete the invariants K_{ij} and L_{ij} [43]). The table is mainly presented to show explicitly in what observable effects the various invariants enter. Since complete formulae for these effects are not presented here the reader should in any particular case use formulae already given in the literature and then generalize them in the same way as has been done for the construction of the table.

In the table, essentially the factors are given which in the various observable quantities appear multiplied by the squared Fermi matrix element, the squared Gamow-Teller matrix element, or products between these two matrix elements. First order Coulomb corrections (terms proportional to $(\alpha Z)^1$) are presented besides the main terms (no dependence upon αZ). Experiments 1, 2, 7 and 12 do not show any violation effects in the Coulomb independent part; the results

[39]) This distribution of imaginary units does, however, not give tensors which are bilinear in Dirac fields and have simple Hermiticity properties.

[40]) T. D. Lee and C. N. Yang: *Phys. Rev.*, **104**, 254 (1956).

[41]) The table has been compiled mainly by Dr. T. Kotani. It is based on recent papers (cf. foornotes [40]) and [42])) and on unpublished work by himself; cf., also his *University of California Radiation Laboratory Report* No. 3798. The present author is very grateful to Dr. Kotani for his permission to publish the table, and for many discussions of its content.

[42]) J. D. Jackson, S. B. Treiman and H. W. Wyld: *Phys. Rev.*, **106**, 517 (1957); M. E. Ebel and G. Feldman: *Phys. Rev.* (to be published); M. Morita and R. S. Morita: *Phys. Rev.*, **107**, 139, 1316 (1957).

[43]) For non-violation effects it is even sufficient to use calculations for parity conserving interactions; cf., also T. D. Lee and C. N. Yang: *Phys. Rev.*, **104**, 254 (1956), especially Eqs. (A.3) through (A.5). For Eq. (A.4) cf. Errata in *Phys. Rev.*, **106**, 1371 (1957).

TABLE I.

	Type of experiment	Fermi		Gamow-Teller		Cross terms	
		$(\alpha Z)^0$	$(\alpha Z)^1$	$(\alpha Z)^0$	$(\alpha Z)^1$	$(\alpha Z)^0$	$(\alpha Z)^1$
1	Spectrum and lifetime — Non-cross term	$K_{SS}+H_{VV}$	—	$K_{TT}+K_{AA}$	—	—	—
	Spectrum and lifetime — Fierz term	$\pm 2/E \operatorname{Re} K_{SV}$	—	$\pm 2/E \operatorname{Re} K_{TA}$	—	—	—
2	β-ν angular correlation	$-K_{SS}+K_{VV}$	$\pm \operatorname{Im} K_{SV}$	$K_{TT}-K_{AA}$	$\mp \operatorname{Im} K_{TA}$	—	—
3	β distribution from oriented nuclei	—	—	$\pm (L_{TT}-L_{AA})$	$\operatorname{Im} L_{TA}$	$-\operatorname{Re}(L_{ST}-L_{VA})$	$\pm \operatorname{Im}(L_{SA}-L_{VT})$
4	Longitudinal polarization of β	$\pm (L_{SS}-L_{VV})$	$\operatorname{Im} L_{SV}$	$\pm (L_{TT}-L_{AA})$	$\operatorname{Im} L_{TA}$	—	—
5	ν distribution from oriented nuclei	—	—	$\mp (L_{TT}+L_{AA})$ $-2m/E \operatorname{Re} L_{TA}$	—	$\operatorname{Re}(L_{SA}+L_{VT})$ $\pm m/E \operatorname{Re}(L_{ST}+L_{VA})$	—
6	β polarization along direction of ν	$2 \operatorname{Re} L_{SV}$ $\pm(m/E)(L_{SS}+L_{VV})$	—	$-2 \operatorname{Re} L_{TA}$ $\pm(m/E)(L_{TT}+L_{AA})$	—	—	—
7a	β polarization from oriented nuclei (*)	—	—	$\pm 2 \operatorname{Re} K_{TA}$ $+(m/2E)(K_{TT}+K_{AA})$	—	$\operatorname{Re}(K_{SA}+K_{VT})$ $\pm(m/E)\operatorname{Re}(K_{ST}+K_{VA})$	—
7b	β polarization from oriented nuclei (*)			$K_{TT}+K_{AA}$ $\mp \operatorname{Re} K_{TA}$	—	$-\operatorname{Re}(K_{SA}+K_{VT})$ $\pm \operatorname{Re}(K_{ST}+K_{VA})$	—
8	β-ν angular correlation from oriented nuclei	—	—	—	—	$\operatorname{Im}(K_{VA}-K_{ST})$	$\mp \operatorname{Re}(K_{SA}-K_{VT})$

9	Correlation of β and ν directions with β polarization	$-\operatorname{Im} K_{SV}$	$\mp(K_{SS}-K_{VV})$	$\operatorname{Im} K_{TA}$	$\pm(K_{TT}-K_{AA})$	—	—
10	Polarization of β perpendicular to plane of decay, for oriented nuclei (+)	—	—	$\pm \operatorname{Im} L_{TA}$	$L_{TT}-L_{AA}$	$\operatorname{Im}(L_{SA}-L_{VT})$	$\mp \operatorname{Re}(L_{ST}-L_{VA})$
11	β polarization correlated with direction of ν, for aligned nuclei	—	—	—	—	$\pm(m/E)\operatorname{Im}(L_{ST}+L_{VA})$ $+\operatorname{Im}(L_{SA}+L_{VT})$	
12	γ distribution from oriented nuclei	$K_{SS}+K_{VV}$ $\pm(2m/E)\operatorname{Re} K_{SV}$	-	$K_{TT}+K_{AA}$ $\pm(2\nu/E)\operatorname{Re} K_{TA}$	—	—	—
13	Correlation between β and polarized γ	—	—	$\mp(L_{TT}-L_{AA})$	$\operatorname{Im} L_{TA}$	$\operatorname{Re}(L_{ST}-L_{VA})$	$\mp \operatorname{Im}(L_{SA}-L_{VT})$
14	β-γ correlation from oriented nuclei	—	—	—	—	$\operatorname{Im}(L_{ST}-L_{VA})$	$\pm \operatorname{Re}(L_{SA}-L_{VT})$

(*) There are two distinct types of such experiments, cf., summary on the next page.

(+) The plane is here defined by the direction of polarization of the decaying nucleus (but not its recoil) and by the direction of emission of the electron.

depend only upon Re K_{ij}. Indications for invariance under charge conjugation and under time reversal can, however, be obtained from the Coulomb term in Experiment 2. Experiments 3, 4, 5, 6 and 13 are typical experiments for testing the violation of parity; in some of the cases conservation or violation of time reversal can be read from the terms proportional to αZ. Experiments 10 and 11 in principle also test parity violation; the main effect vanishes, however, in these cases if time reversal is not violated. Experiments 8 and 9 (depending upon Im K_{ij} in the main term) check invariance with respect to charge conjugation and time reversal whereas the second condition for invariance under time reversal (Im $L_{ij} = 0$) is tested in Experiments 10, 11, and 14. Experiments 12, 13, and 14 are β-γ correlation experiments. The symbol m denotes the mass of the electrons and E its total energy. Where two signs ($\pm$ or $\mp$) are given the upper sign refers to emission of positive electrons, the lower to emission of negative electrons.

In the following we give short formal expressions for the various observable quantities. Notations: $\boldsymbol{J}$ = spin of oriented nucleus, $\boldsymbol{p}$ = electron momentum, $\boldsymbol{\sigma}$ = electron spin, $\boldsymbol{q}$ = neutrino momentum, $\boldsymbol{k}$ = γ momentum, $\tau(-=-1)$ symbol for circular polarization of γ quantum.

2:	$\boldsymbol{p}\cdot\boldsymbol{q}$	8:	$\boldsymbol{J}\cdot\boldsymbol{p}\times\boldsymbol{q}$
3:	$\boldsymbol{p}\cdot\boldsymbol{J}$	9:	$\boldsymbol{\sigma}\cdot\boldsymbol{p}\times\boldsymbol{q}$
4:	$\boldsymbol{p}\cdot\boldsymbol{\sigma}$	10:	$\boldsymbol{\sigma}\cdot\boldsymbol{J}\times\boldsymbol{p}$
5:	$\boldsymbol{q}\cdot\boldsymbol{J}$	11:	$\boldsymbol{\sigma}\cdot\boldsymbol{J}\times\boldsymbol{q}$
6:	$\boldsymbol{q}\cdot\boldsymbol{\sigma}$	12:	$\boldsymbol{k}\cdot\boldsymbol{J}$
7*a*:	$\boldsymbol{J}\cdot\boldsymbol{\sigma}$	13:	$\tau(\boldsymbol{p}\cdot\boldsymbol{k})$
7*b*:	$(\boldsymbol{J}\cdot\boldsymbol{p})(\boldsymbol{p}\cdot\boldsymbol{\sigma})$	14:	$(\boldsymbol{J}\cdot\boldsymbol{p}\times\boldsymbol{k})(\boldsymbol{J}\cdot\boldsymbol{k})^n \quad (n=1,3)$ and $\tau(\boldsymbol{J}\cdot\boldsymbol{p}\times\boldsymbol{k})$.

RIASSUNTO (*)

L'ipotesi di una massa del neutrino tendente a zero porta a un gruppo di trasformazioni del campo neutrinico che trasformano l'interazione di decadimento β in interazioni equivalenti. Con osservazioni fisiche non è possibile distinguere fra interazioni equivalenti. I risultati d'osservazione possono esprimersi in termini di elementi di matrici nucleari e di combinazioni delle costanti di accoppiamento che sono invarianti nel gruppo. Questi invarianti sono stati recentemente proposti da Pursey e messi su una base più generale da Pauli. Essi sono ulteriormente esaminati nel presente lavoro. Se ne studia la matematica e se ne stabiliscono le mutue relazioni. Le condizioni per l'invarianza rispetto alle riflessioni nello spazio, alla coniugazione della carica, e all'inversione del tempo si esprimono in termini di questi invarianti. Le interazioni che conservano la carica leptonica e/o si accoppiano a due sole componenti del campo neutrinico sono caratterizzate da relazioni fra le invarianti. (Per il lettore che non desideri seguire gli argomenti dettagliati i risultati principali sono riassunti nell'ultimo paragrafo). Nell'appendice i possibili esperimenti sul decadimento β si esprimono in termini degli invarianti.

(*) *Traduzione a cura della Redazione.*

Dispersion Relations for Momentum Transfer Heavy Meson-Nucleon Scattering.

D. Amati (*)

Departamento de Física, Faculdad de Ciencias Exactas y Naturales
Universidad de Buenos Aires

B. Vitale (+)

Istituto di Fisica dell'Università - Catania
Centro Siciliano di Fisica Nucleare - Catania

(ricevuto il 29 Settembre 1957)

Summary. — Relativistic dispersion relations for heavy meson-nucleon scattering are obtained for all momentum transfer. All the strong interacting fields are taken into account; results are given for both values of the relative parity of heavy mesons and hyperons. The comparison of the results with the forward dispersion relations obtained in a precedent paper (1) with a fixed source theory shows that the recoil contributions do not alter appreciably the dispersion relations.

1. – Introduction.

In a previous paper (1) (hereafter called I) forward dispersion relations for heavy meson-nucleon scattering were found in a fixed source theory. There it was noted that owing to the rather great mass of the K-mesons, it was not possible to neglect « a priori » the recoil contributions. In this paper we will derive the dispersion relations in relativistic theory for all values of

(*) On summer leave from: Istituto Nazionale di Fisica Nucleare, Sezione di Roma and Istituto di Fisica, Università di Roma.

(+) Now at Istituto di Fisica Teorica, Università di Napoli.

(1) D. Amati and B. Vitale: *Nuovo Cimento*, 6, 1013 (1957).

momentum transfer and write them in a suitable way so to be compared with those derived in I. We want to note that relativistic heavy meson-nucleon dispersion relations have already been announced by SAKURAI (2).

As usual, the dispersion relations do not need the specification of a particular Hamiltonian; the bound state contributions depend only on the spin and parity of the different particles. We shall calculate these bound state contributions for spinless heavy mesons, spin $\frac{1}{2}$ hyperons and for both relative parities.

The method we shall follow in deriving the dispersion relations is similar to those already used for pion-nucleon scattering (3), so we will avoid several details and considerations analogous to those of the aforementioned works.

We shall take into account all the strong interacting fields.

2. – Momentum transfer dispersion relations.

Let call k and k' the 4-vector momenta of initial and final heavy meson, p and p' those of initial and final nucleons. We clearly have the mass shell restrictions

$$k^2 = k'^2 = \mu_{\mathrm{K}}^2 , \qquad p^2 = p'^2 = m_{\mathrm{N}}^2 . \tag{1}$$

The causal matrix element M_i ($\overline{M}_i$) for the scattering of a K ($\bar{\mathrm{K}}$) meson of charge index i on proton is given by (4):

$$M_i = i \int \mathrm{d}_4 z \exp\left[-iz(k+k')/2\right] \cdot \cdot \langle p'v | \theta(z_0)[j_i^+(\tfrac{1}{2}z), j_i(-\tfrac{1}{2}z)] - \delta(z_0)[j_i^+(\tfrac{1}{2}z), \dot{\varphi}_i(-\tfrac{1}{2}z)] | pu \rangle , \tag{2a}$$

(2) J. J. SAKURAI: *Bull. Am. Phys. Soc.*, **2**, 177 (1957).

(3) M. L. GOLDBERGER: *Midwest Conference* (1956) (mimeographed notes); A. SALAM: *Nuovo Cimento*, **3**, 424 (1956); A. SALAM and W. GILBERT: *Nuovo Cimento*, **3**, 607 (1956); R. H. CAPPS and G. TAKEDA: *Phys. Rev.*, **103**, 1877 (1956); BOGOLIUBOV, MEDVEDEV and POLIVANOV: *Mimeographed lectures* (1956); G. F. CHEW, M. L. GOLDBERGER, F. E. LOW and Y. NAMBU: *Phys. Rev.*, **106**, 1337 (1957).

(4) The causal matrix elements M (or $\overline{M}$) coincide for real heavy mesons with the Feynman scattering amplitudes F (or $\overline{F}$) defined by

$$S = I - i(2\pi)^4 \delta_4(k' + p' - k - p) \cdot \frac{m_{\mathrm{N}}}{(4p_0 p_0' k_0 k_0')^{\frac{1}{2}}} \cdot F ,$$

(and analogously for $\overline{F}$), the spinors being normalized so that $\langle u | u \rangle = 1$.

For the charge indices we use the same convention used in I, i.e. $i = \frac{1}{2}$ for K^+ and K^-, $i = -\frac{1}{2}$ for K^0 and $\bar{\mathrm{K}}^0$.

$$(2b) \qquad \overline{M}_i = i \int \mathrm{d}_4 z \exp\left[-iz(k+k')/2\right] \cdot \cdot \langle p'v \,|\theta(z_0)[j_i(\tfrac{1}{2}z),\, j_i^+(-\tfrac{1}{2}z)] - \delta(z_0)[j_i(\tfrac{1}{2}z),\, \dot{\varphi}(-\tfrac{1}{2}z)\,|\, pu\rangle \,,$$

u and v being the spin indices of initial and final nucleons and $\theta(z_0)$ the usual step-function which vanishes for negative z_0 and is unity for positive z_0. The current operators j_i are given by

$$(3) \qquad (\mu_{\mathrm{K}}^2 - \Box)\,\varphi_i(x) = j_i(x) \,,$$

where $\varphi_i(x)$ is the heavy meson field operator. The operator j_i increases by one unit the strangeness of the state to which it is applied while j_i^+ decreases it by the same amount.

In the following we will not consider explicitely the second terms in the right hand side of eq. (2*a*) and (2*b*) (equal time commutators); their inclusion would give rise to arbitrary terms depending only on q, but not on ω (see eq. (5)), to be added to the dispersion relations for the no-spin flip scattering amplitudes (i.e. eq. (25*a*) and (25*b*)). Those terms would anyway vanish if the interaction Hamiltonian contains only three-field interactions.

If strong interactions involving strange particles are charge independent [5] then the scattering amplitudes conserving the total isobaric spin ($T=0$ or $T=1$) are given by:

$$(4a) \qquad M^0 = 2M_{-\frac{1}{2}} - M_{\frac{1}{2}} \,, \qquad M^1 = M_{\frac{1}{2}} \,,$$

$$(4b) \qquad \overline{M}^0 = 2\overline{M}_{\frac{1}{2}} - \overline{M}_{-\frac{1}{2}} \,, \qquad \overline{M}^1 = \overline{M}_{-\frac{1}{2}} \,.$$

As usual it can be shown that the dispersive and absorptive parts (corresponding respectively to the $\varepsilon(z_0)$ and the 1 in the decomposition $\theta(z_0) = \frac{1}{2}(1+\varepsilon(z_0))$) in (2*a*) or (2*b*) are real.

Working in the Breit co-ordinate system, we write [6]

$$(5) \qquad \begin{cases} p = (0,\, 0,\quad q,\, E_q) \,, & k = (s,\, 0,\, -q,\, \omega) \\ p' = (0,\, 0,\, -q,\, E_q) \,, & k' = (s,\, 0,\quad q,\, \omega) \end{cases}$$

[5] Preliminar experimental data seem to indicate the failure of charge independence in these cases J. J. SAKURAI: *Phys. Rev.*, **107**, 908 (1957).

[6] ω and q are related to the center of mass quantities by

$$\omega = [(\boldsymbol{k}^2 + \mu_{\mathrm{K}}^2)^{\frac{1}{2}}(\boldsymbol{k}^2 + m_{\mathrm{N}}^2)^{\frac{1}{2}} + \boldsymbol{k}^2 - q^2]E_q^{-1} \,,$$

$$q^2 = \tfrac{1}{2}\boldsymbol{k}^2(1 - \cos\theta) \,,$$

where $\boldsymbol{k}$ is the momentum and θ the scattering angle in the center of mass system.

so that

$$s = (\omega^2 - \omega_q^2)^{\frac{1}{2}} \quad \text{where} \quad \omega_q^2 = q^2 + \mu_K^2 , \tag{6}$$

q represents the momentum transfer; i.e. $q = 0$ for forward scattering. It is easily seen that if we define

$$M_i = A_i + B_i i(\not{k} + \not{k}')/2 , \qquad \overline{M}_i = \bar{A}_i + \bar{B}_i i(\not{k} + \not{k}')/2 , \tag{7}$$

A, B, $\bar{A}$ and $\bar{B}$ depend only on q^2 and ω, and satisfy the crossing relations

$$A_i^*(-\omega) = \bar{A}_i(\omega) , \qquad B_i^*(-\omega) = -\bar{B}_i(\omega) . \tag{8}$$

It will prove more convenient to work with suitable combinations of particle and antiparticle matrix elements, so we write:

$$\mathcal{M}_i^{(\pm)} = M_i \pm \overline{M}_i , \qquad \mathcal{A}_i^{(\pm)} = A_i \pm \bar{A}_i , \qquad \mathcal{B}_i^{(\pm)} = B_i \pm \bar{B}_i \tag{9}$$

so that the crossing relations (8) can now be written:

$$\mathcal{A}_i^{(\pm)*}(-\omega) = \pm \mathcal{A}_i^{(\pm)}(\omega) , \qquad \mathcal{B}_i^{(\pm)*}(-\omega) = \mp \mathcal{B}_i^{(\pm)}(\omega) . \tag{10}$$

From (7) (and (9)) we see that

$$\mathcal{M}_i^{(\pm)} = \mathcal{C}_i^{(\pm)}(\bar{v}u) + \mathcal{B}_i^{(\pm)} \frac{i}{m_N} (\bar{v}\boldsymbol{\sigma} \cdot \boldsymbol{kxp}\, u) , \tag{11}$$

where $\mathcal{C}_i$ and $\mathcal{B}_i$ are respectively the no-spin flip and spin flip scattering amplitudes. $\mathcal{C}$ is related to $\mathcal{A}$ and $\mathcal{B}$ by

$$\mathcal{C}_i^{(\pm)}(\omega) = \mathcal{A}_i^{(\pm)}(\omega) - \frac{m_N \omega}{E_l} \mathcal{B}_i^{(\pm)}(\omega) . \tag{12}$$

From (11) and (12) we can obtain in the usual way the dispersion relations

$$\mathrm{Re}\, \mathcal{F}(\omega) = \frac{2}{\pi} \int_0^\infty \frac{\mathrm{Im}\, \mathcal{F}(\omega')\omega' \mathrm{d}\omega'}{\omega'^2 - \omega^2} \quad \text{for} \quad \mathcal{F} = \mathcal{A}_i^{(+)}, \mathcal{B}_i^{(-)} \text{ or } \mathcal{C}_i^{(+)}, \tag{13}$$

$$\mathrm{Re}\, \mathcal{F}(\omega) = \frac{2\omega}{\pi} \int_0^\infty \frac{\mathrm{Im}\, \mathcal{F}(\omega')\, \mathrm{d}\omega'}{\omega'^2 - \omega^2} \quad \text{for} \quad \mathcal{F} = \mathcal{A}_i^{(-)}, \mathcal{B}_i^{(+)} \text{ or } \mathcal{C}_i^{(-)} . \tag{14}$$

In order to isolate the contributions of the discrete spectrum we write the absorptive part of the matrix element in the following way,

$$(15)\quad \mathcal{M}^{(\pm)}_{a_i} = \frac{(2\pi)^4}{2}\sum_n \big[\langle p'v|j_i^+(0)|n\rangle\langle n|j_i(0)|pu\rangle \pm \langle p'v|j_i(0)|n\rangle\langle n|j_i^+(0)|pu\rangle\big]\cdot \\ \cdot\delta(p_n^{(1)} - p - k) - \big[\langle p'v|j_i(0)|n\rangle\langle n|j_i^+(0)|pu\rangle \pm \\ \pm \langle p'v|j_i^+(0)|n\rangle\langle n|j_i(0)|pu\rangle\big]\,\delta(p_n^{(2)} - p + k')\,,$$

where $|n\rangle$ is a complete set of eigenstates, and

$$(16)\qquad p_n^{(1)} = \tfrac{1}{2}(p + p' + k + k')\,, \qquad p_n^{(2)} = \tfrac{1}{2}(p + p' - k - k')\,.$$

Using (5)

$$(17)\qquad p_n^{(1,2)} = (\pm s, 0\ ,0\ \pm\omega + E_q)$$

so that

$$(18)\qquad \omega = \pm\,\frac{M_n^2 - m_N^2 - \mu_K^2 - 2q^2}{2E_l} = \pm\,\omega_n\,,$$

(the first sign standing for the $p_n^{(1)}$ case and the second for $p_n^{(2)}$) where M_n is the rest mass of the state $|n\rangle$. Formula (18) acts as a definition of ω_n. The terms containing $\langle n|j_i^+(0)|pu\rangle$ in (15) will give discrete contributions to $\mathcal{M}_a$ for $M_n = m_\Lambda$ and $M_n = m_\Sigma$ (masses of Λ and Σ hyperons respectively) corresponding to a value of ω_n given by:

$$(19)\qquad \omega_H = \frac{m_H^2 - m_N^2 - \mu_K^2 - 2q^2}{2E_q}\,.$$

(H stands for Λ and Σ), and a continuous spectrum for $m_\Lambda + \mu_\pi < M_n < \infty$, where μ_π is the pion mass. The ω_n value for the state with $M_n = m_\Lambda + \mu_\pi$ is given by

$$(20)\qquad \omega_0 = \frac{(m_\Lambda + \mu_\pi)^2 - (m_N^2 + \mu_K^2 + 2q^2)}{2E_q}\,.$$

The terms in (15) containing $\langle n|j_i(0)|pu\rangle$ will not give rise to discrete contributions (there are no baryons with positive strangeness) and will have a continuous spectrum for $m_N + \mu_K < M_n < \infty$.

The contribution of the bound state with mass m_H is easily seen to be

$$(21)\qquad \mathcal{M}^{(\pm)}_{a_i H} = \pi\frac{E_H}{E_l}\sum_\varrho \big[\pm\langle p'v|j_i(0)|p_H^{(1)}\varrho\rangle\langle p_H^{(1)}\varrho|j_i^+(0)|pu\rangle\,\delta(\omega - \omega_H) - \\ - \langle p'v|j_i(0)|p_H^{(2)}\varrho\rangle\langle p_H^{(2)}\varrho|j_i^+(0)|pu\rangle\,\delta(\omega + \omega_H)\big]\,,$$

the sum over ϱ being a sum over spin indices, and $E_{\text{H}} = \omega_{\text{H}} + E_q$. The actual evaluation of the bound state contributions is straightforward when spin and parity of the particles are known. Supposing spin 0 for heavy mesons and $\frac{1}{2}$ for hyperons, we will calculate the bound states contributions for the two parity cases, i.e. equal relative parity of heavy mesons and hyperons with respect to the nucleon (called s. case) and opposite relative parity (called p.s. case). We note that it is not necessary to assume equal parity behaviour for the Λ and Σ. Then, with the usual renormalization procedure we find that the contributions of the bound state H to the absorptive parts of $\mathscr{A}_i$ and $\mathscr{B}_i$ are given by

$$\mathscr{A}^{(\pm)}_{a_{i_{\text{H}}}} = g^2_{i_{\text{H}}} G^2_{\text{H}} \frac{\pi}{2m_{\text{H}}} (m_{\text{H}} + m_{\text{N}}) \left[\pm \delta(\omega - \omega_{\text{H}}) - \delta(\omega + \omega_{\text{H}}) \right], \tag{22}$$

$$\mathscr{B}^{(\pm)}_{a_{i_{\text{H}}}} = - g^2_{i_{\text{H}}} G^2_{\text{H}} \frac{\pi}{2m_{\text{H}}} \left[\pm \delta(\omega - \omega_{\text{H}}) + \delta(\omega + \omega_{\text{H}}) \right], \tag{23}$$

for to s. case, and

$$\mathscr{A}^{(\pm)}_{a_{i_{\text{H}}}} = g^2_{i_{\text{H}}} F^2_{\text{H}} \frac{\pi}{2m_{\text{H}}} (m_{\text{H}} - m_{\text{N}}) \left[\mp \delta(\omega - \omega_{\text{H}}) + \delta(\omega + \omega_{\text{H}}) \right], \tag{22'}$$

$$\mathscr{B}^{(\pm)}_{a_{i_{\text{H}}}} = - g^2_{i_{\text{H}}} F^2_{\text{H}} \frac{\pi}{2m_{\text{H}}} \left[\pm \delta(\omega - \omega_{\text{H}}) + \delta(\omega + \omega_{\text{H}}) \right], \tag{23'}$$

for the p.s. case. G_{H} and F_{H} are respectively the s. and p.s. renormalized rationalized coupling constants for the (NKH) interaction [7]. The $g_{i\text{H}}$, are charge factors; if charge independence is valid they are given by

$$g^2_{\frac{1}{2},\Lambda} = \tfrac{1}{2}, \qquad g^2_{-\frac{1}{2},\Lambda} = 0, \qquad g^2_{\frac{1}{2},\Sigma} = \tfrac{1}{2}, \qquad g^2_{-\frac{1}{2},\Sigma} = 1, \tag{24}$$

with the usual isobaric spin assignements (Λ isoscalar, Σ isovector). If charge independence fails to be valid, the g_i define different coupling constants for $i = \frac{1}{2}$ and $i = -\frac{1}{2}$. From (22) and (23), or (22′) and (23′), the bound state contributions to the no-spin flip scattering amplitude is immediately calculated from (12). Then, the bound state contributions to the integrals of (13) and (14) can be easily obtained. We write down directly the dispersion relations

---

(7) The coupling constant F is the ps-ps coupling constants of the conventional theory. That used in I was instead the ps-pv of the conventional theory. A Dyson transformation similar to that commonly used for pion-nucleon interaction (see for instance S. S. Schweber, H. A. Bethe and F. de Hoffmann: *Mesons and Fields*, Vol. I (Row Peterson and Co.), p. 406 and ff., gives $(m_{\text{H}} + m_{\text{N}}) F_{\text{p.v.}} = \mu_{\text{K}} F_{\text{p.s.}}$.

for spin-independent and spin-flip amplitudes for K-proton and $\overline{\mathrm{K}}$-proton scattering, i.e.

$$(25a)\qquad \mathrm{Re}\, T_i(\omega) = \mathrm{Re}\,\frac{1}{2}\left(\mathscr{C}_i^{(+)}(\omega) + \mathscr{C}_i^{(-)}(\omega)\right) = P_i^{\Lambda}(\omega) + P_i^{\Sigma}(\omega) + \\ + \frac{1}{\pi}\int_{\omega_0}^{\infty}\left[\frac{\mathrm{Im}\, T_i(\omega')}{\omega' - \omega} + \frac{\mathrm{Im}\, \overline{T}_i(\omega')}{\omega' + \omega}\right]\mathrm{d}\omega' ,$$

$$(25b)\qquad \mathrm{Re}\, \overline{T}_i(\omega) = \mathrm{Re}\,\frac{1}{2}\left(\mathscr{C}_i^{(+)}(\omega) - \mathscr{C}_i^{(-)}(\omega)\right) = \overline{P}_i^{\Lambda}(\omega) + \overline{P}_i^{\Sigma}(\omega) + \\ + \frac{1}{\pi}\int_{\omega_0}^{\infty}\left[\frac{\mathrm{Im}\, T_i(\omega')}{\omega' + \omega} + \frac{\mathrm{Im}\, \overline{T}_i(\omega')}{\omega' - \omega}\right]\mathrm{d}\omega' ,$$

$$(26a)\qquad \mathrm{Re}\, B_i(\omega) = Q_i^{\Lambda}(\omega) + Q_i^{\Sigma}(\omega) + \frac{1}{\pi}\int_{\omega_0}^{\infty}\left[\frac{\mathrm{Im}\, B_i(\omega')}{\omega' - \omega} - \frac{\mathrm{Im}\, \overline{B}_i(\omega')}{\omega' + \omega}\right]\mathrm{d}\omega',$$

$$(26b)\qquad \mathrm{Re}\, \overline{B}_i(\omega) = \overline{Q}_i^{\Lambda}(\omega) + \overline{Q}_i^{\Sigma}(\omega) + \frac{1}{\pi}\int_{\omega_0}^{\infty}\left[-\frac{\mathrm{Im}\, B_i(\omega')}{\omega' + \omega} + \frac{\mathrm{Im}\, \overline{B}_i(\omega')}{\omega' - \omega}\right]\mathrm{d}\omega' ,$$

where,

$$(27)\qquad \begin{cases} P_i^{\mathrm{H}}(\omega) = \dfrac{g_{i\mathrm{H}}^2 G_{\mathrm{H}}^2}{2m_{\mathrm{H}}}\,\dfrac{(m_{\mathrm{H}} + m_{\mathrm{N}} + (m_{\mathrm{N}}\omega_{\mathrm{H}}/E_0))}{\omega + \omega_{\mathrm{H}}} , \\ \overline{P}_i^{\mathrm{H}}(\omega) = -\dfrac{g_{i\mathrm{H}}^2 G_{\mathrm{H}}^2}{2m_{\mathrm{H}}}\,\dfrac{1}{\omega - \omega_{\mathrm{H}}}\,(m_{\mathrm{H}} + m_{\mathrm{N}} + (m_{\mathrm{N}}\omega_{\mathrm{H}}/E_0)) , \end{cases}$$

$$(28)\qquad Q_i^{\mathrm{H}}(\omega) = \frac{g_{i\mathrm{H}}^2 G_{\mathrm{H}}^2}{2m_{\mathrm{H}}}\,\frac{1}{\omega + \omega_{\mathrm{H}}}, \qquad \overline{Q}_i^{\mathrm{H}}(\omega) = \frac{g_{i\mathrm{H}}^2 G_{\mathrm{H}}^2}{2m_{\mathrm{H}}}\,\frac{1}{\omega - \omega_{\mathrm{H}}},$$

for the s.-case, and

$$(27')\qquad P_i^{\mathrm{H}} = -\frac{g_{i\mathrm{H}}^2 F_{\mathrm{H}}^2}{2m_{\mathrm{H}}}\,\frac{(\Delta_{\mathrm{H}} - (m_{\mathrm{N}}\omega_{\mathrm{H}}/E))}{\omega + \omega_{\mathrm{H}}} , \qquad \overline{P}_i^{\mathrm{H}} = \frac{g_{i\mathrm{H}}^2 F_{\mathrm{H}}^2}{2m_{\mathrm{H}}}\,\frac{(\Delta_{\mathrm{H}} - (m_{\mathrm{N}}\omega_{\mathrm{H}}/E))}{\omega - \omega_{\mathrm{H}}} ,$$

$$(28')\qquad Q_i^{\mathrm{H}} = \frac{g_{i\mathrm{H}}^2 F_{\mathrm{H}}^2}{2m_{\mathrm{H}}}\,\frac{1}{\omega + \omega_{\mathrm{H}}}, \qquad \overline{Q}_i^{\mathrm{H}} = \frac{g_{i\mathrm{H}}^2 F_{\mathrm{H}}^2}{2m_{\mathrm{H}}}\,\frac{1}{\omega - \omega_{\mathrm{H}}},$$

for the p.s. case, have written $\Delta_{\mathrm{H}} = m_{\mathrm{H}} - m_{\mathrm{N}}$. The values of ω_{H} and ω_0 are given by (19) and (20) respectively, both depend on the momentum transfer q. We see that for $q^2 > \frac{1}{2}[(m_\Lambda + \mu_\pi)^2 - (m_{\mathrm{N}}^2 + \mu_{\mathrm{K}}^2)]$, $\omega_0 < 0$; it is easy to see, however, that the dispersion relations as written in eq. (25) to (28) are always valid provided that when computing the integrals over ω' only the first δ

function of (15) (or analogous decomposition for the other ampliutdes) is considered.

If the behaviour of the scattering amplitudes at great energies is such that the integrals of (13) and (14) (or (25) and (26)) do not converge, a set of dispersion relations with more convergent integrals can be obtained with suitable combinations of the previously obtained relations. This procedure has however the disadvantage of introducing new terms in the dispersion relations containing undetermined functions of q. For the no-spin flip amplitude we find [8]:

$$\text{(29}a\text{)} \qquad \operatorname{Re} T_i(\omega) = C_{i_\Lambda}^{(1)} + C_{i_\Sigma}^{(1)} + \frac{1}{2}\left(1+\frac{\omega}{\nu}\right)\operatorname{Re} T_i(\nu) + \frac{1}{2}\left(1-\frac{\omega}{\nu}\right)\operatorname{Re}\overline{T}_i(\nu) + \\ + \frac{(\omega^2-\nu^2)}{\pi}\int_{\omega_0}^{\infty}\frac{\mathrm{d}\omega'}{\omega'^2-\nu^2}\left(\frac{\operatorname{Im} T_i(\omega')}{\omega'-\omega}+\frac{\operatorname{Im}\overline{T}_i(\omega')}{\omega'+\omega}\right),$$

$$\text{(29}b\text{)} \qquad \operatorname{Re}\overline{T}_i(\omega) = C_{i_\Lambda}^{(2)} + C_{i_\Sigma}^{(2)} + \frac{1}{2}\left(1+\frac{\omega}{\nu}\right)\operatorname{Re}\overline{T}_i(\nu) + \frac{1}{2}\left(1-\frac{\omega}{\nu}\right)\operatorname{Re} T_i(\nu) + \\ + \frac{(\omega^2-\nu^2)}{\pi}\int_{\omega_0}^{\infty}\frac{\mathrm{d}\omega'}{\omega'^2-\nu^2}\left(\frac{\operatorname{Im}\overline{T}_i(\omega')}{\omega'-\omega}+\frac{\operatorname{Im} T_i(\omega')}{\omega'+\omega}\right),$$

where ν is an arbitrary fixed value of ω, and the C_i are given by

$$\text{(30)} \qquad C_{i_\mathrm{H}}^{(1,2)} = \mp\frac{g_{i\mathrm{H}}^2 G_\mathrm{H}^2}{2m_\mathrm{H}}\left(m_\mathrm{H}+m_\mathrm{N}+\frac{m_\mathrm{N}\omega_\mathrm{H}}{E_q}\right)\frac{(\omega^2-\nu^2)}{(\nu^2-\omega_\mathrm{H}^2)(\omega\pm\omega_\mathrm{H})},$$

for the s. case, and

$$\text{(30}'\text{)} \qquad C_{i_\mathrm{H}}^{(1,2)} = \pm\frac{g_{i\mathrm{H}}^2 F_\mathrm{H}^2}{2m_\mathrm{H}}\left(\Delta_\mathrm{H}-\frac{m_\mathrm{N}\omega_\mathrm{H}}{E_q}\right)\frac{\omega^2-\nu^2}{(\nu^2-\omega_\mathrm{H}^2)(\omega\pm\omega_\mathrm{H})},$$

for the p.s. case. Similar expressions can be obtained for the spin flip amplitudes B and $\overline{B}$.

It is possible, as usual, to analyse in partial waves the scattering amplitudes, after transforming them to the center of mass system, and use (25) and (26) in order to find relations among the partial scattering amplitudes that depend only on the center of mass energy [9]. Besides the usual difficulties of analytic continuation of Legendre polynomials [10], we would have

---

[8] As noted before, the equal time commutators of eqs. (2) would give rise to extra terms, depending only on q, to be added to the r.h.s. of eqs. (25) if interactions other than the 3-field one are present. However, these terms will give no contributions at all to eqs. (29) because they shall cancel out in the substraction procedure.

[9] See for instance R. H. Capps and G. Takeda, ref. [3].

[10] K. Symanzik: unpublished.

the inconveniences over the pion-nucleon scattering analysis that owing to the absorption processes $\overline{K}+N \to H+\pi$ we cannot neglect inelastic processes (elastic approximation) and we must work with complex phase shifts for all values of the energy.

3. – Forward scattering, comparison with I.

For forward scattering, i.e. $q = 0$, ω is directly the incident meson energy in the laboratory system. From (19) and (20) we see that for $q = 0$

$$\omega_H = \Delta_H - \frac{\mu_K^2 - \Delta_H^2}{2m_N}, \tag{31}$$

$$\omega_0 = \Delta_\Lambda + \mu_\pi - \frac{\mu_K^2 - (\Delta_\Lambda + \mu_\pi)^2}{2m_N}, \tag{32}$$

chosing the arbitrary energy to be the heavy meson rest mass μ_K, we find for the bound state contributions given in (30) and (30′):

$$C_{i_H}^{(1,2)} = \mp \frac{g_{iH}^2 G_H^2 (1 - (\mu_K^2 - \Delta_H^2)/4m_H m_N)\,(\omega^2 - \mu_K^2)}{(\mu_K^2 - \omega_H^2)(\omega \pm \omega_H)} \qquad \text{(s.-case)}, \tag{33}$$

$$C_{i_H}^{(1,2)} = \pm \frac{g_{iH}^2 F_H^2}{4m_H m_N} \frac{(\mu_K^2 - \Delta_H^2)(\omega^2 - \mu_K^2)}{(\mu_K^2 - \omega_H^2)(\omega \pm \omega_H)} \qquad \text{(p.s.-case)}. \tag{33′}$$

The comparison with I is now straightforward. Defining ${}_{p.v.}F_H = (\mu_K F_H)/(m_H + m_N)$ [7] we see that besides constant numerical factors multiplying the coupling constants (that go to 1 in the fixed source limit), the expressions (29), (33) are analogous to the (17), (18), (33), (34) of I [11] with the substitution of Δ_H in the denominators of the bound state terms of I by ω_H as given in (31) of this paper, and changing the low limit of integration in the dispersion relations integrals from the value $Q_H + \mu_\pi$ of I to ω_0 as given in (32).

Even if the bound state energies change considerably due to the recoil terms ($\Delta_\Lambda \approx 300\ m_e$, $\omega_\Lambda \approx 80\ m_e$; $\Delta_\Sigma \approx 450\ m_e$, $\omega_\Sigma \approx 250\ m_e$) this will not change considerably the contribution of the bound state terms owing to the rather great value of the heavy meson mass and then of the minimum meson energy.

---

[11] The normalization of the forward scattering amplitude $f_i(\omega)$ used in I was such that it is related to the scattering amplitude T used in this paper by $f_i(\omega) = (1/4\pi) T_i(\omega)_{q=0}$.

For the forward scattering we can make use of the optical theorem that states

$$\text{Im } T_i(\omega)_{q=0} = |\boldsymbol{k}|\sigma_i(\omega) , \qquad \text{Im } T_i(\omega)_{q=0} = |\boldsymbol{k}|\bar{\sigma}_i(\omega) , \tag{34}$$

where σ_i ($\bar{\sigma}_i$) are the total cross sections for the scattering of a K ($\overline{\text{K}}$) meson of charge index i on proton.

* * *

One of us (D.A.) wishes to thank Dr. J. J. Giambiagi for his kind hospitality and valuable discussions, he is also grateful to the Dirección Nacional de Invectigaciones Científicas for having partially supported this investigation.

RIASSUNTO

Si ottengono relazioni di dispersione per la diffusione di mesoni pesanti da parte di nucleoni per qualsiasi scambio di impulso e senza restringersi alla teoria di sorgente fissa. Supponendo spin $\frac{1}{2}$ per gli iperoni e spin 0 per i mesoni pesanti, si calcola il contributo degli stati legati per entrambi i valori della parità relativa. Si confrontano i risultati con quelli ottenuti in un precedente lavoro nel quale si utilizzava la teoria della sorgente fissa; si trova che il contributo del rinculo non modifica sensibilmente le relazioni di dispersione.

IL NUOVO CIMENTO Vol. VII, N. 2 16 Gennaio 1958

On Possible Regularities Underlying the Scheme of Elementary Particle States (*).

N. Dallaporta

Istituto di Fisica dell'Università - Padova
Istituto Nazionale di Fisica Nucleare - Sezione di Padova

(ricevuto il 3 Ottobre 1957)

Summary. — An approach is made in order to interpret the observed regularities of the known states of elementary particles by assuming that when we disregard secondary perturbations to which the differences of mass between baryons are attributed, the fundamental properties of all baryons should be the same; particularly all baryons should be spinors and isospinors corresponding to the scheme shown in the Fig. 3, where in abscissa are plotted the values of charge, and in ordinate the strangeness. It is assumed that the only possible transitions between baryonic states are those indicated by dotted lines on the scheme, the horizontal lines being due to emission or absorption of $\pi^{\pm}$-mesons, the vertical ones to that of K^0 or $\overline{K}^0$-mesons and the diagonal ones to $K^{\pm}$-mesons. These transitions are ruled by three $\frac{1}{2}$ isospins, τ for pions, ω for K^0, ζ for $K^{\pm}$, with a similar formalism for each as used for ordinary isotopic spin; the three τ, ω and ζ spins representing internal degrees of freedom of the baryon, the quantum number labels for each baryonic state due to these spins being indicated in the brackets for each baryon as $(\tau_3, \omega_3, \zeta_3)$. It is shown that these assumptions are equivalent to the Gell-Mann Nishijima rules and that when suitable perturbations between the mesonic fields are introduced, the doublets Σ^+Z^0 and $Y^0\Sigma^-$ are mixed and give the singlet Λ^0 and the triplet $\Sigma^{+,0,-}$ states as observed; the hamiltonian then goes even into the form proposed by d'Espagnat and Prentki. Finally the physical meaning for the three quantum numbers of the baryons is discussed.

(*) This work has been presented at the Padua-Venice Conference on Mesons and Recently Discovered Particles, September 22, 1957.

1. – The discovery in recent years of a number of new unstable heavy particles has quickly been followed by the formulation of some phenomenological relations between their quantum numbers (1) which have so far appeared quite successful in interpreting some of the most characteristic phenomena observed in their interactions. Moreover the limited number of the particles observed, together with the regularities that are apparent in their characteristic parameters, seem to indicate that their existence is related to some deep seated symmetries in their internal structure as has recently been pointed out by some authors (2). However these possible underlying symmetries seem by no means easy to reach owing to the fact that they are distorted and covered by secondary disturbances which probably alter their true aspect; so that in order to be able to obtain some insight into this matter the first thing to do is to try to distinguish and remove those superposed secondary disturbing features.

Along this line, it has generally been assumed that the differences in mass between the different kinds of baryons are to be considered as due to the secondary perturbation. Another very general idea outlined recently by GELL-MANN (2) assumes that the interactions between all kinds of mesons and all kind of baryons should be fundamentally of the same type. The possibility however, of pushing this idea very far is disturbed by the fact that the isotopic spin quantum numbers given to the different kinds of mesons and baryons in order to agree with experimental data are different; so that it happens that some bosons are isobosons and other are isofermions, while some fermions are isofermions and other isobosons.

In this work, an attempt is made to develop as far as possible the idea of an essentially similar interaction between all kinds of mesons and of baryons by making the further fundamental assumption that the interchanges of types of isostatistics between different kinds of mesons and baryons are due to secondary perturbations and that fundamentally all baryons are fermions and isofermions with spin $\frac{1}{2}$ and isotopic spin $\frac{1}{2}$; while mesons are all bosons and isobosons in a way that will be explained later. This assumption, together with the first one that all masses of baryons are equal when perturbations are turned off will be first used for establishing the states of the baryons and mesons without disturbances acting on them; we will then try to formulate a phenomenological type of general interaction between undisturbed baryons

(1) M. GELL-MANN: *Phys. Rev.*, **92**, 833 (1953); T. NAKANO and K. NISHIJIMA: *Prog. Theor. Phys. Jap.*, **10**, 581 (1953); K. NISHIJIMA: *Prog. Theor. Phys. Jap.*, **12**, 107 (1954); M. GELL-MANN and A. PAIS: *Proc. Glasgow Conf. on Nuclear and Meson Physics*, 1954, p. 324; R. G. SACHS: *Phys. Rev.*, **99**, 1576 (1955).

(2) J. SCHWINGER: *Phys. Rev.*, **104**, 1164 (1956); M. GELL-MANN: *Phys. Rev.*, **106**, 1296 (1957).

able to reproduce the observed GELL-MANN NISHIJIMA (G-N) rules; then we will try to see what kind of perturbations have to be introduced in order to obtain the experimental situation; and finally we will try to find some justification for the quantum numbers introduced to describe the baryon states.

2. – Let us begin by examining what consequences our assumptions will have in determining the undisturbed states of the baryons. If all of them are to be described as fermions with both spin and isotopic spin equal to $\frac{1}{2}$ the main

TABLE I.

	C	S	τ_3	ω_3	ζ_3	A
P	$+1$	$+1$	$+\frac{1}{2}$	$+\frac{1}{2}$	$+\frac{1}{2}$	$+1$
N	0	$+1$	$-\frac{1}{2}$	$+\frac{1}{2}$	$+\frac{1}{2}$	0
Σ^+	$+1$	0	$+\frac{1}{2}$	$-\frac{1}{2}$	$+\frac{1}{2}$	0
Z^0	0	0	$-\frac{1}{2}$	$-\frac{1}{2}$	$+\frac{1}{2}$	-1
Y^0	0	0	$+\frac{1}{2}$	$+\frac{1}{2}$	$-\frac{1}{2}$	$+1$
Σ^-	-1	0	$-\frac{1}{2}$	$+\frac{1}{2}$	$-\frac{1}{2}$	0
Ξ^0	0	-1	$+\frac{1}{2}$	$-\frac{1}{2}$	$-\frac{1}{2}$	0
Ξ^-	-1	-1	$-\frac{1}{2}$	$-\frac{1}{2}$	$-\frac{1}{2}$	-1

change has to affect the Σ and Λ particles which have now to be considered as split into two doublets of isotopic spin $\frac{1}{2}$ as GELL-MANN [2] has already done in this same case. We may then present the whole scheme of the possibile 8 baryon states as given in Table I or Fig. 1, where the Z^0 and Y^0 particles are to be considered as neutral isotopic partners of the Σ^+ and Σ^- thus forming doublets.

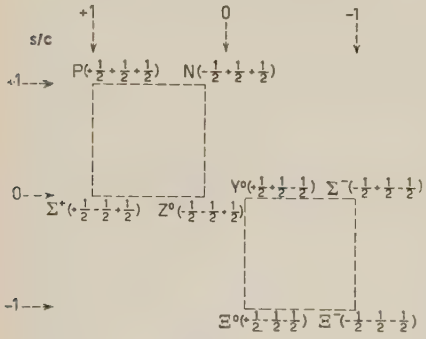

Fig. 1.

In the first column of the table the charge of the particles is given, and in the second one their strangeness. This definition of strangeness coincides with the hypercharge of SCHWINGER [2] and of the strangeness of SALAM [3] and others. According to this definition the 8 states of baryons are situated in a very symmetrical way with respect to the point of zero charge and strangeness, as seen in Fig. 1, i.e. they result arranged in two squares in each of which the values of charge and strangeness are always of the same sign. Each pair of states connected by a horizontal line forms an isotopic spin doublet whose τ_3 values are given in column 3 of Table I. However, on symmetry grounds, one could think that it would also be possible to connect different couples of states by vertical lines as shown in Fig. 1; in this way one can form strangeness doublets,

to whom one could assign a strangeness spin ([3]) ω whose ω_3 values are also given for each particle in column 4 of Table I. If we now consider τ_3 and ω_3 as internal quantum numbers characterizing the different charge and strangeness states of all unperturbed baryons, we see that two different baryons exist, one in each square, for every possible pair of values of τ_3 and ω_3. Therefore in order to distinguish between baryons with the same τ_3 and ω_3, we need a third label which we call for the moment ζ_3 and which we assume to have value $+\frac{1}{2}$ for the baryons in the upper square and value $-\frac{1}{2}$ for those in the lower square.

3. – Let us now go on to consider the mesons. Generally the 7 kinds of them are classified in two distinct groups: the three π-mesons, forming an isotopic spin triplet, and the four K-mesons forming two distinct isotopic doublets, K^0 and K^+ with strangeness 1, and $\overline{K}^0$ and $\overline{K}^-$ with strangeness -1.

TABLE II.

	C	S	τ_3	ω_3	ζ_3	A
π^0	0	0	0	0	0	0
π^+	$+1$	0	$+1$	0	0	$+1$
π^-	-1	0	-1	0	0	-1
K^0	0	$+1$	0	$+1$	0	$+1$
$\overline{K}^0$	0	-1	0	-1	0	-1
K^+	$+1$	$+1$	0	0	$+1$	0
$\overline{K}^-$	-1	-1	0	0	-1	0

However, if we disregard for the moment the difference in mass between π's and K's and if also in this case we further try to stress the symmetry between electric charge and strangeness we can arrive at a quite different kind of grouping, which is presented in Table II and Fig. 2, just according to the different kinds of physical quantities they show: π^0 stands alone as it has neither charge nor strangeness, $\pi^\pm$ form a pair with charge and no strangeness, K^0 and $\overline{K}^0$ another pair with strangeness and no charge, while K^+ and $\overline{K}^-$ possess both charge and strangeness: in such a way that for a given meson the charge and strangeness are always of the same sign.

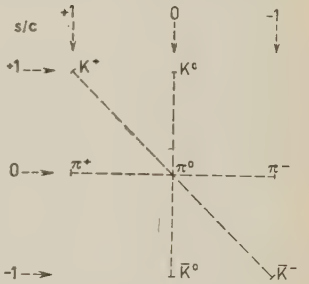

Fig. 2.

The symmetry between the charge and strangeness of this grouping is generally hidden by the mass difference between K's and π's. If however we attribute the small

([3]) A. SALAM and J. C. POLKINGHORNE: *Nuovo Cimento*, **2**, 685 (1955); C. CEOLIN and N. DALLAPORTA: *Nuovo Cimento*, **3**, 586 (1956).

increase in mass of the charged $\pi^{\pm}$ mesons with respect to the π^0 to electromagnetic effects when the field has electric charge, and the big increase of mass of the K-mesons to some as yet unknown effect depending on strangeness we see that for our purposes the mass difference of π's and K's may be overlooked and we can stick to the new grouping of the mesons in the hope of getting a deeper insight of the facts.

Let us now try to connect this assumed grouping for the mesons with the scheme 1 for the baryons. Each baryon may emit or absorb π^0 without changing its nature, while it may emit or absorb $\pi^{\pm}$ and transform by moving along an horizontal line on Fig. 1; this is the usual isotopic spin mechanism. However, on exactly the same lines, one can also assume that a baryon transforms by moving along a vertical line when it emits or absorbs a K^0 or $\overline{K}^0$; this process

TABLE III.

transition	through	transition	through	transition	through
$P \leftrightarrow N$		$P \leftrightarrow \Sigma^+$		$P \leftrightarrow Y^0$	
$\Sigma^+ \leftrightarrow Z^0$	$\pi^{\pm}$	$N \leftrightarrow Z^0$	$K^0\overline{K}^0$	$N \leftrightarrow \Sigma^-$	$K^+\overline{K}^-$
$Y^0 \leftrightarrow \Sigma^-$		$Y^0 \leftrightarrow \Xi^0$		$\Sigma^+ \leftrightarrow \Xi^0$	
$\Xi^0 \leftrightarrow \Xi^-$		$\Sigma^- \leftrightarrow \Xi^-$		$Z^0 \leftrightarrow \Xi^-$	

should then be ruled by a strangeness spin mechanism expressed through the ω operator exactly similar to the τ mechanism.

The question now arises in which way the K^+ and $\overline{K}^-$ should be emitted. One could first think that this could be achieved by a combined τ and ω operation: this however proves not to be consistent with experimental facts as this mechanism would require the existence of K's with charges and strangenesses of all possible signs combined together, in contradiction with the G-N rules; moreover, such a mechanism would never allow the baryons of one of the squares to transform into a baryon belonging to the other square, and this also in contradiction with experiment.

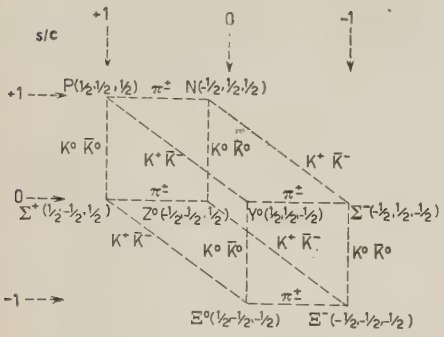

Fig. 3.

Therefore at this point we make the fundamental assumption that $K^{\pm}$ *are emitted or absorbed when baryons make transitions along diagonal lines connecting states with different values of the third quantum number* ζ_3. If we postpone any discussion on the meaning of this number until the end of the paper, we may just interpret it phenomenologically as a third component of a third kind

of iso-strangeness spin ζ, whose rotations rule the emission or absorbtion of charged K's. It may be easily recognized that the proposed transitions for the charged K's, together with those already proposed for neutral K's and pions are exactly equivalent to the G-N rules for associated production. The summary of all possible transitions between all baryon states is presented in Fig. 3 and Table III.

4. – We shall now try to justify the present model by giving to it a qhysical reality; this may be done if we succeed in constructing the observed baryon states by combining the different known mesons with a fundamental baryon.

Let us then consider such a bare baryon which we call B^0 as a fermion with spin $\frac{1}{2}$ and no charge and no strangeness. It is the source of the meson fields and according to a kind of naive Lee model can form different clothed states with the mesons. Let first B^0 be clothed with each kind of a K; we obtain the proton and the neutron

$$p = B^0 + (K^+), \qquad n = B^0 + K^0.$$

Let now these new states absorb a $\bar{K}^0$ or $\overline{K}^-$: we get the 0 strangeness hyperons:

$$\Sigma^+ = p + \overline{K}^0 = B^0 + K^+ + \overline{K}^0, \qquad Z^0 = n + \overline{K}^0 = B^0 + K^0 + \overline{K}^0,$$
$$Y^0 = p + \overline{K}^- = B^0 + K^+ + \overline{K}^-, \qquad \Sigma^- = n + \overline{K}^- = B^0 + K^0 + \overline{K}^-.$$

We see that we thus obtain for these hyperons the compound model configurations that were first proposed by GOLDHABER (4). We may however go a step further to the three mesons configurations obtained by absorbing a pion: We get:

$$p = n + \pi^+ = B^0 + K^0 + \pi^+, \qquad n = p + \pi^- = B^0 + K^+ + \pi^-,$$
$$\Sigma^+ = Z^0 + \pi^+ = B^0 + K^0 + \overline{K}^0 + \pi^+, \qquad Z^0 = \Sigma^+ + \pi^- = B^0 + K^+ + \overline{K}^0 + \pi^-,$$
$$Y^0 = \Sigma^- + \pi^+ = B^0 + \overline{K}^- + K^0 + \pi^+, \qquad \Sigma^- = Y^0 + \pi^- = B^0 + \overline{K}^- + K^+ + \pi^-.$$

At this point let us consider what happens if, according to the general symmetry ideas followed in this work, we begin to clothe our bare B^0 first with $\overline{K}$-mesons: obviously we then obtain the Ξ's built up according to the scheme:

$$\Xi^0 = B^0 + \overline{K}^0, \qquad \Xi^- = B^0 + \overline{K}^-$$

(4) M. GOLDHABER: *Phys. Rev.*, **101**, 433 (1956).

and by adding to these first a K and then a π, the 2 mesons and 3 mesons clothed states of the 0 strangeness hyperons:

$$\Sigma^+ = \Xi^0 + K^+ = B^0 + K^+ + \overline{K}^0 , \qquad Z^0 = \Xi^- + K^+ = B^0 + K^+ + \overline{K}^-$$

$$Y^0 = \Xi^0 + K^0 = B^0 + K^0 + \overline{K}^0 , \qquad \Sigma^- = \Xi^- + K^0 = B^0 + K^0 + \overline{K}^-$$

and

$$\Xi^0 = \Xi^- + \pi^+ = B^0 + \overline{K}^- + \pi^+ , \qquad \Xi^- = \Xi^0 + \pi^- = B^0 + \overline{K}^0 + \pi^- ,$$

$$\Sigma^+ = Z^0 + \pi^+ = B^0 + K^+ + \overline{K}^- + \pi^+ , \qquad Z^0 = \Sigma^+ + \pi^- = B^0 + K^+ + \overline{K}^0 + \pi^- ,$$

$$Y^0 = \Sigma^- + \pi^+ = B^0 + K^0 + \overline{K}^- + \pi^+ , \qquad \Sigma^- = Y^0 + \pi^- = B^0 + K^0 + \overline{K}^0 + \pi^- .$$

It is seen that if we content ourselves by considering the 0 strangeness hyperons as merely built up starting from nucleons, all the two and three mesons compound states are different; if however we consider them as containing also the states btained by starting to build them from the Ξ's, then both Z^0 and Y^0 contain a mixture of the two possible two meson states, but their three meson states remain different; thus in any case Z^0 and Y^0 remain physically different. And generally we see that the assumed transition scheme for all kinds of mesons between the baryon states is consistent with well determined internal structures for them.

5. – The scheme now arrived at for the possible transitions between baryons presents the peculiar and symmetrical feature that unperturbed baryons may be grouped into 4 doublets with respect to meson emission or absorption in three different ways according to the kind of meson considered. This enables us to construct a very simple phenomenological interaction hamiltonian valid for all baryon states,

$$(1) \qquad H = \int \mathrm{d}v\, \overline{\Psi}_{k,l,m} \left[\sum_{\alpha=1,2,3} \tau_\alpha \chi_{\alpha 33} + \sum_{\beta=1,2} \omega_\beta \chi_{3\beta 3} + \sum_{\gamma=1,2} \zeta_\gamma \chi_{33\gamma} \right] \Psi_{k',l',m'} .$$

In this formula, the baryon states $\Psi_{k,l,m}$ are labelled with three indices k, l and m, indicating respectively the values of the third component of the isospin, the strangeness spin and the isostrangeness spin; τ, ω and ζ are vectors represented by the Pauli spin matrices and which operate respectively on k, l and m; $\chi_{\alpha 33}$, $\chi_{3\beta 3}$ and $\chi_{33\gamma}$ are components of the meson field indicating respectively the pions, the neutral K's and the charged K's and are given by a similar expression as in the work of D'Espagnat and Prentki [5]. Summations over indices run from 1 to 2 for β and γ and from 1 to 3 for α, the third component in this case representing π^0 emission or absorption: according

[5] B. D'Espagnat and J. Prentki: *Nucl. Phys.*, **1**, 33 (1956).

to the present scheme this term could have stood alone indipendently from any other, but it has been joined to the $\pi^{\pm}$ terms in order to conform to general use.

If we now introduce as usual

$$\tau_{\pm} = \frac{1}{2}(i\tau_1 \pm \tau_2) \quad \omega_{\pm} = \frac{1}{2}(\omega_1 \pm i\omega_2) \ldots \quad \chi_{\pm 33} = \frac{1}{\sqrt{2}}(\chi_{133} \pm i\chi_{233}) \ldots$$

and so on for all operators, we may get explicitly the different interaction terms. As an example applying (1) to the proton and the neutrons, we obtain

$$\text{(2)} \qquad \mathrm{p} = \mathrm{p}\pi^0 + \sqrt{2}\,\mathrm{n}\pi^+ + \sqrt{2}\,\Sigma^+\mathrm{K}^0 + \sqrt{2}\,\mathrm{Y}^0\mathrm{K}^+$$

$$\mathrm{n} = -\mathrm{n}\pi^0 + \sqrt{2}\,\mathrm{p}\pi^- + \sqrt{2}\,\mathrm{Z}^0\mathrm{K}^0 + \sqrt{2}\,\Sigma^-\mathrm{K}^+$$

and to 0 strangeness hyperons:

$$\Sigma^+ = \sqrt{2}\,\Sigma^0\pi^+ + \Sigma^+\pi^0\,, \qquad \mathrm{Z}^0 = \sqrt{2}\,\Sigma^+\pi^- - \mathrm{Z}^0\pi^0\,,$$

$$\mathrm{Y}^0 = \sqrt{2}\,\Sigma^-\pi^+ + \mathrm{Y}^0\pi^0\,, \qquad \Sigma^- = \sqrt{2}\,\mathrm{Y}^0\pi^- - \Sigma^-\pi^0\,.$$

It may be further remarked that in order to agree with normal isospin formalism, π-mesons should be given isospin 1; and for the same reason, neutral K-meson strangeness spin 1 and charged K-mesons ζ spin 1, if in each case we associate as third component of the triplet the π^0. The values of the other spins for each kind of meson should be 0. These assignements are indicated in the last three columns of Table II ([6]).

6. – Now that, by removing perturbations, we have obtained a possible insight for the regularities underlying the scheme of the particles, we must proceed in the reverse way and try to understand how perturbations have to work in order to alter this scheme and produce the observed more complicated one. The main point concerns the 0 strangeness hyperons which instead of beeing the two doublets here proposed are the Σ triplet and the Λ singlet. In order to rearrange the two doublets into a singlet and a triplet it is necessary that the virtual transitions occurring in the building of the self masses of the hyperons should mix the Z^0 and the Y^0 state. This may be achieved as may be seen from Fig. 3, if the virtual emission-absorption process may go through a succession of the kind: $\mathrm{Y}^0 - \mathrm{p} - \Sigma^+ - \mathrm{Z}^0$, for example, which is accompanied by the emission or absorption of a meson of each kind. Two different types of interactions between them may be thought of as the most easy approaches to this problem:

([6]) An exactly similar assignement of quantum numbers to elementary particles as those indicates in Tables I and II has quite indipendently been recently proposed by J. Tiomno: *Nuovo Cimento*, **6**, 69 (1957).

1) Let us first suppose, following the idea outlined by SCHWINGER (2) and by BUDINI and FONDA (7) that there exists a direct KKπ interaction:

$$\text{(3)} \qquad K \to K + \pi \qquad \text{or} \qquad K + \overline{K} = \pi \,.$$

Then, taking the preceding example, Y^0 goes to p and emits a $\overline{K}^-$, p then goes to Σ^+ and emits a K^0; K^0 and $\overline{K}^-$ interact to form a π^- which is absorbed by Σ^+ which thus transforms in Z^0. It is well known however that interaction (3) requires that parity doublets should exist for the K's; as no experimental evidence for them is actually at hand, one is rather inclined to avoid introducing this interaction, so we may try to look for another possibility.

2) This may be found if we assume that K $\overline{K}$meson pairs are also simultaneously produced or absorbed; as such a reaction goes on without any change in strangeness, it should follow the horizontal lines of our schemes and we should have:

$$\Sigma^+ \to Z^0 + K^+ + \overline{K}^0 \,, \qquad Y^0 \to \Sigma^- + K^+ + \overline{K}^0 \,,$$

$$Z^0 \to \Sigma^+ + K^0 + \overline{K}^- \,, \qquad \Sigma^- \to Y^0 + K^0 + \overline{K}^- \,.$$

Then according to our same example the two K^0 $\overline{K}^-$ produced successively when Y^0 goes first to P and then to Σ^+ may be absorbed simultaneously by Σ^+ which goes to Z^0.

We shall now briefly outline the formalism that has to be used in order to calculate these processes and which turns out to be practically the same for the two possibilities. The possible transformations consisting in the successive emission or absorption of a K and a $\overline{K}$ are obtained by applying twice in succession the K part Γ_K or $\Gamma_{\overline{K}}$ of the hamiltonian (1) to a given initial hyperon state. The resulting operators are as follows:

$$\text{(4)} \qquad \begin{cases} \dfrac{\Gamma_{\overline{K}}\Gamma_K}{2} = \omega_+\omega_-\chi_{3-3}\chi_{3+3} + \zeta_+\zeta_-\chi_{33+}\chi_{33-} + \zeta_+\omega_-\chi_{33-}\chi_{3+3} + \omega_+\zeta_-\chi_{3-3}\chi_{33+} \\ \text{or} \\ \dfrac{\Gamma_K\Gamma_{\overline{K}}}{2} = \omega_-\omega_+\chi_{3-3}\chi_{3+3} + \zeta_-\zeta_+\chi_{33+}\chi_{33-} + \omega_-\zeta_+\chi_{3+3}\chi_{33-} + \zeta_-\omega_+\chi_{33+}\chi_{3-3}. \end{cases}$$

In the following we shall consider only the first of these expressions the treatment of the other being quite similar.

The pairs of meson operators appearing in these formulae may now be rearranged in order to form a triplet and a singlet double meson states which may be labelled with a single letter $\varkappa$ as indicated below. In a similar way, we shall express the pairs of ω and ζ operators appearing in (4) by other new

(7) P. BUDINI and L. FONDA: *Nuovo Cimento*, **5**, 306, 666 (1957).

symbols thus defined:

$$(5)\qquad \begin{cases} \varkappa_{+1} = \chi_{3-3}\chi_{33+} \\ \varkappa_{01} = \dfrac{1}{\sqrt{2}}(\chi_{3-3}\chi_{3+3} - \chi_{33-}\chi_{33+}) \\ \varkappa_{-1} = \chi_{33-}\chi_{3+3} \end{cases} \qquad \begin{cases} \tau'_{+} = \zeta_{+}\omega_{-} \\ \tau'_{3} = \omega_{+}\omega_{-} - \zeta_{+}\zeta_{-} \\ \tau'_{-} = \omega_{+}\zeta_{-} \end{cases}$$

$$\varkappa_{00} = \frac{1}{\sqrt{2}}(\chi_{3-3}\chi_{3+3} + \chi_{33-}\chi_{33+}) \qquad I' = \omega_{+}\omega_{-} + \zeta_{+}\zeta_{-}\,.$$

With these new expressions, the operators (4) become:

$$(6)\qquad \frac{\Gamma_{\bar{K}}\Gamma_{K}}{\sqrt{2}} = (I')\varkappa_{00} + \sqrt{2}\tau'_{+}\varkappa_{-1} + \sqrt{2}\tau'_{-}\varkappa_{+1} + \tau'_{3}\varkappa_{01}.$$

It may now be very easily deduced that the operator I' is a scalar while τ'_{+}, τ'_{3}, τ'_{-} form a three vector which is equivalent to an $\frac{1}{2}$ isotopic spin and is represented by the three Pauli matrices. Therefore transformations between Σ^{+} and Y^{0} and between Z_{0} and Σ^{-} take place according to an isoscalar and an isovector interaction. The application of the same operators (4) to nucleons or Ξ's give instead:

	to nucleons	to Ξ's
$\dfrac{\Gamma_{K}\Gamma_{\bar{K}}}{\sqrt{2}}$	0	$2I'$
$\dfrac{\Gamma_{\bar{K}}\Gamma_{K}}{\sqrt{2}}$	$2I'$	0

Transitions between the doublets $\Sigma^{-}Z^{0}$ and $Y^{0}\Sigma^{-}$ will now obviously take place: in assumption (1) according to the π interaction Γ_{π} of hamiltonian (1); according to assumption 2) according to a $K\bar{K}$ interaction Γ_{2K}

$$(7)\qquad \begin{cases} \Gamma_{\pi} = \sqrt{2}\tau_{+}\chi_{-33} + \sqrt{2}\tau_{-}\chi_{+33} + \tau_{3}(\chi_{-33})\,, \\ \text{or} \\ \Gamma_{2K} = I_{\varkappa 00} + \sqrt{2}\tau_{+}\varkappa_{-1} + \sqrt{2}\tau_{-}\varkappa_{+1} + \tau_{3}\varkappa_{01}\,. \end{cases}$$

These cases are exactly alike relative to the τ dependence. Now the whole interaction term leading to the self mass of the hyperons will be proportional

$$(8)\qquad \frac{1}{\sqrt{2}}\Gamma_{\bar{K}}\Gamma_{K}\Gamma_{\pi} \sim \tau\cdot\tau'\,, \qquad \text{or} \qquad \frac{1}{\sqrt{2}}\Gamma_{\bar{K}}\Gamma_{K}\Gamma_{2K} \sim I\cdot I' + \tau\cdot\tau'\,,$$

which in both assumptions 1) and 2) leads to a $(\tau\cdot\tau')$ term which obviously will split the mass levels into an isosinglet and an isotriplet, the Λ and the Σ hyperon, as is in fact observed.

This way of obtaining the splitting of the hyperon mass levels may be compared with the one proposed according to the Goldhaber compound model and may be seen to be in fact equivalent to it. Here the τ spin characterizes the Σ^+Z^0, and $Y^0\Sigma^-$ pairs while the τ' spin may be thought of as pertaining to the Σ^+Y^0 and $Z^0\Sigma^-$ pairs; therefore each of the states Σ^+, Z^0, Y^0, Σ^- are characterized by the assignment of the values of two isospin third components τ_3 and τ_3', which have to be composed together when interactions are at work to form the total T_3 of the state, in a rather similar way (at least in first approximation) as is done in the Goldhaber model, where the τ_3 values of the nucleon and the K are combined to give the four compound states, $p\overline{K}^0$, $n\overline{K}^0$, $p\overline{K}^-$, $n\overline{K}\tau^-$, which, as was shown in Sect. 4, may de identified with the four unperturbed hyperons. In the present model, the isospin of the $\overline{K}$ has not a fundamental meaning, since it is derived as a combination of the isostrangeness operators ω and ζ. The reason why this concept of isospin of the K works in this case is as usual the smallness of the electromagnetic interaction which, with respect to the large strangeness dependence effect for the mass, makes the charged K's to have about the same mass as the neutral K's.

As a last remark on this question, the mass splitting for the hyperons leads us to define for the observed wave functions of the singlet and triplet neutral hyperon states the symmetric and antisymmetric combinations of Z^0 and Y^0. We then have

$$(9)\qquad \begin{cases} \Sigma^0 = \dfrac{1}{\sqrt{2}}\,(Y^0 - Z^0)\,, \\ Y^0 = \dfrac{1}{\sqrt{2}}\,(Y^0 + Z^0)\,. \end{cases}$$

If we now substitute in every explicit expression of the unperturbed Hamiltonian (1) the definitions of Z^0 and Y^0 obtained from (9), we shall obtain the form for the interaction energy when the perturbation which splits the triplet and singlet hyperonic levels is taken into account. So as an example, the nucleon-K-hyperon and the π-hyperon interactions which were given in (2) now become

$$(10)\qquad \begin{cases} p &= \sqrt{2}\,\Sigma^+K^0 + \Sigma^0K^+ + \Lambda^0K^+ \\ n &= -\Sigma^0K^0 + \sqrt{2}\,\Sigma^-K^+ + \Lambda^0K^0 \\ \Sigma^+ &= \Sigma^+\pi^0 - \Sigma^0\pi^+ + \Lambda^0\pi^+ \\ \Sigma^0 &= \Sigma^-\pi^+ - (\Sigma^+)\pi^- + \Lambda^0\pi^0 \\ \Sigma^- &= \Sigma^0\pi^- - \Sigma^-\pi^0 + \Lambda^0\pi^- \\ \Lambda^0 &= \Sigma^+\pi^- + \Sigma^0\pi^0 + \Sigma^-\pi^+ \end{cases}$$

It may easily be recognized that the new formulae are identical with those obtained from the hamiltonian first proposed by D'ESPAGNAT and PRENTKI ([5]).

7. – The second important question concerning perturbations should be how the differences of mass between baryons ought to be introduced in this scheme, and this point has not yet been carefully considered, so that at present we can only make a few remarks on this subject. Of course, we should expect that the different clothing of the 0 strangeness hyperons with respect to the nucleons and the Ξ's should give a different self mass for them, while the difference of the Σ and Λ masses should then of course be due to the splitting provoked by the interaction term (8). However, the complete symmetry which we have postulated between K and $\overline{\mathrm{K}}$ should bring with it that the mass of the Ξ's should be the same as the mass of nucleons. On this point our model differs from the compound model of Goldhaber, which postulates that Σ and Λ hyperons are compounds of a nucleon and a $\overline{\mathrm{K}}$, while Ξ's are compounds of a nucleon and two K's. Should we try however to modify our scheme in the same sense as GOLDHABER's in order to explain in the same way the greater mass of the Ξ's, we would spoil the assumed fundamental symmetry between K's and $\overline{\mathrm{K}}$'s, which is a characteristic feature of the whole model. There should then be only two ways to preserve its fundamental features and explain the greater mass of the Ξ's 1) First one may assume that the interaction constant Gk between baryon and $\overline{\mathrm{K}}$ is intrinsically different from the interaction constant $G\bar{k}$ between baryon and $\overline{\mathrm{K}}$: so that the self masses of nucleons and Ξ's turn out to be different: this assumption, however, spoils the similarity of all baryon-meson interactions which was one of the leading points of our reasoning. 2) One assumes that according to the present scheme the masses of nucleons and Ξ's should be the same, but for a secondary strangeness-dependent perturbation, of an as yet undetermined nature as long as we do not know what strangess is; this explanation also has to be introduced in a phenomenological way without any true physical insight; so that the question of mass differences is perhaps the weakest point of the present approach.

8. – We shall discuss now the necessity of describing the different states of the hyperons with three different quantum numbers. We wish to give some physical insight to the meaning of these numbers, and try to deduce if, as a reverse procedure of the method used in Sect. 4, when the baryon states are given with their characteristic labels, the nature of the meson emitted or absorbed may be obtained as a consequence of them.

It is easily seen that according to Tables I and II charge and strangeness

of baryons and mesons are given by the following relations:

$$\text{(11)} \qquad \begin{cases} C = \tau_3 + \zeta_3 \,, \\ S = \omega_3 + \zeta_3 \,. \end{cases}$$

Of course, just for symmetry reasons, we could as well define a third quantity which we shall denote by A, according to the relation:

$$\text{(11}a\text{)} \qquad A = \tau_3 + \omega_3 \,.$$

One may observe that by eliminating ω_3 and ζ_3 from these three equations, one obtains:

$$\frac{C + A}{2} = \tau_3 + \frac{S}{2} \,,$$

which may be considered as the equivalent of the Gell-Mann relation between charge, strangeness, and isotopic spin. For nucleons and Ξ's and π's for which $A = C$ (see Tables I and II last column) this relation reduces immediately to the Gell-Mann one; for the other particles no direct comparison between this relation and the Gell-Mann one can be made as the assignments of isotopic spins are different in both cases.

Now the labelling of the baryons with three quantum numbers indicate that we should have three conservation laws. From the relations (11) and (11a) we see, that if we assume that the total value of any three of the six quantities C, S, A, τ_3, ω_3, ζ_3 is conserved in any reaction, then all six of these quantities should be conserved. The effect of these six conservation laws may be most easily visualized if we refer to our baryon scheme: moving along an horizontal line, corresponding to pion emission, ω_3, ζ_3 and S remain constant, while baryonic τ_3, C and A change; along a vertical line, corresponding to neutral K emission, τ_3, ζ_3 and C remain constant, while baryonic ω_3, S and A change; finally, along a diagonal line, corresponding to charged K's emission, τ_3, ω_3 and A remain constant, while baryonic ζ_3, C and S change; therefore, the scheme appears as completely symmetric in the three kinds of transitions. However, as no physical meaning may be as yet attributed to A, it turns out that while π and K^0 transitions are accomplished with the change of only the baryonic charge for the first and only the baryonic strangeness for the second, the transitions connected with the third kind of meson must go on with change of both baryonic charge and strangeness, as is in fact observed for charged K's. Moreover it can easily be shown that for these transitions C and S of the meson must always have the same sign (both positive

or both negative): in fact consider a meson emission from a state I to a state II for which let us say ζ_3 of the meson is > 0. Then baryonic $\zeta_3^{\mathrm{I}} > \zeta_3^{\mathrm{II}}$ and from (11) applied to state I and II of the baryon

$$C_{\mathrm{I}} > C_{\mathrm{II}}\,, \qquad S_{\mathrm{I}} > S_{\mathrm{II}}\,.$$

This corresponds exactly to the characteristic assignment of strangeness to the charged K-mesons of the G-N scheme. To put if in other words: the G-N scheme is apparently based only on two conservation laws, charge and strangeness; but really it contains a further third fundamental assumption; namely the arbitrary assignement of the strangeness to K^+ and $(\overline{\mathrm{K}}^-)$'s; the present scheme, by assuming three conservation laws instead of two and relations (11) explains as a consequence of them also the G-N assignments of strangeness for charged K's.

Now the physical meaning to be given to the quantum numbers can most easily be understood as follows. The baryon possesses two well known kinds of spins: one is the isotopic spin τ and the other the strangeness spin ω, which has been considered already by some authors [3]; just as rotations in the τ space are connected with charge transformations, so rotations in the ω space are connected with strangeness transformations. Moreover both of these two three dimensional isospaces may be considered, as PAIS [8] as shown in a more general case, as subspaces of a four dimensional space, in which it is possible to describe a four dimensional isospin, which may be decomposed in the two dimensional isospins which we observe.

The existence of a third quantum number is now easily understood if we help ourselves with the simple Lee model which we have used for our baryons. If we take the bare baryon B^0 and cloth it with a π^+ a K^+ or a K^0, we complete the states of the upper square; these states are thus obtained just by using mesons of a given sign of strangeness and charge. In order to obtain the states of the lower square, we must reverse the signs of both charge and strangeness of the mesons without touching the bare baryon. This kind of transformation which reverses the signs of the strangeness and charge of the associated fields of the baryons without touching the nature of the baryon itself is considered in another paper [9] and will be called here the CS conjugation, in order to distinguish it from what is generally considered as charge conjugation for the baryons, which consists not only in transforming the signs of charge and strangeness to their opposite values, but also in transforming the baryon into its antibaryon. Thus if this kind of symmetry really exists,

---

([8]) A. PAIS: *Proceedings of the Fifth Annual Rochester Conference on High Energy Nuclear Physics* 1955.

([9]) P. BUDINI and N. DALLAPORTA: *Padua-Venice Conference on Mesons and recently discovered Particles*, September 1957.

the baryons of the lower square are just to be considered as CS conjugates of the baryons of the upper square, so their existence is predicted and justified by this reflection of values of charge and strangeness.

Now according to the choice we have made for the quantum numbers which label the baryon states, it is easily seen that the effect of the CS operation applied to any baryon is to reverse the value of all three τ_3, ω_3, ζ_3,

$$\mathrm{CS}\,\Psi(\psi_p, \psi_n, \psi_{\Sigma^+}, \psi_{Z^0}, \ldots) = \Psi(\pm\psi_{\Sigma^-}, \pm\psi_{\Sigma^0}, \pm\psi_{\Sigma^-}, \pm\psi_{Y^0}, \ldots .$$

The operations of $\exp[\pm i\pi\tau_2]$, $\exp[\pm i\pi\omega_2]$, $\exp[\pm i\pi\zeta_2]$ have the effect of reversing only one of these quantum numbers. It follows that the successive emission or absorption by any baryon of a $\pi^\pm$, a $K^0\overline{K}^0$ and a $K^\pm$ is equivalent to the CS operation, so that we shall have between these operators relations of the type

$$CS = \exp[i\pi(\pm\tau_2 \pm \omega_2 \pm \zeta_2)] . \tag{12}$$

This means that any of the three isospin rotations can be expressed as a function of the other two plus the CS conjugation, and thus that the third quantum number is connected with the reversal of sign of charge and strangeness of the meson fields.

RIASSUNTO

Si cerca di interpretare le osservate regolarità delle particelle elementari note fino ad oggi coll'assumere che, quando si trascurino perturbazioni secondarie alle quali si possono attribuire le osservate differenze di massa tra i barioni, le proprietà fondamentali di tutti i barioni sono le medesime; in particolare, tutti i barioni hanno da essere allora fermioni ed isofermioni secondo uno schema indicato in Fig. 3, sul quale figurano in ascisse le cariche elettriche ed in ordinate le stranezze, mentre tutti i mesoni sono bosoni ed isobosoni. Si assume che le sole transizioni possibili tra stati barionici sono quelle indicate dalle linee tratteggiate in Fig. 3, le linee orizzontali essendo dovute all'emissione od assorbimento di mesoni π carichi, quelle verticali di mesoni K^0 o $\overline{K}^0$, e quelle oblique di mesoni K carichi. Le transizioni sono regolate da tre diversi spin isotopici $\frac{1}{2}$, τ per i pioni, ω per i K neutri, e ζ per i K carichi, con un formalismo identico a quello usato per lo spin isotopico ordinario; i tre spin τ, ω e ζ rappresentano gradi interni di libertà del barione, i numeri quantici per ogni stato barionico dovuti a tali spin essendo indicati tra parentesi per ogni barione $(\tau_3, \omega_3, \zeta_3)$. Si fa vedere come tali ipotesi sono equivalenti alle regole di Gell-Mann-Nishijima e come introducendo opportune perturbazioni tra i campi mesonici, i doppietti Σ^+Z^0 e $Y^0\Sigma^-$ vengano mescolati e diano origine al singoletto Λ^0 ed al tripletto $\Sigma^{+,0,-}$, come in effetti si osserva. L'hamiltoniano qui usato si trasforma allora in quello proposto da d'Espagnat e Prentki. Per finire viene discusso il senso fisico da attribuire ai tre numeri quantici dei barioni.

IL NUOVO CIMENTO Vol. VII, N. 2 16 Gennaio 1958

Gravitational Fields and Quantum Mechanics.

T. Regge

Istituto di Fisica dell'Università - Torino
Istituto Nazionale di Fisica Nucleare - Sezione di Torino

(ricevuto il 7 Ottobre 1957)

Summary. — Several kinds of measurements of gravitational fields are here qualitatively discussed. It is shown that no one of them yields satisfactory results if the region in which the field is measured has linear dimensions smaller than $L = Gh/c^2$.

1. – The problem of the measurability of gravitational fields or more properly of their averages on a given space-time domain (here shortly GFA) from the point of view of quantum mechanics seems to be a hard and a premature one and no satisfactory theory of this subject has been so far constructed.

Most difficulties arise from the non-linearity of Einstein's equations since it is clear that one cannot go very far in studying a linear approximation of these general equations.

In the present note we shall attempt a discussion of some features of the theory of gravitation which can be deduced from simple qualitative arguments like ideal experiments.

No claim of rigor and of completeness is here advocated to our conclusions, we think that they should be more valued as a hint to a further investigation than as a clear cut result.

Our discussion essentially shows that Einstein's field dynamics (following Wheeler here called Geometrodynamics) cannot be a true parallel theory of Electrodynamics and that important differences arise whenever high accuracy is desired and whenever measurements are carried out in small regions of linear dimension D of the order of $L = \sqrt{hG/c^3} \approx 4 \cdot 10^{-33}$ cm, where $G = 6.67\ 10^{-8}\ \mathrm{cm^3\ s^{-2}\ g^{-1}}$ is Newton's constant.

Quite an amount of interesting arguments have been proposed by Wheeler and others ([1-3]) supporting the view that important changes should be expected on the geometrical structure of space at such small distances.

We refer to the original papers by Wheeler and co-workers for a complete discussion of which we wish to give here short account.

1) The field fluctuations over regions of space-time dimensions of the order of L^4 are of the order of magnitude of one in the potentials.

2) Consequently a microcurvature of space over such small distances should be expected.

3) Most likely space shows multiple connectedness if observed on such a detailed scale. There are no *a priori* reasons why a multiple connected space should be rejected as unphysical.

Quantization of geometrodynamics can be carried out in principle with the help of Feynman's method of sum over histories. On this difficult task Misner has made quite important progresses ([4]). In the following the gravitational field will be measured in several different ways. In spite of these differences they all suffer the same limitation thus supporting the view that this may be a general feature of a possible theory.

2. – Before beginning the main problem of the measurement of GFA we would like here to argue about the meaning of « point mass » in general relativity. In the classical physics a point mass is usually meant to be a body satisfying the following properties:

i) It has a given mass $M \neq 0$.

ii) Its acceleration depends on the value which the field of force has in the point where the body is located and it depends only on this value.

In the Newtonian approximation nothing prevents us to think that these two conditions can be realized as closely as wanted.

Elementary particles have been since long treated as locally interacting. Difficulties arise only in connection with the well known self-energy infinities.

In general relativity, once the mass of the body is fixed, condition ii) is hardly realizable in virtue of the non-linearity of Einstein field equations.

([1]) J. A. Wheeler: *Phys. Rev.*, **97**, 520 (1955).

([2]) C. Misner abd J. A. Wheeler: *Classical Physics as Geometry*, in *Rev. Mod. Phys.*, reference in proof.

([3]) J. A. Wheeler: *On the Nature of Quantum Geometrodynamics*, in *Rev. Mod. Phys.* (reference in proof).

([4]) C. Misner: *Rev. Mod. Phys.* (reference in proof).

This is best seen by an analysis of a paper by INFELD and SCHILD [5] on the motion of test particles. These authors give a simple derivation of the geodesic postulate from Einstein equation. They were able to show that a test particle, in the limit in which its mass vanishes, will move along a geodesic. If the mass of the particles has instead a fixed finite value it is impossible to define exactly a geodesic because the body itself will perturbe the metric of the surrounding space in a region of size $\approx MG/c^2$. Moreover it is very unlikely that even if the geodesic can be defined the body will actually follow it. The derivation of the geodesic postulate is there valid only if the background space (defined as the one we would get putting $M = 0$) is with good approximation euclidean in the mentioned region of size MG/c^2 (*). Any departure from this condition will cause the test body to undergo a different motion independently from its internal structure.

The motion of our test body is therefore determined by the structure of the background field over the mentioned region.

In other words the acceleration of the body depends on the values of the field spread over a domain of size $R - MG/c^2$. No particle of this kind will ever behave as a point mass and satisfy ii). R can be regarded as the minimal possible size for a body of mass M. It is worth pointing out that the non-linearity of the field equations plays an essential role in the derivation of this result.

3. – We shall discuss here several methods of measurement of GFA. For the sake of simplicity we shall suppose that the field to be measured can be treated in the linear approximation. Non-linear phenomena will appear only near the test bodies. Furthermore the speed of these bodies will be assumed to be much smaller than c. Under these conditions an obvious experiment could be carried out by determining the momentum change $\Delta \boldsymbol{p}$ of a body of mass M during a given time. We shall call the quantity

$$\Gamma = \frac{\Delta \boldsymbol{p}}{c^2 M \cdot T},$$

GFA over the region of size D covered by the body and during the time T. If the body is localized within the region of size D, $\Delta \boldsymbol{p}$ will be uncertain by the amount h/D. Moreover M cannot exceed Dc^2/G for what said before.

---

[5] L. INFELD and A. SCHILD: *Rev. Mod. Phys.*, **21**, 408 (1949).

(*) Mathematically this is expressed by the condition that $a_{\mu\nu}$ should be small sompared with $\eta_{\mu\nu}$ wherever it is not possible to retain the first term only in the expansion (2.05). It is easy to see that all the following derivations break down in absence of this condition.

Γ is therefore affected by the error

$$\Delta\Gamma \approx \frac{h}{M\cdot c^2 T\cdot D} > \frac{L^2}{D^2\cdot cT}\,.$$

This error depends only on the universal constants h, c, G and on the space-time structure of the measurement. Actually there are other sources of error. One is that the body may radiate gravitational waves during the process. The true nature of gravitational waves is still subjected to some discussion. As a provisional hypothesis we shall assume for them properties strictly similar to those of the electromagnetic waves. We can then follow the discussion of BOHR and ROSENFELD (6) with slight changes in the coupling constants. We should expect then that the uncertainty due to the radiated field is of the kind

$$\Delta\Gamma_R \approx MTDA$$

where $A = cL^2/hTD^2Z$; Z is the largest between D and cT.

If the body is bound to a spring of elastic constant c^2M^2TA the correction entirely cancels out. This method works only if the period of the oscillator body+spring is much larger than T. This leads to the inequality

$$\frac{1}{\sqrt{MTA}} \gg cT\,. \tag{7}$$

This leads again to $M \ll Dc^2/G$ if $D < cT$ and to $M < D^3c^2/(cT)^2\cdot G$ if $D > cT$, thus confirming the adopted limitation for the mass.

We complete the discussion by pointing out that the field induced by a quantum whose frequency may range from 0 to $\frac{1}{2}T$ at the distance D may be as high as $L^2/D^2\cdot cT$. Since such a quantum is needed in order to define a pulse of duration T in the observing radiation an additional uncertainty in Γ is introduced of the same order of magnitude of $\Delta\Gamma$.

4. – The arguments above lead to the conclusion that on a space time region of size D the uncertainty in the Christoffel symbols should be about L^2/D^3 and in the metric tensor (*) correspondingly of the order of L^2/D^2. If D is a macroscopic length the sedeviations are phantastically small and even on the atomic scale they are still negligible. However when D becomes comparable with L it becomes increasingly difficult to mantain the usual notions of space and the effect of the microcurvature becomes evident.

Quite in agreement with these conclusions is the result of a close analysis of the Heisenberg microscope experiment. Apart from the implicit enormous

(6) N. BOHR and D. ROSENFELD: *Danske Vid. Selskab. Math. Phys. Medd.*, **12**, 8 (1933).

difficulties arising from the generalized Carnot principle (7) we meet a fundamental obstacle when high accuracies are desired.

In the Brillouin apparatus the position of the body is measured by sending a suitable superposition of waves through a wave guide. If we wish to narrow down the position of the body to an uncertainty of less than D then forcedly we must use waves of frequency up to hc/D. The metric field inside the region where we know to be the body is then uncertain by the amount $\Delta\Gamma \approx L^2/D^2$ introduced by the observing radiation. There is no use trying to let $D \to L$ because the distance D' of the body from any point is uncertain by an amount $\cong L^2/D$.

From this point of view bodies are never localized. In the non local quantum field theory a question of primary importance was to decide whether or not field operators commute at space like distances or, in other words, if we have local or non-local commutativity. From our point of view before asking this question one should try to give a well defined meaning to the space like or time like attribute when the considered interval is comparable with L.

5. – It may seem premature to base the deduction in Sect. 4 on a single experiment. Therefore we discuss quite different procedures showing that they yield the same qualitative results.

One could, for instance, consider a pendulum. For « pendulum » we mean here a body without internal degrees of freedom hung to a wire (or equivalent constraint). We allow a good deal of ideal properties to our apparatus and suppose that the wire is inextensible. The length of it is Q, the mass of the pendulum is M, its radius R. We measure the period τ of the pendulum and then we deduce $g = c^2\Gamma$ from

$$\Gamma = \frac{4\pi^2 Q}{c^2\tau^2} \quad \text{if} \quad R \ll Q \,. \tag{5}$$

If the oscillations are observed during the time T we expect to make an error $1/T$ in $1/\tau$. We shall have correspondingly

$$\Delta\Gamma \approx 4\pi^2 Q \frac{2}{c^2 T\tau} \gg \frac{8\pi^2 R}{c^2 T\tau} \,. \tag{6}$$

Furthermore if we want a GFA over a region of size D the pendulum should not swing farther than D. In the ground state it still swings as far as $\sqrt{hQ/gM\tau}$. We are forced to require that

$$D^2 > \frac{hQ}{gM\tau} \,. \tag{7}$$

(7) L. Brillouin: *Journ. Appl. Phys.*, **25**, 887 (1954).

From (5) and (7) we get then

$$\frac{1}{\tau} < \frac{D^2 g M}{hQ} \approx \frac{4\pi^2 D^2 M}{\tau^2 h} \quad \text{or} \quad \tau < \frac{4\pi^2 D^2 M}{h} . \tag{8}$$

(6) is then equivalent to (remembering $M < Rc^2/G$)

$$\Delta\Gamma \gg \frac{8\pi^2 R}{c^2 T\tau} \gg \frac{2L^2}{cT \cdot D^2} . \tag{9}$$

The pendulum does not measure Γ with any more accuracy than the first method. Another way to measure the GFA is provided by the dynamometer. An ideal apparatus of this kind consists of a body of mass M hung to a perfectly elastic spring of constant k. Under the pull of the body the spring is lengthened by the amount ξ.

The acceleration of gravity is then given by

$$g = \frac{K\xi}{M} . \tag{10}$$

The hanging body however is not usually at rest and we need to measure its position twice, at the times t at the time $T+t$ (T being a half integer number of periods) and to average the positions then obtained in order to deduce ξ. The energy of the oscillator is therefore uncertain by the amount h/T

If the GFA is to be determined over a region smaller than D the amplitude of the oscillations should not exceed this value. Consequently

$$D^2 > \frac{h}{kT} \quad \text{or} \quad k > \frac{h}{TD^2} . \tag{11}$$

The error in the measure of g arises from the uncertainty in ξ which s larger than MG/c^2. It follows

$$\Delta g = \frac{g\Delta\xi}{M} > \frac{h\Delta\xi}{MTD^2} > \frac{hG}{c^2 T \cdot D^2} = \frac{L^2 c^2}{cT \cdot D^2} .$$

An alternative method consists in placing an atom of radius D, decaying with the emission of a photon of frequency ν, on the region where we wish to measure the GFA. If the gravitational potential γ is not too large we can deduce it from the observed red shift $\Delta\nu$ by the formula

$$\gamma = \frac{\Delta\nu}{\nu} - \gamma_A ;$$

γ_A is the potential induced by the atom itself which must be subtracted in order to measure the background field only. T is the length of the experiment. We suppose $T\nu \gg 1$.

However the larger is ν the larger is the indeterminacy $\Delta\gamma$ in γ_A because the mass of the atom during the transition is only known with the error $h\nu/c^2$.

We have within the atom $\Delta\gamma_A = h\nu G/Dc^4$, this is also the indeterminacy in γ and agrees with the previous experiments (*):

$$\Delta\gamma = \frac{h\nu G}{Dc^4} > \frac{L^2}{cT \cdot D} .$$

6. – We hope that our discussion has helped to point out some of the features and difficulties of a quantum theory of gravitation.

Most probably a satisfactory theory of this kind will proceed along quite different patterns of thought from those to which we have been used in dealing with the classical Riemannian Geometry.

We must expect that the usual space-time continuum will show upsetting features if observed on a scale of distances comparable with L. However, as clearly stressed by WHEELER, classcal Geometrodynamics is already so distinctively well founded from the logical point of view that it is certainly worth giving a close look to quantum Geometrodynamics.

* * *

The author wishes to thank Prof. M. VERDE for a critical reading of the manuscript and many discussions. While this paper was submitted for publication we noticed that similar views had been supported by O. KLEIN in a lecture delivered at the « Congresso Internazionale sulle Costanti Fondamentali della Fisica » (6-11 September 1956) ([8]). We are indebted also to Prof. J. A. WHEELER for many discussions on this subject.

(*) It may not be obvious that if the average of a function F over the space-time region Σ is known with an error F then the average grad F over a region of comparable size D can be measured only with the error $\Delta F/D$. Actually a measurement of grad F could be performed by measuring F on two identical regions Σ_1 and Σ_2 of size D about and shifted apart at the distance D and taking the ratio: $(F_1 - F_2)/D$. Such a ratio can be easily expressed as an average grad F over the region sum of Σ_1 and Σ_2 and the intermediate points. The error in the above measured grad F is clearly $\Delta F/D$ apart from an insignificant numerical factor.

([8]) O. KLEIN: *Suppl. Nuovo Cimento*, **6**, 344 (1957).

RIASSUNTO

In questo lavoro vengono discussi alcuni metodi di misura del campo gravitazionale. Semplici considerazioni di carattere fisico permettono di dedurre che nessuno di essi può considerarsi soddisfacente se la regione in cui il valore medio del campo è determinato ha dimensioni lineari più piccole di $L = Gh/c^2$.

IL NUOVO CIMENTO Vol. VII, N. 2 16 Gennaio 1958

Experimental Determinations of the Λ^0 and Σ^- Spins (*) (+).

F. Eisler, R. Plano, A. Prodell, N. Samios, M. Schwartz and J. Steinberger

Columbia University and Brookhaven National Laboratory - New York

P. Bassi, V. Borelli, G. Puppi, H. Tanaka, P. Waloschek and V. Zoboli

Istituto di Fisica dell'Università - Bologna

M. Conversi, P. Franzini, I. Manelli, R. Santangelo and V. Silvestrini

Istituto di Fisica dell'Università - Pisa

G. L. Brown, D. A. Glaser and C. Graves

University of Michigan - Ann Arbor, Michigan

(ricevuto il 13 Dicembre 1957)

Summary. — We discuss the applicability of the argument of Adair [1] to the determination of the hyperon spins on the basis of the observed distribution in the production angle for the process $\pi+N\to Y+\theta$. Because of the pronounced backward and forward peaking of these distributions it is found possible to use a large fraction of the events without jeopardizing the validity of the argument. We find from measurement of the distribution in the correlation angles between incident and outgoing pions that the spins of both the Λ^0 and Σ hyperons are one half. The only assumptions necessary to this result are 1) that the θ spin is zero and 2) that the interaction radius for strange particle production is not pathologically large.

1. – Introduction.

If the state of polarization of a particle of given spin is known, and the particle decays spontaneously into two others, the distribution in the absolute value of the cosine of the angle of decay relative to the axis of polarization is

(*) This research is supported by the Atomic Energy Commission and the Office of Naval Research.

(+) Presented at the Conference on Elementary Particles, Venice, September 1957.

a consequence of conservation of angular momentum. Conversely, if the angular distribution is measured, the spin can be determined. The difficulty usually is that the state of polarization of the decaying particle is not known. We are indebted to ADAIR [1] for an argument concerning the nature of the polarization of hyperons in the production process which permits the determination of the spins. This paper is an application of the Adair argument to the determination of the Λ^0 and Σ spin.

2. – Adair argument.

Consider the reaction (1) $\pi + N \to Y + \theta$, the production of a heavy meson and hyperon in a π-p collision. Y represents Λ^0, Σ^+, Σ^- or Σ^0, and θ represents θ^0 or θ^+. We assume that the initial nucleon is unpolarized, that the pion has zero spin [2] and that the θ has zero spin. This last assumption will be considered in detail later. Let the axis be along the direction of motion of the incident π. *Consider now only those outgoing waves with z component of orbital angular momentum* $m_L = 0$. For our choice of z axis the incident orbitals has zero z component, so that $m_Y = m_N$. The target proton is unpolarized by assumption, so that the hyperon is produced in the states $m_Y = +\frac{1}{2}$ and $m_Y = -\frac{1}{2}$ with equal probability and no phase correlation.

The state function of the products of the hyperon can now be written in terms of a parity conserving and non-conserving part. For the distribution in $\cos\gamma|$, that is in the absolute value of the cosine angle between the z axis and the decay fragment, the interference term between the two cancels and the distribution is unique. We give the distributions in the decay $Y \to \pi + N$ for the three lower hyperon spin possibilities:

(2)

Spin	$P\lvert\cos\gamma\rvert$
1/2	1
3/2	$\frac{1}{2}(1 + 3\cos^2\gamma)$
5/2	$\frac{3}{4}(1 - 2\cos^2\gamma + 5\cos^4\gamma)$.

In the limit of very large spin, the distribution approaches $P(|\cos\gamma|) = 1/\sin\gamma$ as can easily be seen from a classical argument.

[1] R. ADAIR: *Phys. Rev.*, **100**, 1540 (1955).

[2] W. F. CARTWRIGHT, C. RICHMAN, M. N. WHITEHEAD and H. A. WILCOX: *Phys. Rev.*, **91**, 677 (1953); R. DURBIN, H. LOAR and J. STEINBERGER: *Phys. Rev.*, **83**, 646 (1951); **84**, 581 (1951); D. L. CLARK, A. ROBERTS and R. WILSON: *Phys. Rev.*, **83**, 649 (1951); **85**, 523 (1952).

3. – Useful angular interval in production.

3·1. *Effect of modes with* $m_L \neq 0$. – The important condition $m_L = 0$ is fulfilled identically for production angles in process (1) of zero and 180°. This is an angular interval of measure zero, and there will be no production events at these precise angles. It is therefore of practical importance to see to what extent the argument may be used at other production angles, where the condition $m_L = 0$ is not fulfilled identically.

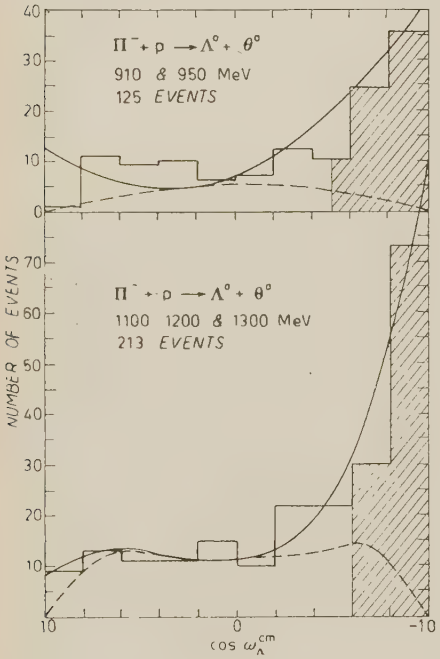

Fig. 1. – Distribution in the center of mass production angle ω for the process $\pi^- + P \to \Lambda^0 + \theta^0$. The solid curves represent fits in terms of S and P and S, P and D waves for the upper and lower figures, respectively. The dotted curves represent the maximum $m_L \neq 0$ contribution to the fit. The shaded areas are the areas accepted for the Adair analysis.

It is then important to notice that the waves of different m_L, $m_L \neq 0$ do, not interfere in amplitude because of their different azimuthal dependence, and the effect of a component with given $m_L \neq 0$ can be found by adding the proper amount of the distribution for this state into the final distribution. We give an example. Consider the effect of a contribution of 10% $m_L = \pm 1$ wave on the distributions (2). If the Y spin is $\frac{1}{2}$, there is of course no change. If the Y spin is $\frac{3}{2}$, then the $m_L = \pm 1$ wave will result in a distribution of the form $\alpha P_{\frac{1}{2}} + \beta P_{\frac{3}{2}}$. $P_{\frac{1}{2}}$ is the distribution $\frac{1}{2} + \frac{3}{2}\cos^2\gamma$ of (2) and $P_{\frac{3}{2}}$ is the distribution for $|m_Y| = \frac{3}{2}$, $P_{\frac{3}{2}} = \frac{3}{2} - \frac{3}{2}\cos^2\gamma$. The relative magnitudes of α and β depend on the details of the strong interaction. If, for example, $\alpha = \beta$ the resulting distribution for 10% $m_L = \pm 1$ will be $P|\cos\gamma| = \frac{1}{2}(1.1 + 2.7\cos^2\gamma)$. For larger Y spin the change in the expected distribution becomes weaker, and disappears entirely in the case of very large spin.

3·2. *Extent of the* $m_L \neq 0$ *contamination.* – Any understanding of the extent of the $m_L \neq 0$ contribution must come, of course, from a study of the production process. In this analysis we are using the processes *a*) $\pi^- + P \to \Lambda^0 + \theta^0$ and *b*) $\pi^- + P \to \Sigma^- + \theta^+$, at pion kinetic energies of 910, 950, 1100, 1200, and 1300 MeV in the laboratory. We will now consider these processes in some

detail. The observed angular distributions ([3]) are shown in Fig. 1 and 2. The energies are sufficiently close to threshold (770 MeV for process *a*), 905 MeV for process *b*)) so that only small angular momenta can be important. The centrifugal barrier limits the higher l value: $l_{max} \lesssim Pr/h$, where P is the center of mass momentum of either of the outgoing particles and r is the interaction radius. We assume that the interaction radius is no more than 10^{-13} cm, and analyse the combined data for Λ^0 production at 910 and 950 MeV in terms of S and P waves, and those at 1100÷1300 MeV in terms of S, P and D. For the Σ^- production, the data at 950 are analyzed in terms of S waves, those at 1100 MeV in terms of S and P, and those at 1200 and 1300 MeV in terms of S, P and D.

It is not possible to find the amplitudes of the different partial waves from the observed distributions since the number of free parameters exceeds the number of observables. The fit can be obtained in an infinite number of ways. In particular, it is possible to fit the distributions without any $m_L \neq 0$ contribution. We have also made a fit to the distributions of Fig. 1 and 2 with *maximal* $m_L \neq 0$ contributions. To illustrate the procedure consider the combined Λ^0 production distribution at 910 and 950 MeV. According to the considerations above, it is to be fitted with S and P waves, that is, with a distri-

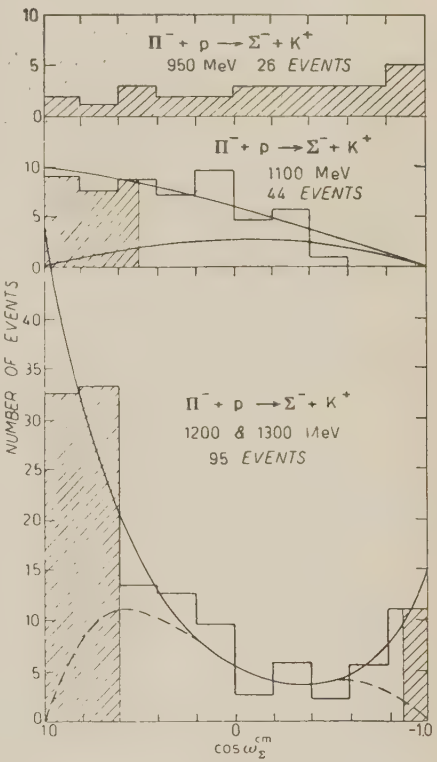

Fig. 2. – Angular distribution in the barycentric system for the process $\pi^- + P \rightarrow \Sigma^- + \theta^+$. The data have been subjected to a small correction for the dependence on the production angle of the efficiency for detecting the Σ^- decay. The solid curves represent fits in terms of S, S and P, and S, P and D waves for the upper, middle and lower figures respectively. The dotted curves represent the maximum $m_L \neq 0$ contribution to the fit. The shaded areas are those accepted for the Adair analysis

([3]) Reported by D. Glaser and P. Waloschek at the Conference on Elementary Particles in Venice, September 1957.

bution of the form

$$|A + B\cos\omega|^2 + |C|^2 \sin^2\omega\,.$$

The $\sin^2\omega$ term corresponds to $m_L = \pm 1$. Because of the arbitrary phase of B relative to A, this can be fitted in an infinite number of ways to the general distribution available to S and P states: $a + b\cos\omega + c\cos^2\omega$. The fit which maximizes $|C|^2$ is shown in Fig. 1. In the cases where S, P and D waves are permitted, the distribution has the form

$$|[A + B\cos\omega + C(3\cos^2\omega - 1)]|^2 + \sin^2\omega\,|(D + E\cos\omega)|^2 + |F|^2 \sin^4\omega\,.$$

The first term is $m_L = 0$, the second $m_L = \pm 1$, the third $m_L = \pm 2$. Again there are many ways of getting the same angular distribution, but the maximum $m_L \neq 0$ contribution is obtained by allowing the interference of the P and D $m_L = \pm 1$ terms (D and E), to simulate as well as possible the observed forward peak. Again the fits with maximum $m_L = 0$ waves are shown in Fig. 1 and 2. These fits are analytically the following:

(3)

1) Λ^0 at 910 and 940 MeV

$$P(X) = (1.4 - 5.0X)^2 + 5(1 - X^2)$$

2) Λ^0 at $1100 \div 1300$ MeV

$$P(X) = (3.3X - 6.17X^2)^2 + (1 - X^2)\,|3.37 + 5.05\exp[1.64i]|^2$$

3) Σ^- at 950 MeV

$$P(X) = \text{constant}$$

4) Σ^- at 1100 MeV

$$P(X) = (1.72 + 1.43X)^2 + 2.8\,(1 - X)^2$$

5) Σ^- at 1200 and 1300 MeV

$$P(X) = (1.69X + 5.4X^2)^2 + (1 - X^2)\,|2.38 + 3.9X\exp[1.0i]|^2\,.$$

Where $X \equiv \cos\omega$.

For the purposes of the spin analysis we have selected the events in the shaded region in a rough attempt to balance the possible systematic error due to the $m_L \neq 0$ contamination, and the statistical error. The maximal contaminations in the angular interval of acceptance for the complete samples, is, according to (3)

11 % in the case of Λ^0 production,

14 % in the case of Σ^- production.

4. – Spin of θ.

It was pointed out in Sect. **1** that an essential condition for application of the Adair argument is that the spin of the θ is zero. This is not yet definitely proven, but there is experimental evidence which makes it appear very probably that the spin is really zero. We list the most relevant:

a) The τ^+ decay. The observed angular and energy correlations agree very well with the predictions (phase space) for spin zero ([4]). Spin 1 is not a fit ([5]) and can also definitely be ruled out on the basis ot the $2\pi^0$ decay of the θ^0 ([6]). The theory ([7]) has no definite prediction for spin 2 but permits a whole continuum of possibilities, depending on the relative amplitudes of different orbital states of the outgoing pions. A particular combination of (2, 0) and (0, 2) states will fit the data, but the fit in the case of zero spin is much more striking since there are no free parameters. In general for higher spin values, it is possible to obtain fits with even, but not with odd spin values.

b) Polarization of the μ in $\theta^+ \to \mu^+ + \nu$ decay. The polarization of the μ-meson has been observed ([8]) to be essentially complete with a 10% precision. This is the result expected for spin zero θ's on the basis of the same models which have been successful in the similar case of pion decay. Again, it is also possible to get the same result for spin 2 θ's, but this is only one result and of many theoretical possibilities for spin 2. In general the μ-polarization would not be expected to be complete for spin 2.

c) Many groups including our own, have searched for correlations in production and decays angles for the θ^0 and θ^+, correlations which would point to polarization and non-zero spin of the θ. No statistically significant correlations have been observed.

d) The γ-stability of the $\theta^+ \to \pi^+ + \gamma$ can only be understood for zero spin ([9]).

We conclude that although the zero spin of the θ has not been established conclusively, there is a large amount of very suggestive evidence pointing in this direction and it would seem to be a good working hypothesis at present.

([4]) See for instance: M. BALDO-CEOLIN, A. BONETTI, W. D. B. GREENING, S. LIMENTANI, M. MERLIN and G. VANDERHAEGHE: *Nuovo Cimento*, **6**, 84 (1957).

([5]) J. OREAR: *Phys. Rev.*, **106**, 834 (1957).

([6]) F. EISLER, R. PLANO, N. SAMIOS, M. SCHWARTZ and J. STEINBERGER: *Nuovo Cimento*, **5**, 1700 (1957).

([7]) R. H. DALITZ: *Phil. Mag.*, **44**, 1068 (1953).

([8]) Report of R. KARPLUS, at the Conference on Elementary Particles, Venice, September 1957.

([9]) R. H. DALITZ: *Phys. Rev.*, **99**, 915 (1955).

5. – Experimental results.

After these somewhat lengthy preliminaries we come to the experimen itself. The same group of bubble chamber exposures which have already been used in an analysis of parity conservation in hyperon decay ([10]) is being used for this spin analysis. For the particulars of the exposures we refer to the previous publication. In all there are 264 Λ^0 decays and 165 Σ^- decays of which 145 and 97 respectively are in the angular interval of acceptance of Fig. 1 and 2 (see Sect. 3·2) ([11]). For these events we have computed the angle γ between the incident pion and the decay pion, after the decay pion (but not the incident pion) is transformed to the center of mass of the decaying hyperon. This method of computation of γ neglects the relativistic transformation of the spin direction, which is small at our center of mass velocities (.15÷.4) ([12]). The resultant distributions in $|\cos\gamma|$ are given in Fig. 3 and 4.

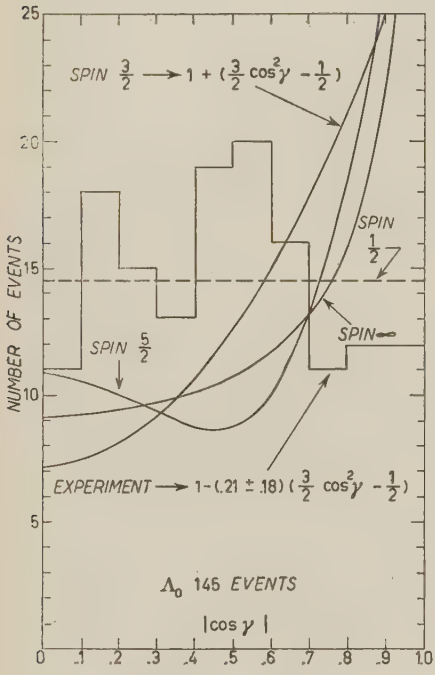

Fig. 3. – Distribution in the correlation angle γ between the incident and decay pion for the process $\pi^- + P \to \Lambda^0 + \theta^0$, $\Lambda^0 \to \pi^- + P$ events with production angle in the acceptance region of Fig. 1.

The data of Fig. 3 include a small correction (2 events) for a certain selection bias. It can happen, in Λ decay, that the decay pion is emitted backwards, and that its laboratory energy is consequently small. The range of the pion may then be so short that the V is not detected unless the associated θ is also visible. In the liquid hydrogen chamber the effect is negligible. In the propane chamber 1.6% of all Λ decays are expected to be of this type.

([10]) Demonstration of Parity Non-Conservation in Hyperon Decay, *NEVIS* no. 58, EISLER *et al.*

([11]) Here we have included some results of R. K. ADAIR and L. LEIPUNER: *Phys. Rev.* (to be published). We wish to thank Drs. ADAIR and LEIPUNER for making their results available to us. The data are at an incident pion energy of 950 MeV and consist of 26 Λ^0 decay events, of which 11 are in the acceptance region.

([12]) We are grateful to Prof. G. C. WICK for clarification of this point.

Although the correction is quite small, it has been included because the missed events are in a particular region of $\cos\gamma$, $-1.0 \leqslant \cos\gamma < -.8$, and the distribution would otherwise be systematically in error.

To compare these observed distributions with those expected for various spin values we have analyzed the experimental result in terms of the distribution

$$P|\cos\gamma| = 1 + A(\tfrac{3}{2}\cos^2\gamma - \tfrac{1}{2}) .$$

We find $A = -.21 \pm .18$ for the Λ^0 and $A = -.44 \pm .24$ for the Σ^-. The error is in the sense of the standard deviation. The comparison between the experimental result and the expectations for the various spin values are given in Table I. The agreement with spin $\frac{1}{2}$ is acceptable, although not as good as one would like. The agreement with higher spin values is not possible. For the Λ^0 of spin $\frac{3}{2}$ the discrepancy would be 7 standard deviations and for the Σ of spin $\frac{3}{2}$ it would be 6 standard deviations. If, for the Λ^0, we take the maximum permissible $m_L \neq 0$ contamination, then the expected A value is somewhere between 1.0 and .68, for spin $\frac{3}{2}$ (see Sect. 3·1), still firmly excluded, and similarly for the Σ. The discrepancy increases with increasing spin.

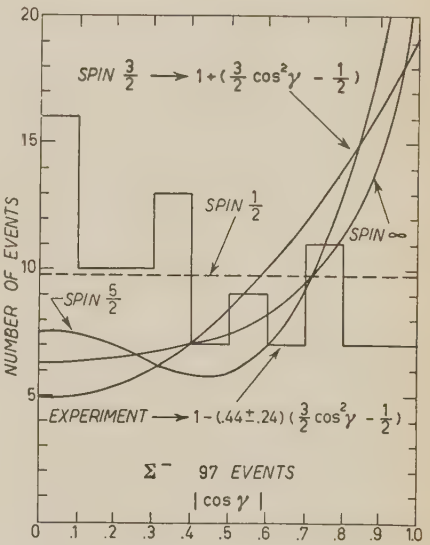

Fig. 4. – Distribution in the correlation angle γ between the incident and decay pion for the process $\pi^- + P \to \Sigma^- + \theta^+$, $\Sigma^- \to \theta^- + N$ for events in the acceptance region of Fig. 2.

TABLE I.

Spin	A expected	(A expected) − (A experiment) for Λ^0	for Σ^-
$\frac{1}{2}$	0	$-.21 \pm .18$	$-.44 \pm .24$
$\frac{3}{2}$	1	$+1.21 \pm .18$	$1.44 \pm .24$
$\frac{5}{2}$	1.14	$1.35 \pm .18$	$1.60 \pm .24$
$\frac{7}{2}$	1.19	$1.40 \pm .18$	$1.65 \pm .24$
∞	1.25	$1.46 \pm .18$	$1.69 \pm .24$

6. – Conclusions.

It is concluded that the spin of both the Λ and Σ hyperon are one half, subject only to conclusive demonstration that the spin of the θ is indeed zero.

RIASSUNTO

Viene discusse la applicabilità dell'argomento di ADAIR per la determinazione dello spin degli iperoni prodotti nel processo $\pi+N \to Y+\theta$. Poichè in questo processo le distribuzioni angolari di produzione mostrano che gli angoli in avanti e in dietro sono favoriti, è possibile usare una notevole parte degli eventi senza intaccare la validità dell'argomento. Viene dimostrato, attraverso l'analisi delle correlazioni angolari tra il piano di decadimento dell'iperone e il piano incidente, che lo spin degli iperoni Λ^0 e Σ^- è $\frac{1}{2}$. Le ipotesi necessariamente fatte per ottenere questo risultato sono: 1) che lo spin della θ sia zero; 2) che il raggio di interazione per la produzione di particelle strane non sia eccezionalmente grande.

NOTE TECNICHE

Photometric Analysis of the Tracks in the Nuclear Emulsions (*).

II. – Measurement of Photometric Width.

P. G. Bizzeti and M. Della Corte

Istituto di Fisica dell'Università - Arcetri (Firenze)

(ricevuto il 12 Settembre 1957)

Summary. — A simple and speedy method for the measurement of the photometrical width of the tracks in nuclear emulsions is described. The independence of this parameter from depth is tested; corrections for dipping tracks are also calculated under reasonable assumptions and successfully compared with experimental results.

In a previous note (1) a device for the photometric analysis of the tracks in nuclear emulsions has been described. In this method the profile of blackening across the track is determined and the photometrical width is obtained therefrom.

As already noted in I, the advantage of this method in regard to other possible photometrical measurements (height of the profile, relative luminous flux, etc.) lays mainly in the independence on the depth of the track in the emulsion and on the intensity of illumination, because the photometrical width so defined is a geometrical, rather than truly photometrical characteristics.

In the present note, we looked for an experimental check of the above statement and we proposed to find the various corrections needed in order to make the method reliable in the greatest number of cases.

Apart from non-essential modifications (+) the experimental device was the same as described in I.

(*) This paper is part of a program of work supported by I.N.F.N., Sezione di Roma.

(1) M. Della Corte: *Nuovo Cimento*, **4**, 1565 (1956), henceforth referred to as I.

(+) I) Substitution of the Koritska Microscope Model « Standard » with another model MS2. II) Substitution of the oscillating system with a similar one, but with bifilar suspension. III) Employment of a cathode follower at the output of photomultiplier and improvement of the linearity of response of the amplifier.

1. – Methods of measurements.

A direct measurement of the width of the profile on the oscillographic screen is extremely troublesome.

An exact method can be to photograph or to trace on transparent paper the profile and then to measure the width on this picture. The advantage of this method is to have a permanent record of the form of the profile and not only of the photometric width.

In order to have the true width of the track on the basis of the width measured on the profile it is necessary to know the overall enlargement I. This is the product of the optical enlargement I_1, which can be measured exactly and is practically constant, by the « electromechanical » enlargement I_2 (*), that must be evaluated in every single case.

This can be done by displacing the slit by a known amount parallel to the direction of oscillation and recording on the same picture the displaced profile.

A simpler and speedier method is possible by introducing at the output of the amplifier a clamping diode which will maintain the peak of the pulse at ground potential (as shown in Fig. 1).

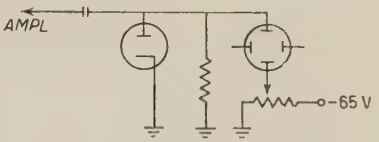

Fig. 1. – Output circuit with clamp.

The peak of the profile is thus approximately (owing to the background) tied up to a fixed reference line a in the oscillograph screen; fine regulation is then achieved by varying the bias of the opposite plate.

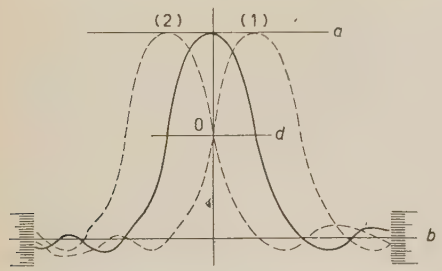

Fig. 2. – Shape of the profile as it appears on the oscillograph screen; full curve: position of the profile for height regulation; dotted curves: positions of the profile for measurement of the width.

By varying the feeding tension of the photomultiplier, the height of the profile is adjusted until the background is brought to reference line b. A third reference line is drown to correspond to the half-height between a and b. By the micrometric displacement of the slit in a direction parallel to the oscillation, it is now possible to bring the left and right side of the profile to coincide with the point 0 of the line d, as shown by the dotted profiles (1) and (2) in Fig. 2.

The corresponding displacement of the slit (which can be accurately measured by a suitable micrometric gauge)

(*) I_2 is the ratio between the distance of two points on the profile and the distance of the corresponding points on the plane of the slit. This ratio depends on many factors (tension applied to the tube, amplitude of the x-oscillation etc.) and particularly on the amplitude of oscillation of the mirror. While the other factors can be considered more or less constant, the amplitude of the mirror oscillation must be varied for every particular segment of the analysed track, in order to include in the profile any δ-ray and part of the background surrounding the track.

when divided by the optical enlargement I_1 gives directly the photometric width, thus dispensing with a separate measure of I_2.

Both for exactness and quickness this method has shown itself definitely the best of the many we tried. We have therefore used it almost exclusively, the photographic recording having been employed only in few particular cases.

2. – Correction for the dip of the tracks.

A serious limitation in most measurements is the uncertainty of the correction for the dipped tracks. In order that measurements of the photometric width can be widely applied in identification of each track or in statistical work, it is necessary to obtain significant results even for very dipped tracks.

A dipped track has a photometric width larger than a plane track having the same intrinsic characteristics. This is due to two indipendent reasons:

a) defocusing, since the different points of the segment of the track under observation are not on the same horizontal plane;

b) clogging of the developed grains during the shrinkage of the emulsion in the drying.

We have made an evaluation of the defocusing effect in the following way.

We choosed a very plane track, and photographed its photometric profile in different conditions of focusing.

As was to be expected both the height and the width of the profile depend strongly on the vertical displacement z from the position of focus as shown by the results in the Table I. It will be noted that the results show a marked symmetry around the point $z = 0$ and that the product λh is approximately constant. This is easily accounted for because the product of the height by the width is strictly related to the total blackening, namely with the amount of light absorbed or scattered by the track, and this amount can reasonably be expected to be independent of z, within certain limits.

Table I.

z defocusing (μm)	h height of the profile (arb. units)	$h_0 \exp[-\alpha z^2]$	λ width of the profile (arb. units)	$h\lambda$ (arb. units)
— 3.5	67.0	61	71.0	$4.76 \cdot 10^4$
— 2.5	85.0	86	51.5	$4.38 \cdot 10^4$
— 1.5	112.0	111	39.5	$4.43 \cdot 10^4$
— 0.5	126.0	126	37.5	$4.72 \cdot 10^4$
+ 0.5	126.5	126	36.5	$4.62 \cdot 10^4$
+ 1.5	110.5	111	39.5	$4.37 \cdot 10^4$
+ 2.5	86.5	86	51.5	$4.46 \cdot 10^4$
+ 3.5	73.5	61	66.5	$4.86 \cdot 10^4$

From the experimental results we can consider a good approximation for the function $h(z)$ the expression

$$h(z) = h_0 \exp\left[-\alpha z^2\right], \tag{1}$$

with $\alpha = 6.12 \cdot 10^{-2}\ \mu m^{-2}$ in our experimental conditions (see Table I). Let us now assume that in the neighbourhood of the point at half height, the dependence of the blackening Y on the distance x from the axis of the track and on the previously defined z is given by

$$\frac{Y(x, z)}{h(z)} = f\left[\frac{x}{\lambda(z)}\right],$$

with the provisions

$$h(z) = Y(0, z) \qquad \text{and} \qquad f[\tfrac{1}{2}] = \tfrac{1}{2}\,.$$

This amounts to admit that on varying z the profile is deformed in a way equivalent to a contraction of the abscissae and a corresponding expansion of the ordinates, so that the area is conserved by the transformation, as required by the experimental results of Table I.

Let us now consider the contribution of the defocusing effect to the enlargement ot the apparent width of the track. Let $2l$ be the slit length and D the dip on the emulsion plane of the track segment intercepted by the slit. If the center of the segment is exactly focused ($z=0$), the average value $\overline{Y}(x, D)$ of the blackening at distance x from the axis of the track will be

$$\overline{Y}(x, D) = \frac{1}{2lD}\int_{-lD}^{+lD} Y(x, z)\,\mathrm{d}z\,.$$

So the factor of enlargement due to the defocusing is obtained. The final result is:

$$\left[\frac{\lambda}{\overline{\lambda}}\right]_{\text{def.}} = \frac{\sqrt{2}\varphi(lD\sqrt{2\alpha})}{\varphi(lD2\sqrt{\alpha})}\,,$$

where the function φ is the normal probability integral. See Appendix for the calculation and Fig. 3 for the results.

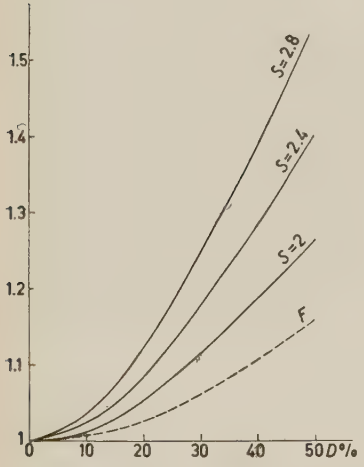

Fig. 3. – Widening factors for dipping tracks. Curve F: defocusing effect. Full curves: clogging effect for different values of the shrinkage factor S.

As for the clogging effect of the grains the problem is intrinsically complex owing to the irregular and inhomogeneous structure of the grains themselves. Some rather drastic schematization is therefore needed; the most simple which suggest themselves most naturally are:

1) In the shrinkage of the emulsion, the dipped track becomes shorter, while the volume remains constant so that the product of the length t by the square λ^2 of the width is constant.

This amounts to treat the track as a plastic cylinder compressed in the direction of its axis.

2) In the shrinkage the area λt of a longitudinal section of the track is constant. This hypothesis corresponds to a dislocation of the grains in an horizontal plane. This assumption is justified if we consider that during the drying the forces which act on the grains of the track are mostly perpendicular to the plane of the emulsion. In this hypothesis, the relation between the width λ' in the shrinked emulsion and the width λ in the unshrinked emulsion is given by

$$\left[\frac{\lambda'}{\lambda}\right]_{\text{shr.}} = \left[\frac{1 + S^2 D^2}{1 + D^2}\right]^{\frac{1}{2}},$$

where S is the shrinkage factor and D is the dip.

We carried out the calculation on both assumptions and the experimental results showed a definite indication for the second one. The results for this case are plotted in Fig. 3 for various values of the shrinkage factor.

The total correction for the dip is obviously obtained by multiplying the two widening factors just evaluated.

The calculated corrections have been checked experimentally on a group of 70 α-particles from radioactive stars in a Ilford G-5 200 μm plate (*).

The average shrinkage factor of the emulsion was 1.6. The photometric measurements have been made with a slit whose equivalent length and width, on the plane of the emulsion, were respectively 12 μm and 0.2 μm. Five overlapping cells were used for a total length on every α-track of 36 μm.

The mean values of the width as a function of the dip and the curve calculated in the aforesaid hypothesis are shown in Fig. 4.

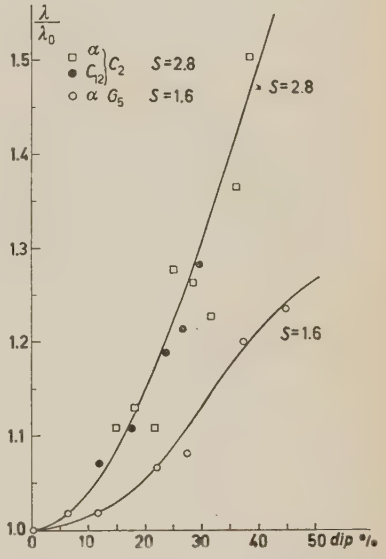

Fig. 4. – Comparison of calculated widening factors for dipping tracks with experimental results.

Further experimental verification has been obtained by measuring the mean width on the last 120 μm of the range of tracks of carbon ions, and also on a group of monoenergetic α-particles found on the same plate. The plate was a Ilford C 2 100 μm thick with shrinkage factor 2.8. In spite of the fact that in this case our hypothesis about the clogging effect does not seem completely justified because the tracks appear grey, the calculated correction agrees with the experimental results (Fig. 4).

We can conclude that at least for a dip in the shrinked emulsion which does not exceed 40% the evaluated correction is quantitative.

(*) The plate was impregnated with a Thorium Nitrate solution and developped with the standard procedure at 20 °C.

3. – Independence of the photometric width of the depth in the emulsions.

The same experimental data collected by measuring the photometric widths of the tracks of α-particles from radioactive stars, have been used also for a verification of the independence of the photometric width from the depth in the emulsion.

The 70 measured tracks have been divided in four groups according to their depth in the emulsion. The tracks having a dip greater than 35% have been discarded, and the correction for the dip has been applied to all others.

The results are shown in Table II.

TABLE II.

Depth in the emulsion in μm	$0 \div 20$	$20 \div 40$	$40 \div 80$	$80 \div 125$
Photometric width in μm	0.940 ± 0.009	0.953 ± 0.006	0.936 ± 0.006	0.926 ± 0.016

The overall mean value of the width comes out to be 0.940 μm, and it is easily seen that there is no depth effect within the experimental error, the fluctuations between the groups being less than 1.5%.

We can observe that the independence from the depth has been verified in spite of a noticeable background of dispersed grains in the plate.

4. – Effect of the finite width of the slit.

The width of the slit being finite and not infinitesimal, one can expect an effect on the width λ of the profile. This effect will depend not only on the width ε of the slit but also on the true shape of the blackening profile.

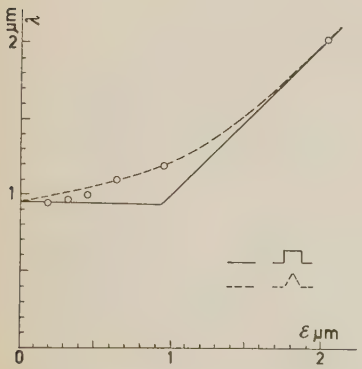

Fig. 5. – Effect of the finite width of the slit; curves evaluated for extreme cases. Experimental points.

The evaluation of the correction term which thus arises has been carried out in the two extreme cases of a rectangular or respectively triangular shape of the original profile; the actual profile will be certainly included between the two. The results are compared in Fig. 5 with the experimental curve obtained by repeating the measurement of the same track segment with different slit-widths.

As expected, the experimental points lie between the two limiting curves and with a slit width equivalent to about 0.2 μm in the plane of the track as in our standard experimental set-up, the error is less than 2% in any case.

5. – Conclusions.

From the above results the photometric width as defined by us (*) comes out to be independent of the depth in the emulsion, while for dipped tracks a correction factor can be applied which allows measurements to be carried out up to a dip of 40%. This extends considerably the range of application of the method.

The practical measurement is very simple and fast; about forty profiles can be obtained in one hour. This corresponds, with an equivalent length of the slit of 12 μm, to a total length on the track of about 500 μm. If the device is applied on the scattering microscope MS2 the time required to line-up the track and to adjust the illumination is also considerably reduced.

Finally, the first group of measurements carried out to date allows us to state that the measurement of photometirc width permits the identification of the charge for single tracks with residual range of some hundred μm, namely in a field well outside the range of other methods (δ-ray counting, scattering, etc.). Results will be published soon.

* * *

We thank most heartily Prof. R. Chastel of the Collège de France, Prof. J. H. Fremlin of the University of Birmingham and Dr. M. René of the Université Libre de Bruxelles who kindly supplied us the plates on which the measurements have been carried out.

The encouragement and advice of Prof. Simone Franchetti, Director of the Institute of Physics of the University of Florence, is gratefully acknowledged.

Thanks are also due to Dr. M. G. Dagliana and Dr. L. Tocci for their help in the measurements.

One of us (P.G.B.) is indebted to the Foundation « Della Riccia » for a grant, during the tenure of which this work was done.

Appendix

Calculation of the correction of defocusing.

In the neighbourhood of the point of half height we can write

$$\frac{Y(x, z)}{Y(0, z)} = f\left[\frac{x}{\lambda(z)}\right].$$

We now expand $f[x/\lambda(z)]$ in the neighbourhood of $x/\lambda(z) = \frac{1}{2}$ to the first term, which is a reasonable approximation throughout the interval of interest.

(*) Width at half height of the transversal photometric profile.

We obtain

$$\frac{Y(x, z)}{Y(0, z)} = a - b\,\frac{x}{\lambda(z)}\,.$$

From the condition $Y[\lambda(z)/2, z]=\frac{1}{2}Y(0, z)$ we get $a=\frac{1}{2}(1+b)$ and then

$$\overline{Y}(x, D) = \frac{1}{2}\,(1 + b)\,\overline{Y}(0, D) - b\,\frac{x}{lD}\int_0^{lD}\frac{Y(0, z)}{\lambda(z)}\,\mathrm{d}z\,.$$

To evaluate $\bar{\lambda}(D)$, we must solve the equation (definition of photometric width)

$$\overline{Y}\left[\frac{\bar{\lambda}(D)}{2}, D\right] = \frac{1}{2}\,\overline{Y}(0, D)\,,$$

from which

$$\bar{\lambda}(D) = \frac{\overline{Y}(0, D)}{\dfrac{1}{lD}\displaystyle\int_0^{lD}\frac{Y(0, z)}{\lambda(z)}\,\mathrm{d}z}\,.$$

We observe that the value of $\bar{\lambda}(D)$ is independent from the parameter b, therefore from the steepness of the profile.

Introducing for $Y(0, z)$ the formula (1), namely

$$Y(0, z) = Y(0, 0)\exp\left[-\alpha z^2\right],$$

we obtain

$$\overline{Y}(0, D) = Y(0, 0)\sqrt{\frac{\pi}{2}}\,\frac{1}{lD\sqrt{2\alpha}}\,\varphi(lD\sqrt{2\alpha})\,,$$

or taking into account the relation $Y(0, z)\lambda(z)=\text{const.}$ (see Table I)

$$\frac{1}{lD}\int_0^{lD}\frac{Y(0, z)}{\lambda(z)}\,\mathrm{d}z = \sqrt{\frac{\pi}{2}}\,\frac{1}{lD\,2\sqrt{\alpha}}\,\varphi(lD\,2\sqrt{\alpha})\,.$$

Here φ is the integral

$$\varphi(u) = \frac{1}{\sqrt{2\pi}}\int_{-u}^{+u}\exp\left[-\tfrac{1}{2}t^2\right]\mathrm{d}t\,.$$

At last we find for the widening factor for the defocusing:

$$\frac{\bar{\lambda}(D)}{\lambda(0)} = \frac{\sqrt{2}\,\varphi(lD\sqrt{2\alpha})}{\varphi(lD\,2\sqrt{\alpha})}\,. \tag{2}$$

We observe that for the form of the expression (2) a relative error in the estimate of the α-parameter affects the results to half the extent of the same relative error in the dip.

RIASSUNTO

Viene descritto un metodo semplice e rapido per la misura della larghezza fotometrica delle tracce nelle emulsioni nucleari, facendo uso di un apparecchio descritto in un precedente lavoro. Si discute la correzione da apportare per tracce inclinate. Tale correzione consiste di due termini, uno dovuto allo « sfocamento » e l'altro all' « affastellamento » dei granuli nella contrazione dell'emulsione. Il calcolo di questi termini effettuato con ragionevoli ipotesi, è stato trovato in buon accordo con l'esperienza. È stata verificata l'indipendenza della larghezza fotometrica dalla profondità della traccia nell'emulsione. L'effetto della larghezza finita della fenditura è stato preso in considerazione.

On the Theory of the Neutrino with Oriented Spin.

A. Sokolov

State University - Moscow

(ricevuto il 20 Luglio 1957)

Lee and Yang [1] have proved that the invariance under space inversion can be violated in weak interactions.

Developing this idea Lee and Yang [2], Salam [3] and Landau ( ) have supposed that the parity non-conservation may be connected with a new property of the neutrino.

They assume that the mass of the neutrino is zero, then its motion can be described by the equation:

$$[\hat{E} - c(\boldsymbol{\sigma}'\hat{\boldsymbol{p}})]\begin{pmatrix}\varphi_1\\ \varphi_2\end{pmatrix} = 0\,, \tag{1}$$

where

$$\hat{E} = -\frac{\hbar}{i}\frac{\partial}{\partial t}\,, \qquad \hat{\boldsymbol{p}} = \frac{\hbar}{i}\nabla\,, \tag{2}$$

$\boldsymbol{\sigma}'(\sigma_1', \sigma_2', \sigma_3')$ are the usual 2×2 Pauli matrices. According to this theory the neutrino spin is always parallel to its momentum, while the spin of an antineutrino is always anti-parallel to its momentum. This is the new definition of the neutrino and anti-neutrino.

The theory of these authors is not invariant under space inversion. However, Landau and Lee and Yang have shown the theory to be invariant under the combined inversion. Combined inversion means a simultaneous transformation of a particle into an antiparticle and space inversion.

We shall use the Dirac equation in order to solve the problem of a neutrino with oriented spin.

(1) T. D. Lee and C. N. Yang: *Phys. Rev.*, **104**, 254 (1956).
(2) T. D. Lee and C. N. Yang: *Phys. Rev.*, **105**, 1671 (1957).
(3) A. Salam: *Nuovo Cimento*, **5**, 299 (1957).
(4) L. Landau: *Nucl. Phys.*, **3**, 127 (1957); *Žu. Èksper. Teor. Fis.*, **32**, 405 (1957).

The Dirac equation for a free particle can be written as:

$$(3)\qquad \begin{cases} (\hat{E} - m_0c^2)\begin{pmatrix}\psi_1\\ \psi_2\end{pmatrix} = c(\boldsymbol{\sigma}'\hat{\boldsymbol{p}})\begin{pmatrix}\psi_3\\ \psi_4\end{pmatrix}, \\ (\hat{E} + m_0c^2)\begin{pmatrix}\psi_3\\ \psi_4\end{pmatrix} = c(\boldsymbol{\sigma}'\hat{\boldsymbol{p}})\begin{pmatrix}\psi_1\\ \psi_2\end{pmatrix}. \end{cases}$$

Once the mass of the neutrino is zero ($m_0 = 0$), one obtains the linear relation between the functions

$$(4)\qquad \begin{pmatrix}\psi_1\\ \psi_2\end{pmatrix} = \varepsilon\begin{pmatrix}\psi_3\\ \psi_4\end{pmatrix}$$

where $\varepsilon = \pm 1$.

We can choose for the quantity ε the four values:

a) $\varepsilon = 1$ (the state with $E > 0$ and $E < 0$ will describe the neutrino).

b) $\varepsilon = -1$ (the state with $E > 0$ and $E < 0$ will describe the antineutrino).

c) $\varepsilon = E/|E|$ (the state with $E > 0$ corresponds to the neutrino and the state $E < 0$ to the antineutrino).

d) $\varepsilon = -E/|E|$ (the state with $E > 0$ corresponds to the antineutrino and the state $E < 0$ to the neutrino).

Now we shall consider the case:

$$(5)\qquad \varepsilon = \frac{E}{|E|}.$$

In this case the neutrino is a particle in the positive energy state and the antineutrino is a hole in the negative energy state.

Then the equation (3) can be written as:

$$(6)\qquad [\hat{E} - \varepsilon c(\boldsymbol{\sigma}'\hat{\boldsymbol{p}})]\begin{pmatrix}\psi_1\\ \psi_2\end{pmatrix} = 0.$$

The wave function $\begin{pmatrix}\psi_3\\ \psi_4\end{pmatrix}$ will satisfy a similar equation. The solution of Eqs. (3) can be presented in the form [5,6]:

$$(7)\qquad \begin{cases} \begin{pmatrix}\psi_1\\ \psi_2\end{pmatrix} = L^{-\frac{3}{2}}\sum_{\boldsymbol{k}}\frac{1}{\sqrt{2}}\exp[i\boldsymbol{kr}]\begin{pmatrix}\cos\theta/2\\ \sin(\theta/2)\exp[i\varphi]\end{pmatrix}[C(\boldsymbol{k})\exp[-ickt] + \tilde{C}^{+}(-\boldsymbol{k})\exp[ickt]], \\ \begin{pmatrix}\psi_3\\ \psi_4\end{pmatrix} = L^{-\frac{3}{2}}\sum_{\boldsymbol{k}}\frac{1}{\sqrt{2}}\exp[i\boldsymbol{kr}]\begin{pmatrix}\cos\theta/2\\ \sin(\theta/2)\exp[i\varphi]\end{pmatrix}[C(\boldsymbol{k})\exp[-ickt] - \tilde{C}^{+}(-\boldsymbol{k})\exp[ickt]], \end{cases}$$

(5) A. Sokolov: *Journ. of Phys. USSR*, **9**, 363 (1945).
(6) A. Sokolov and B. Kerimov: *Nuovo Cimento*, **5**, 921 (1957).

where $E = c\hbar k$ is the energy of the particle, $\boldsymbol{p} = \hbar\boldsymbol{k}$ its momentum, (k, θ, φ) are the spherical coordinates of the vector $\boldsymbol{k}$.

One obtains the following expressions for the total energy $\overline{E}$, the total momentum $\overline{\boldsymbol{G}}$ and the total projection of the spin on the direction of the momentum S ([5,7]):

$$(8)\qquad \overline{E} = c\int \mathrm{d}^3x \left[(\psi_3^+\psi_4^+)(\boldsymbol{\sigma}'\hat{\boldsymbol{p}})\begin{pmatrix}\psi_1\\ \psi_2\end{pmatrix} + (\psi_1^+\psi_2^+)(\boldsymbol{\sigma}'\hat{\boldsymbol{p}})\begin{pmatrix}\psi_3\\ \psi_4\end{pmatrix}\right] = \sum_{\boldsymbol{k}} c\hbar\boldsymbol{k}[C^+(\boldsymbol{k})C(\boldsymbol{k}) - \tilde{C}(-\boldsymbol{k})\tilde{C}^+(-\boldsymbol{k})]\,,$$

$$(9)\qquad \overline{\boldsymbol{G}} = \int \mathrm{d}^3x \left[(\psi_1^+\psi_2^+)\hat{\boldsymbol{p}}\begin{pmatrix}\psi_1\\ \psi_2\end{pmatrix} + (\psi_3^+\psi_4^+)\hat{\boldsymbol{p}}\begin{pmatrix}\psi_3\\ \psi_4\end{pmatrix}\right] = \sum_{\boldsymbol{k}} \hbar\boldsymbol{k}[C^+(\boldsymbol{k})C(\boldsymbol{k}) + \tilde{C}(-\boldsymbol{k})^+\tilde{C}(-\boldsymbol{k})]\,,$$

$$(10)\qquad \overline{S} = \int \mathrm{d}^3x \left[(\psi_1^+\psi_2^+)\frac{(\boldsymbol{\sigma}'\hat{\boldsymbol{p}})}{|\boldsymbol{p}|}\begin{pmatrix}\psi_1\\ \psi_2\end{pmatrix} + (\psi_3^+\psi_4^+)\frac{(\boldsymbol{\sigma}'\hat{\boldsymbol{p}})}{|\boldsymbol{p}|}\begin{pmatrix}\psi_3\\ \psi_4\end{pmatrix}\right] = \sum_{\boldsymbol{k}} [C^+(\boldsymbol{k})C(\boldsymbol{k}) + \tilde{C}(\quad \boldsymbol{k})\tilde{C}^+(-\boldsymbol{k})]\,.$$

If the amplitudes of the neutrino field satisfy the Fermi-commutation relations, we have

$$(11)\qquad C^+(\boldsymbol{k})C(\boldsymbol{k}) = N(\boldsymbol{k})\,, \qquad \tilde{C}(\boldsymbol{k})\tilde{C}^+(\boldsymbol{k}) = 1 - \tilde{N}(\boldsymbol{k})\,.$$

It is seen from (8) and (10) that a neutrino (their number being N) and an antineutrino (their number being $\tilde{N}$) have positive energy and the spin of a neutrino is parallel to its momentum, while the spin of an antineutrino is antiparallel to its momentum.

In this neutrino theory we have only two states (and not four as in the theory of electrons) since the neutrino has no charge. Therefore the states having different charge but the same spin projection become non-distinguishable.

The Spur of a neutrino wave function can be easily evaluated by means of the formula for the Spur of the electron wave function, the spin state being fixed. This formula can be written in the form ([8]):

$$(12)\qquad b'^+\beta'bb^+\beta b' = \frac{1}{16}\,\mathrm{Sp}\left[\beta'\left(1 + \varrho_1\varepsilon's'\frac{k'}{K'} + \varrho_3\varepsilon'\frac{k'_0}{K'}\right)\left(1 + s'\frac{(\boldsymbol{\sigma}\boldsymbol{k}')}{k'}\right)\cdot \beta\left(1 + \varrho_1\varepsilon s\frac{k}{K} + \varrho_3\varepsilon\frac{k_0}{K}\right)\left(1 + s\frac{(\boldsymbol{\sigma}\boldsymbol{k})}{k}\right)\right],$$

where $b = b(\boldsymbol{k}, s, \varepsilon)$ and $b' = b(\boldsymbol{k}', s', \varepsilon')$ are the spin amplitudes of the wave function; all the others matrices are the well known Dirac matrices, moreover β and β' can be any of the 16 independent Dirac matrices.

([7]) D. IVANENKO and A. SOKOLOV: *Phys Zeits. d. Sowjet.*, **11**, 590 (1937).

([8]) A. SOKOLOV and A. MUCHTAROV: *Vestnik Moskovskogo Gosudarstvennogo Universiteta*, **8**, 63 (1948); A. SOKOLOV and D. IVANENKO: *Quantum Theory of Fields* (Moscow-Leningrad, 1952), pp. 110-113.

If one of the particles is a new neutrino (antineutrino) we have to take the corresponding mass to be equal zero ($k_0 = 0$, $K = k$). Then the two non-distinguishable states ($\varepsilon = 1$, $s = 1$ and $\varepsilon = -1$, $s = -1$) will describe the neutrino and two other states ($\varepsilon = 1$, $s = -1$ and $\varepsilon = -1$, $s = 1$) the antineutrino.

We can also use the equation (12) for the Dirac-particle with oriented spin, if the rest mass is not equal zero (for example, when the rest mass of the neutrino would not be equal zero). In this case the state $\varepsilon = 1$, $s = 1$ would differ from the state $\varepsilon = -1$, $s = -1$ and we would have again four states but not two as in the new theory of neutrino.

Nuclear Moments of Inertia.

H. M. Foley (*)

Institute of Theoretical Physics - Copenhagen

(ricevuto il 30 Luglio 1957)

Skyrme [1] has made an application of his interesting variational principle to the calculation of the moments of inertia of heavy nuclei. The result (Skyrme, eq. (17)) is expressed in terms of the two particle excitation matrix elements of the interaction potential, which are not included in the usual self consistent field. Further approximations, discussed below, lead to the « simplified formula » (eq. (20))

$$I = \frac{2\langle|J_x^2|\rangle^2}{\langle|J_x(H'-\langle H'\rangle)J_x|\rangle},$$

in which expectation values are to be calculated in the wave function of the ground state of a self consistent single particle model, for which H' is the effective hamiltonian operator. This is the formula actually employed by Skyrme to calculate moments of inertia. The values he obtains are about one half the « rigid » values, and are in general agreement with the upper limit of the observed values for even-even nuclei.

Inasmuch as the Skyrme formula given above, is expressed wholly in terms of the operators of the single particle model, it is rather surprising that it is not equivalent to the Inglis « cranking model » formula, which yields just the « rigid » values for the moments of inertia. It may be shown that the Skyrme formula is in fact equivalent to a simple but crude approximation to the « cranking model » expression. If in a standard second order energy perturbation expression

$$E_2 = \sum_n \frac{\langle 0|v|n\rangle\langle n|v|0\rangle}{E_0 - E_n},$$

one replaces the numerators, according to the sum rule, by

$$\langle 0|v^2|0\rangle,$$

($\langle 0|v|0\rangle$ is zero in these applications), and the denominators by an « average excitation », each level weighted by the factor $\langle 0|v|n\rangle\langle n|v|0\rangle$ then we obtain

$$E_2 \sim -\frac{\langle 0|v^2|0\rangle^2}{\langle|v[H,v]|\rangle}.$$

This approximate formula, derived by the author [2], is in some cases a rough

(*) Permanent address: *Phys. Dept.*, Columbia University, New York.

(1) T. H. R. Skyrme: *Proc. Phys. Soc.*, **70**, 433 (1957).

(2) Unpublished.

but useful estimate of a second order perturbation, and, with the required change of sign, is just Skyrme's formula in this case. In the « cranking » formula there occur excitations within a shell and between shells, which are of quite different energies. Thus the Skyrme formula gives a quite different result from the Inglis expression, and, as Skyrme pointed out, always a lower value of I.

In the derivation of his « simplified » formula Skyrme found it necessary to neglect the « exchange » two particle matrix elements compared with the « direct » matrix elements. Now in such double excitation processes there is no real difference in magnitude between « direct » and « exchange » matrix elements. It appears that neglect of the « exchange » elements is hardly justified, for any range of the forces, and can lead to considerable error. For these reasons it appears that the Skyrme formula does not give reliable values for the nuclear moments of inertia.

* * *

The writer has had the benefit of a communication from Dr. SKYRME on this subject.

Non-Conservation of Parity in the Radiative π-Meson Decay.

G. W. Bund and P. Leal Ferreira
Instituto de Física Teórica - São Paulo, Brasil

(ricevuto il 14 Ottobre 1957)

The radiative decay of the charged π-mesons [1] ($\pi^{\pm} \to \mu^{\pm} + \nu + \gamma$) is recalculated in order to take into account possible effects due to the non-conservation of parity in the interaction hamiltonian. The neutrino is described by the two-component theory of Lee and Yang [2], the process beeing of second order with the following matrix elements ($\hbar = c = 1$):

$$(1) \qquad (f|H|i) = \frac{e}{\sqrt{2K_0}} \frac{g}{\sqrt{2P_0}} \left\{ \bar{u}(p) \gamma a_\varrho \frac{\gamma q + i\mu}{q^2 + \mu^2} (1 - \gamma_5) v(k) \right\},$$

where $P(\boldsymbol{P}, iP_0)$, p, k, K are the momentum four-vectors of the π-meson, muon, neutrino and photon respectively, $q = P - k = p + K$, a_ϱ beeing the polarization vector of photon ($a_0 = 0$).

If $\boldsymbol{a}_x$, $\boldsymbol{a}_y$, $\boldsymbol{a}_z = \boldsymbol{K}/K_0$, for each $\boldsymbol{K}$, are three unit vectors, forming a right-handed orthogonal system then we define $\sqrt{2}\boldsymbol{a}_\varrho = \boldsymbol{a}_x - i(-1)^\varrho \boldsymbol{a}_y$, where $\varrho = 1, 2$ corresponds to the right and left circular polarization of the light quantum, respectively. We have:

$$(2) \qquad a_\varrho^2 = 0\,, \qquad a_\varrho a_\varrho^* = 1\,, \qquad \boldsymbol{a}_\varrho \wedge \boldsymbol{a}_\varrho^* = -i(-1)^\varrho \frac{\boldsymbol{K}}{K_0}\,.$$

Choosing as independent variables K_0 and p_0 we get, by the usual methods, the following expression for the probability of radiative desintegration per unit time

---

(1) W. F. Fry: *Phys. Rev.*, **83**, 1268 (1951); T. Eguchi: *Phys. Rev.*, **85**, 943 (1952); T. Nakano, J. Nishimura and Y. Yamaguchi: *Progr. Theor. Phys.*, **6**, 1028 (1951); H. Primakoff: *Phys. Rev.*, **84**, 1255 (1951); G. E. A. Fialho and J. Tiomno: *Notas de Física*, No. 1 (1952).

(2) F. D. Lee and C. N. Yang: *Phys. Rev.*, **105**, 1671 (1957).

of the π-meson (mass M) at rest:

$$(3) \qquad \mathcal{P}(p_0, K_0)\,\mathrm{d}p_0\,\mathrm{d}K_0 = \frac{e^2g^2}{(2\pi)^3}\,\frac{p_0k_0}{2M^2}\,\frac{\mathrm{d}p_0\,\mathrm{d}K_0}{(p_m-k_0)^2}\cdot$$

$$\cdot\left\{E_m - \frac{\mu^2}{p_0} - \frac{p_m}{p_0k_0}\,\frac{(K_0^2+\boldsymbol{pK})\boldsymbol{pK}}{K_0^2} + \frac{(-1)^\varrho}{K_0p_0k_0}\left[(E_mp_0 - p_mk_0 - \mu^2)\boldsymbol{pK} + (E_mp_0-\mu^2)K_0^2\right]\right\},$$

where p_m and E_m are the maximum momentum and energy of the muon (mass μ):

$$p_m = \frac{M^2-\mu^2}{2M}, \qquad E_m = \frac{M^2+\mu^2}{2M},$$

$$k_0 = M - p_0 - K_0, \qquad \boldsymbol{pK} = p_0K_0 - M(p_m - k_0).$$

In terms of the variables p_0 and θ, θ beeing the angle between the directions of the muon and light quantum, the probability of desintegration per unit time reads:

$$\mathcal{P}(p_0, \theta)\,\mathrm{d}p_0\sin\theta\,\mathrm{d}\theta = \frac{1}{(2\pi)^3}\,\frac{e^2g^2}{2M}\,\frac{|\boldsymbol{p}|\,\mathrm{d}p_0\sin\theta\,\mathrm{d}\theta}{\lambda^2}\cdot$$

$$\cdot\left\{\frac{p_m|\boldsymbol{p}|^2\sin^2\theta}{E_m-p_0} + \frac{M(E_m-p_0)\lambda}{M-\lambda} - \frac{(-1)^\varrho M}{M-\lambda}\left[\lambda^2 - \lambda(E_m+p_0)+\mu^2\right]\right\},$$

where $\lambda = p_0 - |\boldsymbol{p}|\cos\theta$.

The first terms in (3), which do not depend on ϱ, correspond exactly to the expression derived by EGUCHI [1]. The corresponding terms in formula (5) are also known and have been derived by FIALHO and TIOMNO [1], so the two formulas can be shown to be in agreement. The terms proportional to $(-1)^\varrho$ in both (3) and (5) give the contribution due to the non conservation of parity. It is clear that if we sum over the two polarization states of the photon, the contribution of the $(-1)^\varrho$ terms vanishes. Formula (5) then shows that the angular correlation between the directions of the muon and the emitted photon presents an asymmetry with respect to the polarization state of the photon. This means that if the state of circular polarization of the photon is detected, the number of coincidences (γ,μ) differs according to whether the measured polarization of the γ-ray is left or right.

However, the effect involved is difficult to detect because the total probability of the radiative process is small (3 radiative to 10^4 non-radiative events). The asymmetry effect obtained can be understood in a qualitative way by using the fact that the right-circular polarized photons carry their spin of magnitude 1, in the direction of motion, the left ones in the opposite direction. Then, for instance, for small momentum of the muon, the γ-ray and the antineutrino have nearly opposite momenta. Considering that the antineutrino is polarized in the direction opposite to its motion, it follows, from conservation of angular momentum that the right-polarized photons are forbidden, so that in this region of the μ-spectrum the photons are almost completely left polarized, a result which can be obtained directly from (3). If a neutrino, instead of an antineutrino, were emitted (π^+-decay), the left polarized photons would be forbidden.

It should be pointed out that (5) is divergent for $|\boldsymbol{p}|$ tending to p_m ($\theta \neq 0, \pi$)

which corresponds to the well-known « infrared catastrophe ». Such divergent behaviour is also apparent in (3) for K_0 tending to zero and means the breakdown of the perturbation method.

Finally, it might be mentioned that similar correlation asymmetries can occur in the inner-bremsstrahlung of β-rays in allowed transitions [3] and in the radiative decay of polarized muons, the analysis in this last case beeing more involved in view of the fact that four light particles occur in the final state.

* * *

We are very grateful to Prof. J. TIOMNO for the suggestion of the argument.

---

[3] In this connection see G. W. FORD: *Phys. Rev.*, **107**, 321 (1957). See also, R. E. CUTKOSKI: *Phys. Rev.*, **107**, 330 (1957).

IL NUOVO CIMENTO Vol. VII, N. 2 16 Gennaio 1958

Über die Symmetrien des Diracfeldes.

H. Rollnik

Institut für theoretische Physik der Freien Universität - Berlin

(ricevuto il 15 Ottobre 1957)

Die Symmetrieeigenschaften eines quantenphysikalischen Systems können entweder auf eine unitäre oder antiunitäre Abbildung des Hilbertraumes zurückgeführt werden(1). Seit Wigner(2) wird die Bewegungsumkehr durch einen antiunitären Operator beschrieben, sodaß z.B. für ein Diracfeld diese Transformation durch

$$\psi'(\mathrm{r}, t) = C^{-1}\gamma_5\psi(\mathrm{r}, -t)\,, \tag{1}$$

beschrieben wird, statt durch die Racahsche « Zeitspiegelung »

$$\psi'(\mathrm{r}, t) = \gamma_1\gamma_2\gamma_3\psi(\mathrm{r}, -t)\,, \tag{2}$$

die mit der Diracgleichung ebenfalls verträglich wäre. In der Literatur schließt man (2) z.B. mit dem Argument aus, daß die Vertauschungsrelationen eine antilineare Transformation für die Bewegungsumkehr erfordern (3). Man sieht aber leicht, daß dies nur für Bosonenfelder richtig ist. Für ein Diracfeld läßt die Transformation (2) die Vertauschungsrelationen invariant. (Der innere Grund für diesen Unterschied liegt darin, daß die kanonisch konjugierten Felder im Bosonenfalle die zeitliche Ableitung der Feldoperatoren sind). Andererseits läßt (2) die Lagrangefunktion nicht invariant, aber zur Ausschließung von (2) sollte man nur Argumente benutzen, die sich auf Observable beziehen oder wenigstens auf letzlich beobachtbare Konsequenzen stützen. In der Tat gibt es ein solches Argument: die Operatoren (2) geben eine Darstellung der Vertauschungsrelationen, die zu der üblichen Darstellung der Löchertheorie inäquivalent ist, und in der es kein Vakuumzustand gibt (4).

Wir führen das etwas näher an dem allgemeinen Problem aus: welche Transformationen der Dirac-Operatoren in der Form

$$\psi'(x) = A\psi(Lx) + \overline{\psi}(Lx)B\,, \tag{3}$$

führen auf unitäre oder antiunitäre Transformationen im Hilbertraum. Dabei seien A und B zunächst beliebige Dirac-

(1) Vergl. z.B. G. Ludwig: *Grundlagen der Quantenmechanik* (Berlin, 1954), III, § 10.

(2) *Göttinger Nachrichten*, **31**, 546 (1932).

(3) J. Jauch and F. Rohrlich: *Theory of Photons and Electrons* (Cambridge, 1955).

(4) Zu den benutzten Begriffen vgl. z.B. A. Wightman und S. Schweber: *Phys. Rev.*, **98**, 812 (1955).

Matrizen. Lx symbolisiert eine allgemeine, inhomogene Lorentztransformation: $x'^{\mu} = l^{\mu}{}_{\nu} x^{\nu} + l^{\mu}$ wobei also auch alle Spiegelungen zugelassen sein sollen. Durch Rechnungen im Ring der γ-Matrizen kann man zeigen, daß (3) *genau* dann die (freie) Diracgleichung und die Vertauschungsrelationen invariant läßt, wenn gilt:

$$\text{(U)} \qquad A = \mu \Lambda^{-1}, \qquad B = \lambda \Lambda C .$$

Dabei gibt die Matrix Λ die Darstellung von L im Raum der Dirac-Spinoren: $\gamma_{\mu} l^{\mu}{}_{\nu} = \Lambda \gamma_{\nu} \Lambda^{-1}$. μ und λ sind komplexe Zahlen, die die Bedingung $|\mu|^2 + |\lambda|^2 = 1$ erfüllen müssen. C ist ebenso wie in (1) die von SCHWINGER [5] eingeführte Matrix der Ladungskonjugation. Wir betonen, daß (U) für beide Vorzeichen von l^4_4 die genannte Invarianzeigenschaft besitzt. Ebenso folgt, daß (3) den Feldgleichungen und Vertauschungsrelationen genügt, die einer antiunitären Transformation entsprechen (d.h. wo alle c-Zahlen durch ihre konjugiert Komplexen ersetzt sind), wenn die Matrizen die Form

$$\text{(A)} \qquad A = \mu C^{-1} \gamma_4 \Lambda^{-1}, \qquad B = \lambda \Lambda \gamma_4 ,$$

haben, mit derselben Bedingung für Λ, μ und λ wie oben. Damit (U) und (A) die physikalischen Aussagen nicht ändern, darf bei geladenen Feldern der Operator der Ladung Q höchstens sein Vorzeichen ändern. Daraus folgt, daß entweder λ verschwinden muß ($Q' = Q$) oder aber μ ($Q' = -Q$). Wichtiger noch ist die Wirkungsweise auf den Energie-Impuls-Vektor P_{μ} (vergl. dazu W. PAULI [6]). Bei Transformationen ohne Zeitspiegelung ($l^4_4 > 0$) macht (A) aus der Energie P_4 einen negativ definiten Operator; dasgleiche gilt für (U) bei Transformationen mit Zeitspiegelung. Mathematisch wird dies möglich, weil dabei die Erzeugungsoperatoren in Linearkombinationen von Vernichtungsoperatoren verwandelt werden. Z.B. wird nach (A) für $L=1$ und $\mu=1$ aus dem Erzeugungsoperator eines Teilchens der entsprechende Vernichtungsoperator des Antiteilchens: $a_r^{(+)*}(k)' = a_r^{(-)}(k)$. Für die Racahsche Zeitspiegelung gilt: $a_r^{(+)*}(k)' = -a_r^{(-)}(-k)$. In allen diesen Fällen werden alle Vektoren des Hilbertraumes der Löchertheorie — außer dem Vakuum — auf Null abgebildet; es existiert also keine isomorphe Abbildung *dieses* Hilbertraumes auf sich, die $\psi(x)$ in $\psi'(x)$ überführt.

[5] *Phys. Rev.*, **74**, 1439 (1948).

[6] In *Niels Bohr and the Development of Physics* (1955).

On the Mechanical Activation of Thermoluminescence in Calcite.

Arturo Debenedetti (*)

(ricevuto il 26 Ottobre 1957)

1. – Many investigators (1) have shown that natural calcite (or limestone), when thermoluminescent, gives a glow curve with *two* peaks, at about 230° and 360°. The height of the peaks may vary greatly from case to case.

The cause of the thermoluminescence of natural crystals and rocks is usually ascribed to impurities of radioactive elements. Cosmic radiation may be another factor (possibly overlooked) of natural activation.

Not-thermoluminescent calcite, or limestone, (like other substance) may be activated by exposure to X- or γ-rays. After exposure to a γ-ray source (as ^{60}Co), a glow curve with *four* peaks, at about 135°, 175°, 230°, 360°, is obtained (2).

The usual absence of the two low-temperature peaks in the glow curve of calcite or limestone not artificially irradiated, has been interpreted by supposing that these peaks have been drained out, as a consequence of the geothermic gradient. The rock is supposed to have stayed at a depth below the surface, where the temperature was higher than that of the missing peaks (2).

2. – In the course of an investigation about the use of thermoluminescence data as geologic thermometer, glow curves of many samples of a Tertiary limestone were recorded.

They all have also shown only two peaks, at 230° and 360°.

A test by nuclear plates did not show the presence of radioactive elements in the limestone.

On the other side, from the local geological conditions, it can be presumed that the rock has never been at a depth of more than some hundred meters from the surface.

Therefore, neither the presence of the high-temperature, nor the absence of the low-temperature peaks can be satisfactory explained.

3. – To remove the uncertainty unavoidable when using natural substances, it was decided to study the thermoluminescence behaviour of artificial, pure calcite.

Pure Merck $CaCO_3$, *pro analysi*, was employed. Under the microscope it was seen to be composed of very small

(*) Writer's address: Torino, corso Sommeiller, 21.

(1) For instance: F. Daniels, C. A. Boyd and D. F. Saunders: *Science*, **117**, n. 3040, 343 (1953); E. J. Zeller: *Compt. Rend. XIX Congr. Géol. Intern.*, **12**, 365 (1954); E. J. Zeller, in H. Faul *et al.*: *Nuclear Geology*, 180 (1954).

(2) J. Parks jr.: *Bull. Amer. Ass. Petrol. Geol.*, **37**, n. 1, 125 (1953); D. F. Saunders: *Bull. Amer. Ass. Petrol. Geol.*, **37**, n. 1, 114 (1953); R. E. Bergstrom: *Bull. Amer. Ass. Petrol. Geol.*, **40**, n. 5, 918 (1956); C. W. Pitrat: *Bull. Amer. Ass. Petrol. Geol.*, **40**, n. 5, 943 (1956).

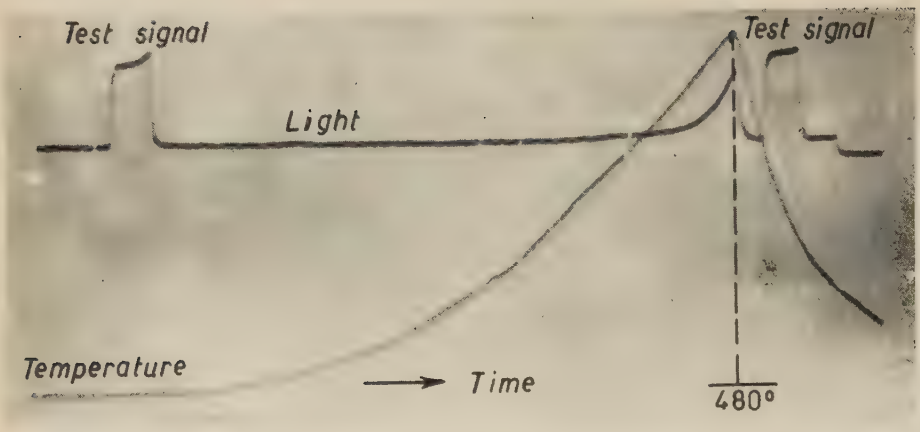

Fig. 1.

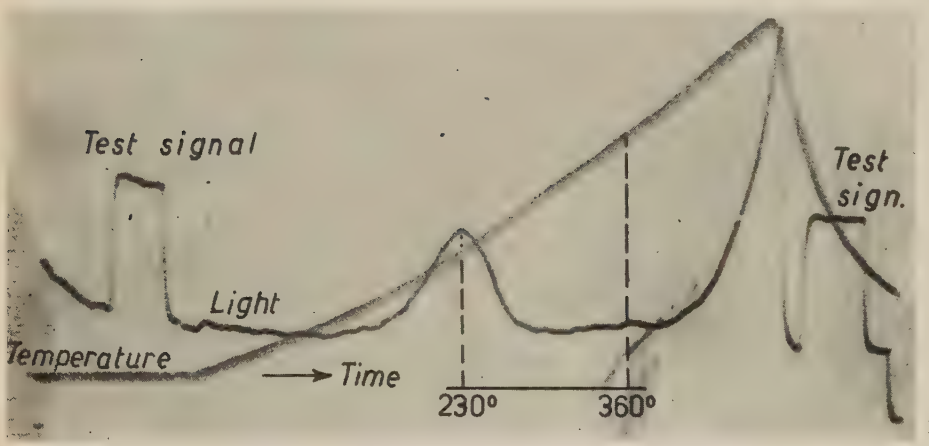

Fig. 2.

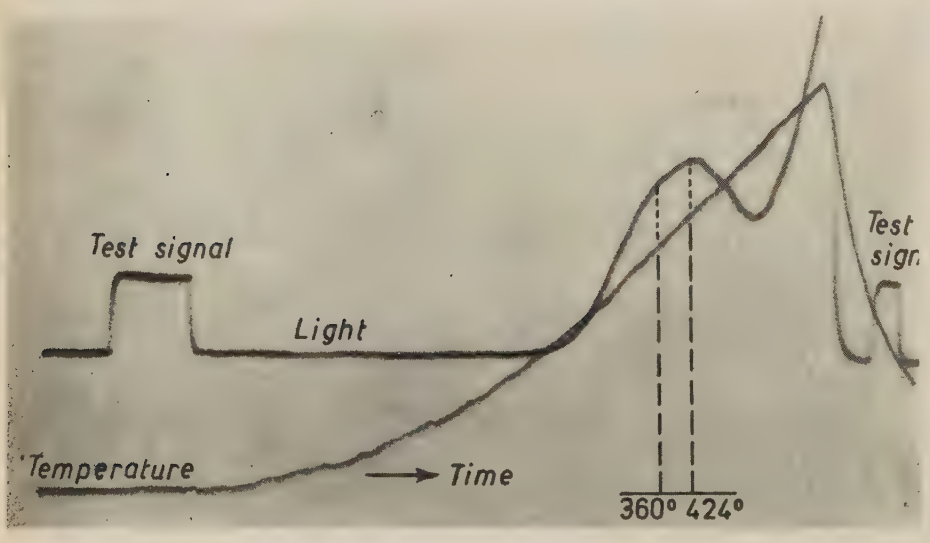

Fig. 3.

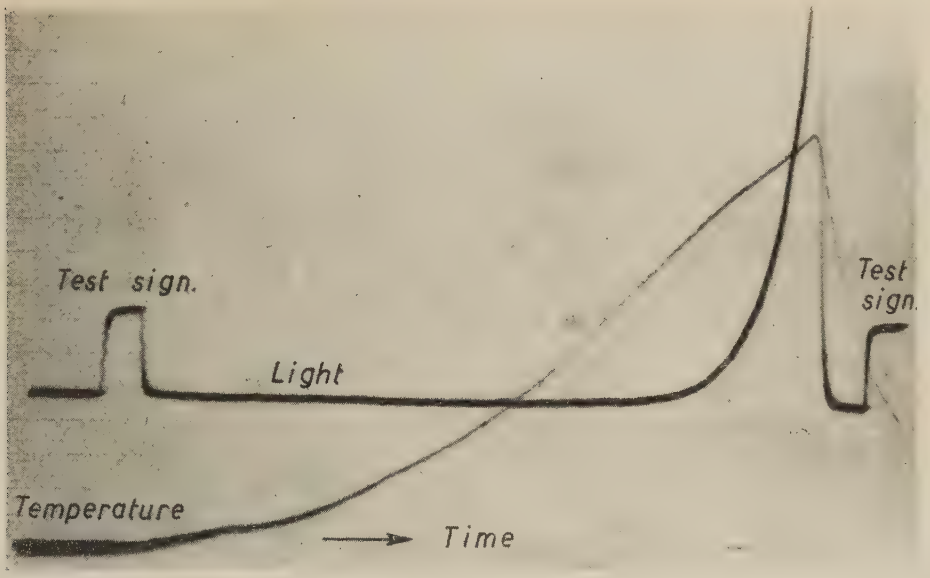

Fig. 4.

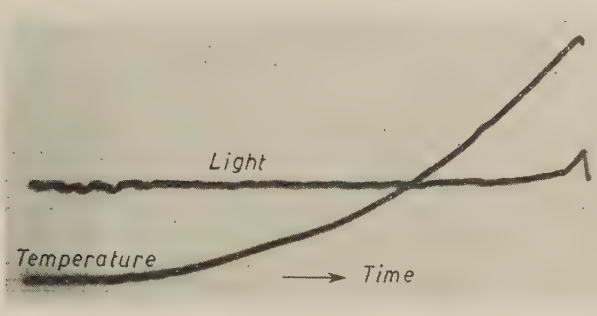

Fig. 5.

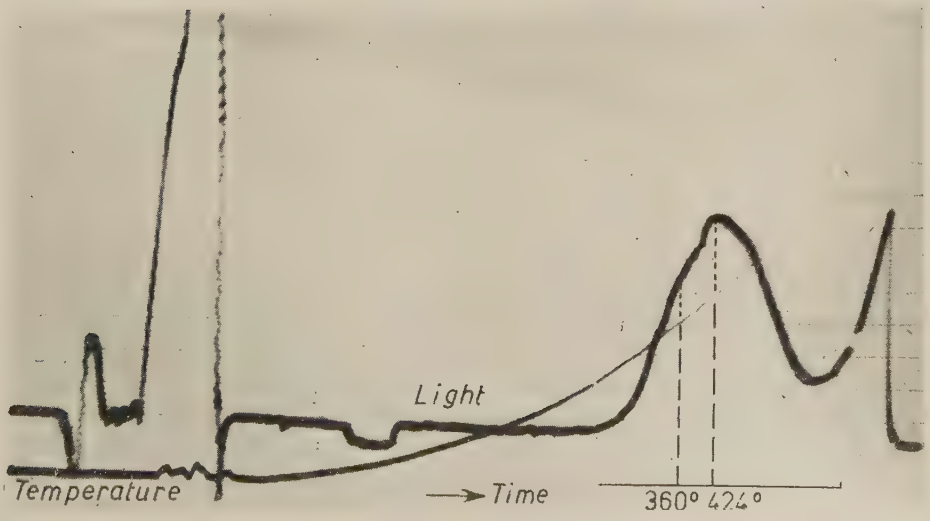

Fig. 6.

rhombohedra of calcite; it was not necessary to crush or grind it.

As it was to be expected, a first sample, not irradiated, did not give off any luminescence. The curve of emitted light began to raise only as the temperature of normal thermal emission was reached (Fig. 1).

A second sample, irradiated with X-rays (~ 25 kV), in order to test a less energetic radiation agent than γ-rays, gave a two-peak glow curve, similar to those obtained from natural limenstones (Fig. 2).

A third sample, not irradiated, but which had been compressed for 12 hours at about 700 kg/cm^2, gave a glow curve with a peak which seems to be the resultant of two curves, one with a peak at 360°, the other with a peak at 424° (Fig. 3).

On the contrary, glow curve of not irradiated quartz, ground to minus 200 mesh and compressed in the same conditions, did not show any peaks (Fig. 4).

4. – These facts seem to suggest:

a) Thermoluminescence is probably activated by pressure in calcite, because calcite crystals are very easily cleaved and twinned by pressure;

b) The same occurrence is, therefore, to be expected in other crystalline species having similar properties;

c) It is probable that thermoluminescence may result, in pulverized limestones, from activation in crushing and grinding the samples.

It seems noteworthy that, in the present experiments, high-temperature peaks appear to be activated by less energetic agents (like mechanical ones), while low-temperature peaks are produced by more energetic agents (like X- and γ-rays).

5. – The paper by ZELLER, WRAY and DANIELS [3], describing the same pressure effect, became known later.

Only some of the results and interpretations of the present investigations are in good agreement with ZELLER's and coll.

It was necessary, therefore, to verify the supposition that thermoluminescence activation in calcite results from pulverizing.

Two more glow curves were recorded, one directly from a part of a single calcite crystal, the other from another part of it, which had been ground, in an Abich mortar, to minus 200 mesh.

The glow curve of the not crushed crystal did not show any peaks (Fig. 5); that of the pulverized crystal was very similar to that of compressed calcite, showing the two adjacent peaks, at 360° and 424° (Fig. 6).

6. – This result seems to prove that calcite may become thermoluminescent by the mere fact of having been pulverized.

Moreover, as the pressure action in grinding in the Abich mortar is not a lasting one, it seems that the thermoluminescence activation does not result from compression, but from crushing, an effect that could be named *tribophosphorescence*.

The fact should be remembered when natural thermoluminescence of pulverized limestone is studied.

It should be interesting to know whether the calcite in which ZELLER and coll. have discovered crystallization thermoluminescence had been ground or not.

7. – The writer is glad to express his warmest thanks to Prof. G. BONFIGLIOLI, who friendly allowed the access to the thermoluminescence apparatus which he has devised, and who gave many valuable suggestions; and to Dr. C. CORTESE, who kindly performed the greatest part of the experimental task involved.

[3] E. J. ZELLER, J. L. WRAY and F. DANIELS: *Journ. Chem. Phys.*, **23**, 11, 2187 (1955).

Kinematic Depolarization of μ-Mesons Emitted in π-Meson Decays.

J. Werle

Institute for Nuclear Research - Warsaw

(ricevuto il 31 Ottobre 1957)

The presence of an asymmetry in the angular distribution of electrons emitted in the π-μ-e chain, predicted by the two-component variant of the neutrino field [1], has been already confirmed by several laboratories [2]. However, no quantitative conclusions can be drawn so far because of very big differences between the values of the asymmetry parameter obtained by different laboratories [2,3]. Evidently some part of these discrepancies can be explained by different experimental arrangements. E.g. different bubble chambers or nuclear emulsions, different magnetic fields etc., may lead to different depolarization rates during the slowing down process of the μ-meson, and consequently, to different experimental values of the asymmetry parameter. Depolarizing influence of the stopping medium has been discussed in [4]. However, some cases are known when two laboratories using just the same equipment (e.g. the same plates) obtained different results. Therefore, we shall study another possible source of error which is of purely kinematic origin and might have been overlooked or underestimated by some laboratories.

First let us consider a monokinetic beam of π^+-mesons of momentum $\boldsymbol{P}$ decaying in flight into μ^+ and ν. We assume that a μ^+-meson emitted by a π^+-meson decaying at rest (i.e. at $\boldsymbol{P}=0$) is completely polarized in direction of its momentum $\boldsymbol{p}_0$. The longitudinal component of the polarization vector of a μ^+-meson emitted by a π^+-meson of momentum $\boldsymbol{P}$ can be shown to be given by the formula

$$l = \frac{2(pE - \varepsilon P\cos\theta)}{m^2 - \mu^2}\,, \tag{1}$$

---

[1] T. D. Lee and C. N. Yang: *Phys. Rev.*, **105**, 1671 (1957); L. D. Landau: *Nuclear Phys.*, **3**, 127 (1957).

[2] R. L. Garvin, L. M. Lederman and M. Weinrich: *Phys. Rev.*, **105**, 1415 (1957); J. Friedman and V. L. Telegdi: *Phys. Rev.*, **105**, 1681 (1957); G. B. Chadwick, S. A. Durrani, L. M. Eisberg, P. B. Jones, J. W. G. Wignall and D. H. Wilkinson: *Phil. Mag.*, **2**, 684 (1957); B. Bhowmik, D. Evans and D. J. Prowse: *Nuovo Cimento*, **5**, 1663 (1957); N. N. Biswas, M. Ceccarelli and J. Crussard: *Nuovo Cimento*, **5**, 756 (1957); C. Castagnoli, C. Franzinetti and A. Manfredini: *Nuovo Cimento*, **5**, 684 (1957); J. M. Cassels, T. W. O. Keefe, M. Rigby, A. M. Wetherell and J. R. Wormald: *Proc. Phys. Soc.*, A **70**, 543 (1957); see also *Report to the 1957 Rochester Conference.*

[3] D. H. Wilkinson: *Nuovo Cimento*, **6**, 516 (1957).

[4] J. Friedman and V. L. Telegdi: *Phys. Rev.*, **106**, 1290 (1957).

where θ denotes the angle between the π-meson and μ-meson momenta, i.e. $\cos\theta = \boldsymbol{P}\cdot\boldsymbol{p}/Pp$. The symbols μ, $\boldsymbol{p}$, ε and m, $\boldsymbol{P}$, E denote the mass, momentum and energy of μ^+ and π^+ respectively. For a decay at rest $P=0$ and we have

$$p_0 = \frac{m^2-\mu^2}{2m}, \qquad \varepsilon_0 = \frac{m^2+\mu^2}{2m}, \qquad E_0 = m . \tag{2}$$

Putting $P = 0$ and inserting (2) into (1) we obtain $l_0 = +1$, i.e. complete longitudinal polarization.

In general, the conservation equations lead to the following expressions for μ-meson energy and momentum as functions of P and θ

$$\varepsilon_{1,2} = \mu\,\frac{E'E \pm P\cos\theta\sqrt{P'^2 - P^2\sin^2\theta}}{m^2 + P^2\sin^2\theta}, \tag{3}$$

$$p_{1,2} = \mu\,\frac{E'P\cos\theta \pm E\sqrt{P'^2 - P^2\sin^2\theta}}{m^2 + P^2\sin^2\theta}, \tag{4}$$

with

$$P' = \frac{m^2-\mu^2}{2\mu}, \qquad E' = \frac{m^2+\mu^2}{2\mu} . \tag{5}$$

Now we must discuss separately two different cases.

CASE A. – If $P < P'$, i.e. if

$$E_{\text{kin}} = E - m < E'_{\text{kin}} = E' - m = 5.37\ \text{MeV}, \tag{6}$$

we must reject the (—) sign in (3) and (4). Inserting p_1 and E_1 taken with (+) sign into (1) we find for this region of π-meson energies

$$l_1 = \sqrt{1 - (P^2/P'^2)\sin^2\theta} . \tag{7}$$

For fixed P the function (7) has a minimum for $\theta = 90°$.

CASE B. – If $P > P'$, i.e. if

$$E_{\text{kin}} > 5.37\ \text{MeV} \tag{8}$$

the angles θ are restricted to the interval

$$0 \leqslant \theta \leqslant \theta_k = \arcsin\frac{P}{P'} \leqslant 90°, \tag{9}$$

but for any P and θ from this interval we have now two values of ε and p given by (3) and (4). Inserting these two expressions into (1) we find correspondingly two values of l

$$l_{1,2} = \pm\sqrt{1 - (P^2/P'^2)\sin^2\theta} . \tag{10}$$

Thus we see that in this region of π-mesons energies the beam of μ-mesons emitted at an angle θ consists actually of two beams of different energies ε_1, ε_2 and opposite longitudinal polarizations $l_1 = -l_2$. It should be noted that for $\theta \to \theta_k$ the difference $\varepsilon_1 - \varepsilon_2 \to 0$ as well. A few plots of $l_1(P, \theta)$ for some chosen values of E_{kin} are shown in Fig. 1.

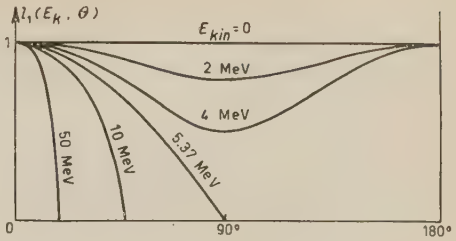

Fig. 1.

The normalized probability of finding the μ-meson emitted at an angle θ with momentum p_i given by (4) has the following form

$$W_i(P, \theta)\,\mathrm{d}\Omega = \frac{1}{4\pi p_0^2}\,\frac{p_i^2\,\mathrm{d}\Omega}{\sqrt{1-(P^2/P'^2)\sin^2\theta}}. \tag{11}$$

By means of the formulae (3)-(11) we can now calculate the mean values of l according to the kind of experiment.

As an example we shall calculate the average of $l(P, \theta)$ over all angles. For the sake of simplicity we restrict ourselves to energies $E_{\text{kin}} < 5.37$ MeV. For this range of π-meson energies we find

$$\tilde{l}(P) = 2\pi \int_0^{\pi} W_1(P, \theta) l_1(P, \theta) \sin\theta\,\mathrm{d}\theta = \frac{1}{V'^2} - \frac{1-V'^2}{2VV'^2} \ln\frac{1+V}{1-V} = \tag{12}$$

$$= 1 - \frac{1-V'^2}{3}\,\frac{V^2}{V'^2}\left(1 + \frac{3}{5}V^2 + \frac{3}{7}V^4 + \ldots\right),$$

where

$$V = \frac{P}{E}, \qquad V' = \frac{P'}{E'} \approx 0.27, \qquad V < V'. \tag{13}$$

For $P = P'$, i.e. for $E_{\text{kin}} = 5.37$ MeV, we find $\tilde{l}(P') = 0.68$. We see that $\tilde{l}(P)$ decreases quite rapidly with increasing P. Neglecting terms of higher order in V^2 we can reduce (12) to a simpler form

$$\tilde{l}(P) = 1 - 0.061\,E_{\text{kin}}, \tag{14}$$

where E_{kin} is to be expressed in MeV.

In order to avoid the difficulties connected with decays in flight many laboratories selected only such cases which could be ascribed to decays at rest. Since measurements of π-meson momentum are often not accurate enough one uses the length of μ-meson track (i.e. μ-meson energy) as a check distinguishing a decay at rest from a decay in flight. However, it can easily be seen that for $P < P'(2E'/m)$ one can always find a value θ'' such that either

$$\varepsilon_1(P, \theta'') = \varepsilon_0 \qquad \text{or} \qquad \varepsilon_2(P, \theta'') = \varepsilon_0. \tag{15}$$

In practice we have always a continuous spectrum of π-meson momenta in the beam which can be characterized by the probability $R(P)\,\mathrm{d}P$. The mean value of l averaged over all angles and momenta is then given by

$$l = \frac{\sum_{i=1}^{2} \iint R(P)\, W_i(P,\theta)\, l_i(P,\theta)\, G(\varepsilon_i - \varepsilon_0)\, \mathrm{d}P \sin\theta\, \mathrm{d}\theta}{\sum_{i=1}^{2} \iint R(P)\, W_i(P,\theta)\, G(\varepsilon_i - \varepsilon_0)\, \mathrm{d}P \sin\theta\, \mathrm{d}\theta}, \tag{16}$$

where the function G characterizes the accuracy of μ^+-meson track measurements. Thus we see that even in this case we may have some contribution from decays in flight which will result in a diminishing factor. However, it follows from (3), (4) and (15) that the angles θ'' lie in the interval $0 \leqslant \theta'' \leqslant 90°$. Therefore, if the length of the track is measured with sufficient accuracy we can avoid all the difficulties connected with kinematic depolarization simply by selecting only such cases in which $90° < \theta < 180°$.

Summarizing we can say that kinematic effects may lead to some quite substantial lowering of the mean longitudinal polarization of the μ-meson beam. Kinematic effects may be therefore responsible for at least some part of the still persisting confusion in π-μ-e experiments.

* * *

This work has been done during my visit to the United Institute for Nuclear Research at Dubna.

Generalization of the Variation Principle in the Theory of Electrical Conductivity.

V. Glaser and B. Jakšić

Institute R. Bošković and the University of Zagreb - Zagreb, Yugoslavia

(ricevuto il 5 Novembre 1957)

The most powerful method for solving the Bloch integral equation in the theory of conductivity is the variational method set up by Kohler [1]. This integral equation expresses the stationarity condition for the electron distribution, assuming the thermal equilibrium distribution for phonons. If one does not make this assumption, one arrives to a system of two coupled integral equations expressing the stationarity condition for electrons and phonons separately. It is our intention to generalize Kohler's variation principle to this general stationarity condition.

As usually, $f_0(E)$ and $N_0(\omega)$ denote the thermodynamic equilibrium distributions of electrons and phonons, respectively. Small deviations from these distributions $\Phi(\boldsymbol{k})$ and $\Psi(\boldsymbol{q})$ will be defined as follows

$$f(\boldsymbol{k}) = f_0(E) - \frac{\mathrm{d}f_0}{\mathrm{d}E}\Phi(\boldsymbol{k}), \qquad N(\boldsymbol{q}) = N_0(\omega) - \frac{\mathrm{d}N_0}{\mathrm{d}(\hbar\omega)}\Psi(\boldsymbol{q}). \tag{1}$$

In order to simplify the notation, the spin variable σ for the electron and the polarization variable s for the phonon are not written down explicitely. Therefore the integrals $\int \mathrm{d}^3k$ and $\int \mathrm{d}^3q$ ought to be understood as $\sum_\sigma \int \mathrm{d}^3k$ and $\sum_s \int \mathrm{d}^3q$. With this convention in mind both integral equations can be written in the form [2]

$$\begin{aligned}
&\int K_{\mathrm{e,\,irr}}(\boldsymbol{k};\boldsymbol{k}')[\Phi(\boldsymbol{k}) - \Phi(\boldsymbol{k}')]\,\mathrm{d}^3k' + \int \{K_{\mathrm{e,\,ph}}(\boldsymbol{k},\boldsymbol{q};\boldsymbol{k}')[\Phi(\boldsymbol{k}) + \Psi(\boldsymbol{q}) - \Phi(\boldsymbol{k}')] + \\
&\quad + K_{\mathrm{e,\,ph}}(\boldsymbol{k}',\boldsymbol{q};\boldsymbol{k})[\Phi(\boldsymbol{k}) - \Psi(\boldsymbol{q}) - \Phi(\boldsymbol{k}')]\}\,\mathrm{d}^3k'\,\mathrm{d}^3q + \\
&\quad + \int K_{\mathrm{e,\,e}}(\boldsymbol{k},\boldsymbol{k}';\boldsymbol{k}'',\boldsymbol{k}''')[\Phi(\boldsymbol{k}) + \Phi(\boldsymbol{k}') - \Phi(\boldsymbol{k}'') - \Phi(\boldsymbol{k}''')]\,\mathrm{d}^3k'\,\mathrm{d}^3k''\,\mathrm{d}^3k''' = \\
&\quad = -\frac{e}{(2\pi)^3}\frac{\mathrm{d}f_0}{\mathrm{d}E}v\,,
\end{aligned} \tag{2a}$$

[1] M. Kohler: *Zeits. Phys.*, **124**, 772 (1948); **125**, 679 (1949).
[2] R. E. Peierls: *Quantum Theory of Solids* (1955).

$$
(2b)\quad \left\{ \begin{aligned} &\int K_{\mathrm{ph,\,irr}}(\boldsymbol{q};\boldsymbol{q}')[\Psi(\boldsymbol{q})-\Psi(\boldsymbol{q}')]\,\mathrm{d}^3q' + \\ &\quad + \int K_{\mathrm{e,\,ph}}(\boldsymbol{k},\boldsymbol{q};\boldsymbol{k}')[\Phi(\boldsymbol{k})+\Psi(\boldsymbol{q})-\Phi(\boldsymbol{k}')]\,\mathrm{d}^3k\,\mathrm{d}^3k' + \\ &\quad + \int\Big\{K_{\mathrm{ph,\,ph}}(\boldsymbol{q},\boldsymbol{q}';\boldsymbol{q}'')[\Psi(\boldsymbol{q})+\Psi(\boldsymbol{q}')-\Psi(\boldsymbol{q}'')] + \\ &\quad + \tfrac{1}{2}K_{\mathrm{ph,\,ph}}(\boldsymbol{q}',\boldsymbol{q}'';\boldsymbol{q})[\Psi(\boldsymbol{q})-\Psi(\boldsymbol{q}')-\Psi(\boldsymbol{q}'')]\Big\}\,\mathrm{d}^3q'\,\mathrm{d}^3q'' = 0\,. \end{aligned} \right.
$$

Only terms linear in the external electric field F_i have been retained in (2), so that $\Phi = \Phi_i F_i$ and $\Psi = \Psi_i F_i$. The quantity v is equal to $v_i F_i$, $v_i = (1/\hbar)(\partial E/\partial k_i)$. The kernels of the integral equations (2) are due to different interactions of electrons and phonons. The possibility of representing in (2*a*), (2*b*) each of the interaction processes by a single kernel is due to the principle of detailed balance. The symmetric functions $K_{\mathrm{e,\,irr}}(\boldsymbol{k};\boldsymbol{k}')$ and $K_{\mathrm{ph,\,irr}}(\boldsymbol{q};\boldsymbol{q}')$ represent the elastic scattering of electrons, respectively phonons on irregularities in the crystal. They are proportional to the square of the matrix element and to $\delta[E(\boldsymbol{k})-E(\boldsymbol{k}')]$ respectively $\delta[\hbar\omega(\boldsymbol{q})-\hbar\omega(\boldsymbol{q}')]$. The kernel $K_{\mathrm{e,\,ph}}(\boldsymbol{k},\boldsymbol{q};\boldsymbol{k}')$ is identical to the Bloch kernel

$$
K_{\mathrm{e,\,ph}}(\boldsymbol{k},\boldsymbol{q};\boldsymbol{k}') = \frac{\Omega_0}{2(2\pi)^3 MkT}\,\frac{|\int_{\Omega_0}\psi^*_{\boldsymbol{k}'}U\psi_{\boldsymbol{k}}\,\mathrm{d}\tau|^2}{\omega(\boldsymbol{q})}\cdot
$$

$$
\cdot\,\frac{\delta[E(\boldsymbol{k})+\hbar\omega(\boldsymbol{q})-E(\boldsymbol{k}')]\sum_{\boldsymbol{n}}\delta[\boldsymbol{k}+\boldsymbol{q}-\boldsymbol{k}'+\boldsymbol{K}_{\boldsymbol{n}}]}{(e^{\varepsilon}+1)(e^{\varepsilon'}+1)\,|\,e^{-\varepsilon}-e^{-\varepsilon'}\,|}\,,
$$

where

$$
\varepsilon = \frac{E(\boldsymbol{k})-\zeta}{kT}\,,\qquad \varepsilon' = \frac{E(\boldsymbol{k}')-\zeta}{kT}\,,\qquad \psi_{\boldsymbol{k}} = \frac{1}{(2\pi)^{\frac{3}{2}}}\exp[i\boldsymbol{k}\cdot\boldsymbol{r}]u_{\boldsymbol{k}}(\boldsymbol{r})\,,
$$

$$
U = \sum_{\boldsymbol{n}}\boldsymbol{e}(\boldsymbol{q})\cdot\nabla V(\boldsymbol{r}-\boldsymbol{a}_{\boldsymbol{n}})\exp[i\boldsymbol{q}\cdot\boldsymbol{a}_{\boldsymbol{n}}]
$$

and $\boldsymbol{K}_{\boldsymbol{n}}$ is a vector of the reciprocal lattice. $K_{\mathrm{e,e}}(\boldsymbol{k},\boldsymbol{k}';\boldsymbol{k}'',\boldsymbol{k}''')$ is due to the electron-electron scattering and it contains the factor

$$
\delta[E(\boldsymbol{k})+E(\boldsymbol{k}')-E(\boldsymbol{k}'')-E(\boldsymbol{k}''')]\sum_{\boldsymbol{n}}\delta[\boldsymbol{k}+\boldsymbol{k}'-\boldsymbol{k}''-\boldsymbol{k}'''+\boldsymbol{K}_{\boldsymbol{n}}]\,.
$$

Finally $K_{\mathrm{ph,\,ph}}(\boldsymbol{q},\boldsymbol{q}';\boldsymbol{q}'')$ is a phonon-phonon interaction due to the anharmonicity of crystal vibrations and proportional to

$$
\delta[\hbar\omega(\boldsymbol{q})+\hbar\omega(\boldsymbol{q}')-\hbar\omega(\boldsymbol{q}'')]\sum_{\boldsymbol{n}}\delta(\boldsymbol{q}+\boldsymbol{q}'-\boldsymbol{q}''+\boldsymbol{K}_{\boldsymbol{n}})\,.
$$

Higher order phonon-phonon interactions, due to the same cause, can be introduced in the same way. We have dropped them for the sake of simplicity.

It is immediately clear from the equations (2*a*, *b*) that they can be derived from the variation principle

$$\delta L[\Phi, \Psi] = 0 \,, \tag{3a}$$

with

$$\begin{cases} L = -\frac{1}{4}\int K_{\mathrm{e,irr}}(\boldsymbol{k};\boldsymbol{k}')[\Phi(\boldsymbol{k}) - \Phi(\boldsymbol{k}')]^2 \,\mathrm{d}^3k\,\mathrm{d}^3k' - \\ \quad -\frac{1}{4}\int K_{\mathrm{ph,irr}}(\boldsymbol{q};\boldsymbol{q}')[\Psi(\boldsymbol{q}) - \Psi(\boldsymbol{q}')]^2 \,\mathrm{d}^3q\,\mathrm{d}^3q' - \\ \quad -\frac{1}{2}\int K_{\mathrm{e,ph}}(\boldsymbol{k},\boldsymbol{q};\boldsymbol{k}')[\Phi(\boldsymbol{k}) + \Psi(\boldsymbol{q}) - \Phi(\boldsymbol{k}')]^2 \,\mathrm{d}^3k\,\mathrm{d}^3k'\,\mathrm{d}^3q - \\ \quad -\frac{1}{4}\int K_{\mathrm{ph,ph}}(\boldsymbol{q},\boldsymbol{q}';\boldsymbol{q}'')[\Psi(\boldsymbol{q}) + \Psi(\boldsymbol{q}') - \Psi(\boldsymbol{q}'')]^2 \,\mathrm{d}^3q\,\mathrm{d}^3q'\,\mathrm{d}^3q'' - \\ \quad -\frac{1}{8}\int K_{\mathrm{e,e}}(\boldsymbol{k},\boldsymbol{k}';\boldsymbol{k}'',\boldsymbol{k}''')[\Phi(\boldsymbol{k}) + \Phi(\boldsymbol{k}') - \Phi(\boldsymbol{k}'') - \Phi(\boldsymbol{k}''')]^2 \,\mathrm{d}^3k\,\mathrm{d}^3k'\,\mathrm{d}^3k''\,\mathrm{d}^3k''' - \\ \quad -\frac{e}{(2\pi)^3}\int \frac{\mathrm{d}f_0}{\mathrm{d}E}\, v\Phi \,\mathrm{d}^3k \,. \end{cases} \tag{3b}$$

For the conductivity tensor σ_{ij} defined by

$$\sigma_{ij} = -\frac{e}{(2\pi)^3}\int \frac{\mathrm{d}f_0}{\mathrm{d}E}\, v_i \Phi_j \,\mathrm{d}^3k \,, \tag{4}$$

one can derive some important properties. By multiplying (2*a*) and (2*b*) by some arbitrary function $g(\boldsymbol{k})$ respectively $h(\boldsymbol{q})$ and integrating, one can prove the following equality

$$\begin{cases} -\frac{e}{(2\pi)^3}\int \frac{\mathrm{d}f_0}{\mathrm{d}E}\, vg \,\mathrm{d}^3k = \frac{1}{2}\int K_{\mathrm{e,\,irr}}(\boldsymbol{k};\boldsymbol{k}')[\Phi(\boldsymbol{k}) - \Phi(\boldsymbol{k}')][g(\boldsymbol{k}) - g(\boldsymbol{k}')]\,\mathrm{d}^3k\,\mathrm{d}^3k' + \\ + \frac{1}{2}\int K_{\mathrm{ph,\,irr}}(\boldsymbol{q};\boldsymbol{q}')[\Psi(\boldsymbol{q}) - \Psi(\boldsymbol{q}')][h(\boldsymbol{q}) - h(\boldsymbol{q}')]\,\mathrm{d}^3q\,\mathrm{d}^3q' + \\ + \int K_{\mathrm{e,\,ph}}(\boldsymbol{k},\boldsymbol{q};\boldsymbol{k}')[\Phi(\boldsymbol{k}) + \Psi(\boldsymbol{q}) - \Phi(\boldsymbol{k}')][g(\boldsymbol{k}) + h(\boldsymbol{q}) - g(\boldsymbol{k}')]\,\mathrm{d}^3k\,\mathrm{d}^3k'\,\mathrm{d}^3q + \\ + \frac{1}{2}\int K_{\mathrm{ph,\,ph}}(\boldsymbol{q},\boldsymbol{q}';\boldsymbol{q}'')[\Psi(\boldsymbol{q}) + \Psi(\boldsymbol{q}') - \Psi(\boldsymbol{q}'')]\cdot \\ \qquad \cdot[h(\boldsymbol{q}) + h(\boldsymbol{q}') - h(\boldsymbol{q}'')]\,\mathrm{d}^3q\,\mathrm{d}^3q'\,\mathrm{d}^3q'' + \\ + \frac{1}{4}\int K_{\mathrm{e,\,e}}(\boldsymbol{k},\boldsymbol{k}';\boldsymbol{k}'',\boldsymbol{k}''')[\Phi(\boldsymbol{k}) + \Phi(\boldsymbol{k}') - \Phi(\boldsymbol{k}'') - \Phi(\boldsymbol{k}''')]\cdot \\ \qquad \cdot[g(\boldsymbol{k}) + g(\boldsymbol{k}') - g(\boldsymbol{k}'') - g(\boldsymbol{k}''')]\,\mathrm{d}^3k\,\mathrm{d}^3k'\,\mathrm{d}^3k''\,\mathrm{d}^3k'''. \end{cases} \tag{5}$$

By taking $g(\boldsymbol{k}) \equiv \Phi_j(\boldsymbol{k})$ and $h(\boldsymbol{q}) \equiv \Psi_j(\boldsymbol{q})$, which satisfy $(2a, b)$ and therefore solve the variational problem, we obtain

$$\sigma_{ij} = \sigma_{ji} \,, \tag{6}$$

i.e. the symmetry property of the conductivity tensor. The second consequence follows from a similar choice: $g(\boldsymbol{k}) \equiv \Phi(\boldsymbol{k})$ and $h(\boldsymbol{q}) \equiv \Psi(\boldsymbol{q})$. One obtains for the extremal value of L:

$$L_{\text{extr}} = \tfrac{1}{2}\sigma_{ij}F_iF_j > 0 \,, \qquad \text{for } \boldsymbol{F} \neq 0, \tag{7}$$

and this means that σ_{ij} is a positive definite tensor.

These two consequences are valid for the exact solution of the variational problem or the equivalent system of integral equations $(2a, b)$.

But in practice it is usually impossible to find the exact solution. In this case we have to restrict our functions Φ, Ψ to a certain class of functions for which the variational problem is manageable. Let us denote the functions belonging to the chosen class of functions by $\Phi^{(n)}(\boldsymbol{k})$, $\Psi^{(n)}(\boldsymbol{q})$. The variational principle will now give us the integral equations for $\Phi^{(n)}$, $\Psi^{(n)}$ which differ from $(2a, b)$ by an unknown function orthogonal to our class of functions. The same procedure as before can be applied now. We multiply the integral equations with some arbitrary functions $g^{(n)}(\boldsymbol{k})$ and $h^{(n)}(\boldsymbol{q})$ belonging to our class, and we integrate. Through this integration we get rid of the unknown functions orthogonal to our class of functions. What is left is exactly the expression (5), but here valid for the functions $\Phi^{(n)}$, $\Psi^{(n)}$, $g^{(n)}$, $h^{(n)}$. The immediate consequences of this result are that $\sigma_{ij}^{(n)}$, calculated by means of $\Phi^{(n)}$ inserted in the formula (4), is a symmetric positive definite tensor. On the other hand we can choose $g \equiv \Phi^{(n)}$, $h \equiv \Psi^{(n)}$ in (5), so that we are able to express $\sigma_{ij}^{(n)}$ in two different ways

$$\begin{aligned} \sigma_{ij}^{(n)}F_iF_j &= \frac{1}{2}\int K_{\text{e, irr}}(\boldsymbol{k};\boldsymbol{k}')[\Phi^{(n)}(\boldsymbol{k}) - \Phi^{(n)}(\boldsymbol{k}')]^2 \,\mathrm{d}^3k\,\mathrm{d}^3k' + \ldots = \\ &= \frac{1}{2}\int K_{\text{e, irr}}(\boldsymbol{k};\boldsymbol{k}')[\Phi(\boldsymbol{k}) - \Phi(\boldsymbol{k}')][\Phi^{(n)}(\boldsymbol{k}) - \Phi^{(n)}(\boldsymbol{k}')]\,\mathrm{d}^3k\,\mathrm{d}^3k' + \ldots . \end{aligned} \tag{8}$$

Since our kernels, being probabilities for different processes, are never negative, we can write down, for any A, $A^{(n)}$, the inequality

$$\int K(\boldsymbol{k}, \boldsymbol{q}, \ldots)[A(\boldsymbol{k}, \boldsymbol{q}, \ldots) - A^{(n)}(\boldsymbol{k}, \boldsymbol{q}, \ldots)]^2 \,\mathrm{d}^3k\,\mathrm{d}^3q \ldots \geqslant 0 \,. \tag{9}$$

From (8) and (9) we obtain the very important inequality

$$(\sigma_{ij} - \sigma_{ij}^{(n)})F_iF_j \geqslant 0 \,, \qquad \boldsymbol{F} \neq 0 \,. \tag{10}$$

It says that $(\sigma_{ij} - \sigma_{ij}^{(n)})$ is a positive semi-definite tensor, so that the approximate value of the conductivity, in the direction of the principal axis calculated by means of $\Phi^{(n)}$, $\Psi^{(n)}$ determined by the generalized variation principle $\delta L[\Phi^{(n)}, \Psi^{(n)}] = 0$, with $L[\Phi, \Psi]$ given by $(3b)$, is never bigger than the exact value. For the special case of the Bloch integral equation this inequality has been found by KOHLER [1].

IL NUOVO CIMENTO Vol. VII, N. 2 16 Gennaio 1958

Relativistic Electron-Proton Scattering According to Meson Theory.

L. K. Pandit

Seminar für theoretische Physik der Universität - Zürich

(ricevuto il 5 Novembre 1957)

Scattering of high energy electrons by protons, for electron energies ranging up to 550 MeV, has recently been measured by Hofstädter and coworkers [1]. These experimenters were able to account for their experimental results on the basis of phenomenological models describing the proton as having an extended charge and magnetic moment distribution. The experiments quite definitely establish the extended structure of the proton. That meson theory also leads to a certain extended structure for the nucleons has been known for a long time. The charge distribution of the nucleons, on the basis of meson theory, was first calculated by Slotnick and Heitler [2].

The high energies involved require any theory, undertaking to explain these experiments, to be completely relativistic. In the following, we describe the results of our first order perturbation calculations for electron-proton scattering on the basis of covariant charge-symmetrical pseudoscalar meson theory with both pseudoscalar and pseudovector couplings. In these calculations, we have employed, for the virtual mesons, the relativistic cut-off formulated recently by Arnous and Heitler [3]. The special feature of this cut-off is that it is applied in a relativistically invariant way to the three-dimensional momenta of the virtual particles. It is characterized by a cut-off momentum K_0 for the virtual mesons when the whole nucleon is at rest. From various experimental data it was concluded that K_0 is of the order M (nucleon mass). It has been felt for a long time that such a universal cut-off is needed for the present day field theories, as expressing a limit of their validity. For example, we may mention the recent success in explaining the pion-nucleon scattering using a similar cut-off theory [4].

Let us, for the sake of visualizing the process, use the non-relativistic terminology of the meson-cloud round the fixed heavy nucleon-core. The charge is distributed between the point core (actually a Dirac particle) and the cloud.

[1] R. Hofstädter and R. McAllister: *Phys. Rev.*, **98**, 217 (1955); R. Hofstädter and E. E. Chambers: *Bull. Am. Phys. Soc.* II, **1**, 10 (1956); R. Hofstädter: *Proc. Sixth Rochester Conference* (1956); E. E. Chambers: *Stanford Univ. Dissertation* (1956).

[2] M. Slotnick and W. Heitler: *Phys. Rev.*, **75**, 1645 (1949).

[3] E. Arnous and W. Heitler: *Nuovo Cimento*, **2**, 1282 (1955).

[4] G. F. Chew: *Phys. Rev.*, **94**, 1748, 1755 (1954); and subsequent papers.

Then the cut-off, K_0, has the effect that, as it decreases from infinity towards the value zero, the meson-cloud extends more and more, but the total charge on it becomes less and less till the whole of the charge is on the proton core. Similarly, the anomalous magnetic moment

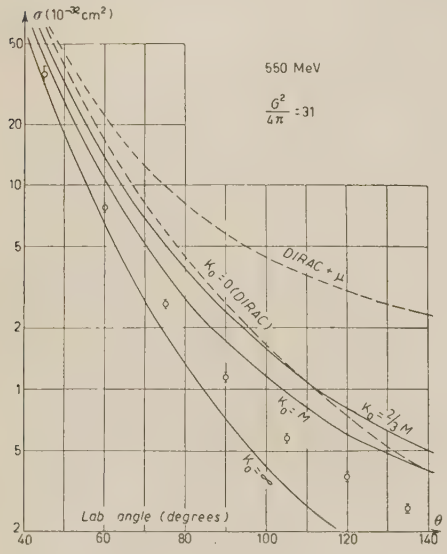

Fig. 1.

of the proton vanishes for $K_0=0$. Thus, for $K_0=0$, we have the proton simply as a point Dirac-particle.

To illustrate the results of our calculations, we give, in the accompanying figure, a graphical plot of the theoretical cross-sections for the scattering of 550 MeV electrons as a function of the laboratory angle of scattering (shown on the figure by continuous curves). The experimental points, given for comparison, have been taken from the Stanford dissertation of CHAMBERS [1]. Calculations without cut-off (i.e., $K_0=\infty$) were first performed by ROSENBLUTH [5], but surprisingly, they have not been compared with experiments in the literature so far. The curves given here have been calculated with $G^2/4\pi=31$ (*). Two of the curves on the figure are shown dotted. The lower one of these corresponds to the proton considered as a point Dirac-particle, and the higher one to the point Dirac-proton along with a point anomalous magnetic moment of 1.78 nuclear magnetons (described by a Pauli-term). The curves with cut-off values M or $\frac{2}{3}M$ are shown and a value of about $\frac{3}{2}M$ would give a good fit at all energies for the coupling constant chosen. The agreement can, naturally, not be expected to be perfect, for firstly the calculations are only to the first order in perturbation, and secondly this theory can have only an approximate nearness to the future correct theory. The results are not very sensitive to the values of K_0 and G. Without cut-off, i.e., $K_0=\infty$, the situation is slightly different and one could even get a rather nice fit for about half the above value of $G^2/4\pi$. Furthermore, with our cut-off we are able to use the otherwise divergent pseudovector coupling also. When K_0 is not much larger than M, the two couplings give results so close to each other that it is difficult to decide, from these calculations, in favour of either of them; but other effects, like pion-nucleon scattering, seem to favour strongly the pseudovector coupling. It can thus be concluded that the extension of the charge and magnetic moment provided by meson theory certainly accounts for the electron-proton scattering. A cut-off of the order M gives a reasonable fit with either of the two couplings, but the value of K_0 can hardly be determined with reliability from these experiments.

As another study of this cut-off, we would like to mention our results on the anomalous magnetic moments of the

(*) G is the pseudoscalar coupling constant. It also represents $(2M/\mu)F$, where F is the pseudovector coupling. Hence $F^2/4\pi=0.17$. This value for F, with the cut-off chosen, is likely to warrant the use of perturbation theory.

(5) M. N. ROSENBLUTH: *Phys. Rev.*, **79**, 615 (1950).

nucleons. As is well known, one gets, without cut-off, a value of about 8 for the ratio of the magnitude of the anomalous magnetic moment of the neutron to that of the proton. With $K_0 = M$, this ratio drops down to 4.1 and with $K_0 = \frac{2}{3}M$ to 3.15 (all in first order perturbation theory). The experimental value is about 1.08. Thus, here also the cut-off improves the situation a great deal. It is clear, however, that higher orders are needed and it might be hoped that their inclusion will lead to a more satisfactory agreement.

We would like to emphasize that this cut-off, being applied in an invariant way, takes account of the deformation of the source when the nucleon has a non-vanishing momentum (even, in some cases, in the limiting case of a nucleon at rest). As a result, we find that on going over to the non-relativistic limit of our theory in a consistent way, we obtain for example a value of the nucleon magnetic moment which is essentially different from the often quoted value obtained from the present day non-relativistic models of the meson theory [6] (the well known fixed and extended source).

A detailed account of this work will be published in the near future.

* * *

The author wishes to express his deepest gratitude to Prof. W. HEITLER for his kind guidance. To Dr. E. ARNOUS and Dr. CH. TERREAUX he is indebted for many useful discussions. His grateful thanks are due to the Government of India for the award of the Central States Scholarship.

---

[6] See, for example, G. SALZMANN: *Phys. Rev.*, **105**, 1076 (1957).

On the Locality of β-Interaction.

G. F. Dell'Antonio and P. Gulmanelli

Istituto di Scienze Fisiche dell'Università - Milano
Istituto Nazionale di Fisica Nucleare - Sezione di Milano

(ricevuto il 6 Dicembre 1957)

K. Nishijima [1] has recently derived a general system of equations for the vacuum expectation values of retarded products of field operators in the Heisenberg representation. The deduction is accomplished on the ground of a few general postulates, such as the existence of the energy-momentum four-vector and a complete set of state vectors, defined by means of a recurrent system of equations [eq. (2.9*a*)], to which the vacuum and the one particle states belong.

In the afore-mentioned paper the perturbation solution is worked out on the hypothesis of Lorentz invariance of the theory and with the additional requirement of microscopic causality; finally the formalism is applied to electrodynamics. The purpose of this note is to investigate the conclusions one can draw, if one applies the same method to the present formulation of β-theory.

For definiteness we shall compute, to the second order in the coupling constants, the electron propagation function, defined as $g_{\alpha\alpha'}(x-y) \equiv \langle \Omega, R[\psi^e_\alpha(x) : \overline{\psi}^e_{\alpha'}(y)]\Omega\rangle$. From this definition immediately follows:

$$\langle \Omega, R[\overline{\psi}^e_\alpha(x) : \psi^e_\alpha(y)]\Omega\rangle = -g^\dagger_{\alpha\alpha'}(x-y) .$$

The R-products are defined according to [1]. For future convenience we recall the following formula:

$$(1) \qquad R(\psi : \psi_1\psi_2\psi_3) = (-i)^3\{[\{\psi, \psi_1\}, \psi_2], \psi_3\}\theta(x-x_1)\theta(x-x_2)\theta(x-x_3) .$$

It turns out that for g and $g^\dagger$ the following equations hold:

$$(2) \qquad g_{\alpha\alpha'}(x-y) + g^\dagger_{\alpha\alpha'}(y-x) + i\langle \Omega, \{\psi^e_\alpha(x), \overline{\psi}^e_{\alpha'}(y)\}\Omega\rangle = 0 .$$

---

[1] K. Nishijima: *Progr. Theor. Phys.*, **17**, 765 (1957); cfr. also H. Lehmann, K. Symanzik and W. Zimmermann: *Nuovo Cimento*, **1**, 205 (1955); **6**, 319 (1957).

With the usual form of β-interaction, one has:

$$(\gamma_\mu \partial_\mu - m)\psi^e = \sum_i f^i O^i \psi^\nu \bar{\psi}^P O^i \psi^N . \tag{3}$$

One finds immediately that the zero-order solution of eq. (2) is:

$$g^{(0)}_{\alpha\alpha'}(x-y) = S^{\mathrm{ret}}_{\alpha\alpha'}(x-y) .$$

To the second order eq. (2) becomes:

$$\begin{aligned} g^{(2)}_{\alpha'\alpha}(x-y) + g^{\dagger(2)}_{\alpha\alpha'}(y-x) = &- i\langle \Omega, \psi^e_\alpha(x)\Phi^{(+)}_e\rangle\langle\Phi^{(+)}_e, \bar{\psi}^e_{\alpha'}(y)\Omega\rangle + \\ &+ i\langle \Omega, \bar{\psi}^e_{\alpha'}(y)\Phi^{(+)}_e\rangle\langle\Phi^{(+)}_e, \psi^e_\alpha(x)\Omega\rangle + \\ &+ i\langle \Omega, \psi^e_\alpha(x)\Phi^{(+)}_{PN\nu}\rangle\langle\Phi^{(+)}_{PN\nu}, \bar{\psi}^e_\alpha(y)\Omega\rangle + \\ &+ i\langle \Omega, \bar{\psi}^e_{\alpha'}(y)\Phi^{(+)}_{P\bar{N}\nu}\rangle\langle\Phi^{(+)}_{P\bar{N}\nu}, \psi^e_\alpha(x)\Omega\rangle \ (^2) . \end{aligned} \tag{4}$$

With the help of eqs. (1) and (3), eq. (4) may be rewritten as follows:

$$\begin{aligned} g^{(2)}_{\alpha\alpha'}(x-y) + g^{\dagger(2)}_{\alpha'\alpha}(y-x) + \int \mathrm{d}z' \, [&S_{\alpha\beta}(x-z')D^{z'}_{\beta\gamma} g^{\dagger(2)}_{\alpha'\gamma}(y-z') + \\ &+ S_{\beta\alpha'}(z'-y)\widetilde{D}^{z_j}_{\beta'\gamma} g^{(2)}_{\alpha\gamma}(x-z')] = \\ = \iint \mathrm{d}u \, \mathrm{d}v [&S^{\mathrm{ret}}(x-u)Q(u-v)S^{\mathrm{av}}(v-y)]_{\alpha\alpha'} , \end{aligned} \tag{5}$$

where:

$$D = \gamma_\mu \partial_\mu + m ; \qquad \widetilde{D} = \gamma^{\top}_\mu \partial_\mu - m ,$$

and

$$Q(u-v) = A(u-v) + A^\dagger(v-u) ,$$

$$A(u-v) = \sum_{i,j} f_j f^*_j O^i S^{(+)}(u-v)\bar{O}^j \, \mathrm{Spur}\,[O^i S^{(+)}(u-v)\bar{O}^j S^{(-)}(v-u)] .$$

The retarded solution of eq. (5) is:

$$\begin{aligned} g^{(2)}(x-y) = \iint \mathrm{d}u \, \mathrm{d}v S^{\mathrm{ret}}(x-u)\theta(u-v)Q(u-v)S^{\mathrm{ret}}(v-y) + \\ + i\lambda \int \mathrm{d}u S^{\mathrm{ret}}(x-u)S^{\mathrm{ret}}(u-y) , \end{aligned}$$

where λ is a differential operator of the second order in the coupling constants, and otherwise arbitrary to a large extent.

(²) The intermediate states $\Phi^{(+)}$ belong to the complete set of incoming states.

A polarization operator Π is defined in the usual way through the relation:

$$g^{(2)}(x-y) = \iint \mathrm{d}u\,\mathrm{d}v S^{\mathrm{ret}}(x-u)\,\Pi^{(2)}(u-v)S^{\mathrm{ret}}(v-y)\,.$$

If one assumes the coupling to be scalar (this restriction is ineffective for the conclusions we shall draw), the expression for $\Pi^{(2)}$ takes the following form:

$$(6) \qquad \Pi^{(2)}(x-y) = |f|^2 \int \mathrm{d}h \exp\left[ih\,(x-y)\right] \int \mathrm{d}s\theta(s_0)\theta(h_0-s_0)(is\gamma - m_v)\cdot$$

$$\cdot \frac{[-M^2 - \frac{1}{4}(h-s)^2]^{\frac{3}{2}}}{\sqrt{-(h-s)^2}}\,\theta\left(-M^2 - \frac{(h-s)^2}{4}\right) \frac{\delta\left(s_0 - \sqrt{|\mathbf{s}|^2 + m_v^2}\right)}{2\sqrt{|\mathbf{s}|^2 + m_v^2}} + i\lambda\delta(x-y)\,.$$

On grounds of invariance, the operator λ shall be of the form:

$$\lambda = C_0 + C_1\gamma_\mu\partial_\mu + C_2\,\Box + C_3\gamma_\mu\partial_\mu\,\Box + \ldots\,.$$

The integral which appears in eq. (6) is divergent; it may be shown that, if one tries to eliminate this divergence by a suitable choice of the arbitrary coefficients C_i, one cannot obtain finite results assuming that only the first three terms are different from zero.

This implies that when one goes to higher orders of approximation the number of counter terms becomes increasingly large. The appearance of higher and higher order derivatives reveals an essentially non-local feature of the theory. The foregoing discussion rests of course upon the validity of the perturbation approach.

* * *

We wish to thank Prof. P. CALDIROLA for his kind interest.

Direttore responsabile: G. POLVANI Tipografia Compositori - Bologna

Questo fascicolo è stato licenziato dai torchi il 28-I-1958